

Large-System Analysis of Joint Channel and Data Estimation for MIMO DS-CDMA Systems

Keigo Takeuchi, *Member, IEEE*, Mikko Vehkaperä, *Member, IEEE*, Toshiyuki Tanaka, *Member, IEEE*,
and Ralf R. Müller, *Senior Member, IEEE*

Abstract

This paper presents a large-system analysis of the performance of joint channel estimation, multiuser detection, and per-user decoding (CE-MUDD) for randomly-spread multiple-input multiple-output (MIMO) direct-sequence code-division multiple-access (DS-CDMA) systems. A suboptimal receiver based on successive decoding in conjunction with linear minimum mean-squared error (LMMSE) channel estimation is investigated. The replica method, developed in statistical mechanics, is used to evaluate the performance in the large-system limit, where the number of users and the spreading factor tend to infinity while their ratio and the number of transmit and receive antennas are kept constant. The performance of the joint CE-MUDD based on LMMSE channel estimation is compared to the spectral efficiencies of several receivers based on one-shot LMMSE channel estimation, in which the decoded data symbols are not utilized to refine the initial channel estimates. The results imply that the use of joint CE-MUDD significantly reduces rate loss due to transmission of pilot signals, especially for multiple-antenna systems. As a result, joint CE-MUDD can provide significant performance gains, compared to the receivers based on one-shot channel estimation.

Manuscript received February 24, 2010; revised March , 2011. The work of K. Takeuchi was in part supported by the Grant-in-Aid for Young Scientists (Start-up) (No. 21860035) from MEXT, Japan and by the Grant-in-Aid for Scientific Research on Priority Areas (No. 18079010) from MEXT, Japan. The work of M. Vehkaperä was supported by the Norwegian Research Council under grant 171133/V30. The work of T. Tanaka was in part supported by the Grant-in-Aid for Scientific Research on Priority Areas (No. 18079010) from MEXT, Japan. The material in this paper was presented in part at the 2008 IEEE International Symposium on Information Theory, Toronto, Canada, July 2008 and at the 2nd Workshop on Physics-Inspired Paradigms in Wireless Communications and Networks, Seoul, Korea, June 2009.

K. Takeuchi is with the Department of Communication Engineering and Informatics, the University of Electro-Communications, Tokyo 182-8585, Japan (e-mail: takeuchi@ice.uec.ac.jp).

M. Vehkaperä was with the Department of Electronics and Telecommunications, the Norwegian University of Science and Technology (NTNU), NO-7491 Trondheim, Norway. He is currently with the School of Electrical Engineering, Royal Institute of Technology (KTH), SE-100 44 Stockholm, Sweden (e-mail: mikkok@kth.se).

T. Tanaka is with the Department of Systems Science, Graduate School of Informatics, Kyoto University, Kyoto, 606-8501, Japan (e-mail: tt@i.kyoto-u.ac.jp).

R. R. Müller is with the Department of Electronics and Telecommunications, the Norwegian University of Science and Technology (NTNU), NO-7491 Trondheim, Norway (e-mail: ralf@iet.ntnu.no).

Index Terms

Multiple-input multiple-output (MIMO) systems, direct-sequence code-division multiple-access (DS-CDMA) schemes, channel estimation, multiuser detection (MUD), linear minimum mean-squared error (LMMSE) estimation, iterative receivers, successive decoding, large-system analysis, replica method, statistical mechanics.

I. INTRODUCTION

Direct-sequence code-division multiple-access (DS-CDMA) schemes are used in the air interface of third-generation (3G) mobile communication systems [1]–[3]. In order to improve the spectral efficiency of DS-CDMA systems, the extension to multiple-input multiple-output (MIMO) DS-CDMA systems has been actively considered [4]–[13]. As a drawback of using multiple antennas at the transmitters, the receiver structure of MIMO DS-CDMA systems becomes more complex than that of conventional DS-CDMA systems. Therefore, it is important in MIMO DS-CDMA systems to construct receivers achieving an acceptable tradeoff between performance and complexity.

A goal in this research area is to construct receivers which achieve near-optimal performance by using acceptable computational costs, since optimal joint decoding is infeasible in terms of complexity. Separation of detection and decoding significantly reduces the complexity of the receiver, although it is suboptimal in terms of performance. In multiuser detection (MUD) [14], certain statistical properties of multiple-access interference (MAI) are used to detect data symbols. Large-system analysis is a powerful approach for evaluating the performance of MUD followed by per-user decoding for randomly-spread DS-CDMA systems. In this analysis an asymptotic limit is assumed, referred to as the large-system limit, in which the number of users and the spreading factor tend to infinity while their ratio is kept constant. A series of large-system analyses [15]–[20] have revealed that the linear minimum mean-squared error (LMMSE) detection followed by per-user decoding achieves near-optimal performance for lightly-loaded systems with perfect channel state information (CSI) at the receiver. Furthermore, it has been shown numerically [21]–[24] and analytically [25], [26] that iterative LMMSE-based multiuser detection and per-user decoding (MUDD) can achieve near-optimal performance even for highly-loaded systems with perfect CSI at the receiver. See [4], [12], [13] for the extension of these results to MIMO DS-CDMA systems with perfect CSI at the receiver. In the large-system analysis for MIMO DS-CDMA systems the numbers of transmit and receive antennas are commonly fixed, while the number of users and the spreading factor tend to infinity with their ratio fixed. Note that a many-antenna limit, in which the numbers of transmit and receive antennas tend to infinity, may be taken after this large-system limit [27]. In this paper, the numbers of transmit and receive antennas are kept finite.

It is worth considering the no-CSI case since CSI is unknown in advance for practical MIMO DS-CDMA systems. Iterative MUDD was extended to iterative channel estimation (CE) and MUDD (CE-MUDD) in [28]. In this scheme, the channel estimator utilizes soft feedback from the per-user decoders for refining the initial channel estimates. In terms of complexity, iterative CE-MUDD requires updating the filter coefficients of the channel estimator and the detector in every iteration. This implies that the computational complexity of iterative CE-MUDD is higher than that for receivers based on one-shot channel estimation, in which data estimation is performed without refining the initial channel estimates. In order to reduce the complexity of iterative CE-MUDD, linear channel estimators, such

as the LMMSE channel estimator, have been commonly used. Linear channel estimators use known pilot symbols to obtain the initial channel estimates, while the optimal channel estimator can attain the initial channel estimates with no pilot symbols. Numerical simulations [28]–[30] demonstrated that iterative LMMSE-based CE-MUDD can provide significant performance gains for highly-loaded systems, compared to receivers based on one-shot channel estimation. However, these works did not discuss how to design the length of symbol periods assigned for transmission of pilot symbols, called training phase. Increasing the length of the training phase improves the accuracy of channel estimation, while transmission of pilot symbols reduces the transmission rate. Thus, how to design the length of the training phase should provide a great impact on achievable spectral efficiency for the no-CSI case. The goal of this paper is to optimize the length of the training phase on the basis of information-theoretical capacities.

Simple modulation schemes, such as quadrature phase shift keying (QPSK) or quadrature amplitude modulation (QAM), are commonly used for coherent receivers that estimate CSI explicitly. Thus, the channel capacity for a fixed modulation scheme, called constrained capacity, corresponds to a performance bound¹ for iterative receivers, while the true capacity might be achieved by using complicated modulation [31]. It is a challenging issue to derive analytical formulas for the constrained capacities of wireless communication systems with no CSI, since the optimal channel estimator is nonlinear. Lower bounds for the constrained capacities have been derived instead [32], [33]. The basic idea in these works for obtaining lower bounds is to replace the noise due to channel estimation errors by additive white Gaussian noise (AWGN). This replacement reduces optimal nonlinear channel estimation to LMMSE channel estimation. In this paper, this type of a lower bound is referred to as a lower bound based on LMMSE channel estimation.

We derive a lower bound for the constrained capacity of randomly-spread MIMO DS-CDMA systems with no CSI, on the basis of LMMSE channel estimation. The lower bound can be regarded as a performance index for iterative CE-MUDD based on LMMSE channel estimation. In an information-theoretical point of view, both LMMSE channel estimates and covariances of the estimation errors should be used in MUD [34], while the use of the covariances is uncommon in practice. In this paper, we consider *suboptimal* LMMSE channel estimation in which only a part of the covariances for the LMMSE estimation errors are used, while all covariances are used in the *true* LMMSE channel estimation. The use of suboptimal LMMSE channel estimation allows us to evaluate a lower bound for the constrained capacity. We refer to this lower bound as the performance of the joint CE-MUDD based on suboptimal LMMSE channel estimation, or simply as the performance of the joint CE-MUDD. In order to investigate the benefits obtained by using iterative CE-MUDD, we also analyze the performance of three receivers based on one-shot LMMSE channel estimation: one-shot CE-MUDD, an optimum separated receiver, and an LMMSE receiver. Table I lists the four receivers considered in this paper. The one-shot CE-MUDD performs joint MUDD based on one-shot LMMSE channel estimation. Intuitively, the performance of the one-shot CE-

¹ Intuitively, one may expect that the optimal CE-MUDD can be implemented with iterative CE-MUDD. However, it is unclear whether the solution of the iterative CE-MUDD converges to the global optimal solution. Therefore, the constrained capacity might be a loose bound for the performance of iterative CE-MUDD.

TABLE I
FOUR RECEIVERS CONSIDERED IN THIS PAPER.

	channel estimation(CE)	MUD	feedback	
			to CE	to detector
joint CE-MUDD	suboptimal LMMSE	optimal	available	available
one-shot CE-MUDD	suboptimal LMMSE	optimal		available
optimum separated receiver	suboptimal LMMSE	optimal		
LMMSE receiver	suboptimal LMMSE	LMMSE		

MUDD corresponds to a performance bound for an iterative receiver obtained by eliminating the feedback from the per-user decoders to the channel estimator in iterative CE-MUDD. The optimum separated receiver performs separated optimal detection and decoding on the basis of one-shot LMMSE channel estimation. The performance of the optimum separated receiver corresponds to a performance bound for a non-iterative receiver obtained by eliminating the feedback from the per-user decoders to the channel estimator and to the detector. The LMMSE receiver is obtained by replacing the optimal detector in the optimum separated receiver by the LMMSE detector. To the best of our knowledge, no analytical results for joint CE-MUDD are obtained, except for non-iterative linear receivers [34] and iterative CE-MUDD based on hard decision feedback [35]. The methodology developed in this paper is applicable to the analysis of iterative LMMSE-based CE-MUDD. See [36] for details.

Our large-system analysis is based on the replica method [37]–[39], which is a powerful method for analyzing randomly-spread DS-CDMA systems [11], [18]–[20], [40] and MIMO systems [41]–[44]. The replica method is based on several non-rigorous procedures at present time. In this paper, we assume that results obtained by using these procedures are correct since their proof is beyond the scope of this paper. See [45]–[47] for recent progress with respect to the assumptions of the replica method.

This paper is organized as follows: After summarizing the notation used in this paper, in Section II we introduce a discrete-time model of MIMO DS-CDMA systems. In Section III, the joint CE-MUDD based on suboptimal LMMSE channel estimation is defined. In Section IV, we define the three receivers based on one-shot LMMSE channel estimation. Section V presents the main results of this paper. In Section VI, we compare the performance of the joint CE-MUDD with that of the three receivers based on one-shot LMMSE channel estimation. Numerical simulations for finite-sized systems are also performed to demonstrate the usefulness of our large-system analysis. In Section VII, we conclude this paper. The derivations of the main results are summarized in the appendices.

A. Notation

For a complex number $z \in \mathbb{C}$ and a real number $x \in \mathbb{R}$, $\text{Re}(z)$, $\text{Im}(z)$, i , z^* , $\log x$, and $\ln x$ denote the real part, imaginary part, imaginary unit, complex conjugate, $\log_2 x$, and $\log_e x$, respectively. $|\mathcal{A}|$ stands for the number of elements of a set \mathcal{A} . For a matrix \mathbf{A} , \mathbf{A}^T , \mathbf{A}^H , $\text{Tr}(\mathbf{A})$, and $\det(\mathbf{A})$ denote the transpose, conjugate transpose,

trace, and the determinant, respectively. \mathbf{I}_N stands for the $N \times N$ identity matrix. $\mathbf{1}_N$ denotes the N -dimensional vector whose elements are all one. $\mathbf{e}_N^{(n)}$ represents the N -dimensional vector in which the n th element is one and the other elements are all zero. \mathcal{M}_n^+ denotes the set of all positive definite $n \times n$ Hermitian matrices. \otimes denotes the Kronecker product operator between two matrices. $\delta(\cdot)$ represents the Dirac delta function, while $\delta_{i,j}$ denotes the Kronecker delta. $p(x)$ and $p(y|x)$ stand for the probability density function (pdf) of a continuous random variable x and the conditional pdf of a continuous random variable y given x , respectively. We use the same symbol $p(x)$ for the probability mass function (pmf) of a discrete random variable x . $a \sim P(a)$ indicates that the distribution of a random variable a equals a distribution $P(a)$. If the pdf $p(a)$ of a exists, we use the notation $a \sim p(a)$ to represent that a follows the distribution whose pdf is given by $p(a)$. $\mathcal{CN}(\mathbf{m}, \mathbf{\Sigma})$ denotes a proper n -dimensional complex Gaussian distribution with mean $\mathbf{m} \in \mathbb{C}^N$ and a covariance matrix $\mathbf{\Sigma} \in \mathcal{M}_n^+$ [48]. The pdf of the n -dimensional complex Gaussian random vector $\mathbf{x} \sim \mathcal{CN}(\mathbf{m}, \mathbf{\Sigma})$ is defined as $p(\mathbf{x}) = g_n(\mathbf{x} - \mathbf{m}; \mathbf{\Sigma})$, given by

$$g_n(\mathbf{y}; \mathbf{\Sigma}) = \frac{1}{\pi^n \det \mathbf{\Sigma}} e^{-\mathbf{y}^H \mathbf{\Sigma}^{-1} \mathbf{y}}. \quad (1)$$

$D(\mathbf{A} \parallel \mathbf{B})$ stands for the Kullback-Leibler divergence with the logarithm to base 2 between $\mathcal{CN}(\mathbf{0}, \mathbf{A})$ and $\mathcal{CN}(\mathbf{0}, \mathbf{B})$. $I(x; y|z)$ denotes the conditional mutual information with the logarithm to base 2 between a random variable x and a random variable y conditioned on a random variable z .

The indices of chips, symbol periods, users, transmit antennas, and replicas are denoted by l , t , k , m , and a , respectively. In this paper, indices themselves have meanings, like the argument of distributions. Symbols with several superscripts or subscripts are used in this paper. We write sets of the symbols as follows: For a symbol $a_{i,j}^k$ and a subset \mathcal{J} of indices $\{j\}$, the set $\mathcal{A}_{i,\mathcal{J}}^k$ denotes a subset $\{a_{i,j}^k : j \in \mathcal{J}\}$ for fixed i and k . When \mathcal{J} equals the set of all indices $\{j\}$, $\mathcal{A}_{i,\mathcal{J}}^k$ is also written as \mathcal{A}_i^k . The sets \mathcal{A}_i , \mathcal{A} , and so on are defined in the same manner. The two sets \mathcal{A}_i^k and \mathcal{A}_j^k should not be confused with each other. The set $\mathcal{J} \setminus \{j\} = \{j' \in \mathcal{J} : j' \neq j\}$ denotes the set obtained by eliminating the element j from \mathcal{J} . When \mathcal{J} equals the set of all indices $\{j\}$, $\mathcal{J} \setminus \{j\}$ is simply written as $\setminus \{j\}$. As notational convenience for subsets of the natural numbers \mathbb{N} , we use $[a, b) = \{i \in \mathbb{N} : a \leq i < b\}$ for integers a and $b (> a)$, which is always used as subscripts or superscripts for discrete sets. The other sets $[a, b]$, (a, b) , and so on are defined in the same manner. As exceptions, the two sets $\{t' \in \mathbb{N} : 1 \leq t' \leq t\}$ and $\{t' \in \mathbb{N} : t \leq t' \leq T_c\}$ for coherence time T_c are denoted by \mathcal{T}_t and \mathcal{C}_t , respectively, instead of $[1, t]$ and $[t, T_c]$.

We use symbols with tildes and hats to represent random variables for postulated channels and estimates of random variables, respectively. Underlined symbols are used to represent random variables for decoupled single-user channels. Note that there are several exceptions in the replica analyses presented in Appendix C and Appendix D.

II. MIMO DS-CDMA CHANNEL

We consider the uplink of a synchronous K -user frequency-flat fading MIMO DS-CDMA system with spreading factor L , in which each user and the receiver have M transmit antennas and N receive antennas, respectively. A per-antenna spreading scheme is investigated in this paper: Different spreading sequences are used for different transmit antennas of each user. See [49] for a generalization of spreading schemes. We assume block-fading channels with

coherence time T_c , i.e., fading coefficients do not change during T_c symbol periods, and they are independently sampled from a distribution at the beginning of the next coherent interval.

The input symbol $u_{t,k,m} \in \mathbb{C}$ for the m th transmit antenna of user k in symbol period t is spread with a spreading sequence $\{s_{l,t,k,m} : l = 1, \dots, L\}$. The chip-sampled received vectors $\{\mathbf{y}_{l,t} \in \mathbb{C}^N : l = 1, \dots, L\}$ in symbol periods $t = 1, \dots, T_c$ are given by

$$\mathbf{y}_{l,t} = \frac{1}{\sqrt{L}} \sum_{k=1}^K \sum_{m=1}^M \mathbf{h}_{k,m} s_{l,t,k,m} u_{t,k,m} + \mathbf{n}_{l,t}. \quad (2)$$

In (2), $\mathbf{n}_{l,t} \sim \mathcal{CN}(\mathbf{0}, N_0 \mathbf{I}_N)$ represents the AWGN vector with variance N_0 . Furthermore, $\mathbf{h}_{k,m} \in \mathbb{C}^N$ denotes the channel vector between transmit antenna m of the k th user and the receiver. Note that the channel vectors are fixed during T_c symbol periods.

The assumption of frequency-flat fading channels might be an unrealistic assumption since practical MIMO DS-SS systems commonly operate over frequency-selective fading channels. For the sake of simplicity, however, we consider frequency-flat fading channels. An extension to frequency-selective fading channels is possible by considering the assumption of independent spreading sequences across different resolvable paths [4], [34]. For details, see [50].

The receiver does not have CSI in advance, which is information about all realizations of the channel vectors $\{\mathbf{h}_{k,m} : \text{for all } k, m\}$, while it knows all spreading sequences, the variance N_0 of the AWGN, and the statistical properties of all channel vectors and input symbols. In order for the receiver to estimate the channel vectors, consider that the first τ symbol periods $\mathcal{T}_\tau = \{1, \dots, \tau\}$ in each coherent interval are assigned to a training phase, and that the remaining $\tau' = T_c - \tau$ symbol periods $\mathcal{C}_{\tau+1} = \{\tau + 1, \dots, T_c\}$ are assigned to a communication phase. The length of the training phase τ is a design parameter, which will be optimized on the basis of large-system results. User k transmits pilot symbols $\{x_{t,k,m} \in \mathbb{C}\}$ known to the receiver from the m th transmit antenna in the training phase $t \in \mathcal{T}_\tau$, and subsequently sends data symbols $\{b_{t,k,m} \in \mathbb{C}\}$ in the communication phase $t \in \mathcal{C}_{\tau+1}$. Therefore, the input symbol $u_{t,k,m}$ is given by

$$u_{t,k,m} = \begin{cases} x_{t,k,m} & \text{for } t \in \mathcal{T}_\tau, \\ b_{t,k,m} & \text{for } t \in \mathcal{C}_{\tau+1}. \end{cases} \quad (3)$$

Throughout this paper, we assume that the input symbols $\{u_{t,k,m}\}$ are mutually independent for all t, k, m , and that each $u_{t,k,m}$ is a zero-mean random variable satisfying $|u_{t,k,m}|^2 = P/M$. In numerical results, unbiased QPSK input symbols with $|u_{t,k,m}|^2 = P/M$ are used. Furthermore, it is straightforward to extend the results to the unequal power case. Next, we assume that the channel vectors $\{\mathbf{h}_{k,m}\}$ are mutually independent for all k, m , and that each $\mathbf{h}_{k,m}$ has independent and identically distributed (i.i.d.) circularly symmetric complex Gaussian (CSCG) elements with unit variance. Finally, we assume that the spreading sequences $\{s_{l,t,k,m} : \text{for all } l, t, k, m\}$ are i.i.d. for all l, t, k, m , and that each $s_{l,t,k,m}$ is a CSCG random variable with unit variance. We have made the CSCG assumption of each chip for the sake of simplicity in analysis. We believe that the main results presented in this paper hold for a general distribution of $s_{l,t,k,m}$ with zero mean and finite moments, as shown numerically in Section VI.

We shall present several sets used in this paper: The set $\mathcal{Y}_t = \{\mathbf{y}_{l,t} \in \mathbb{C}^N : l = 1, \dots, L\}$ denotes the received vectors in symbol period t . The set $\mathcal{S}_t = \{s_{l,t,k,m} : \text{for all } l, k, m\}$ represents the spreading sequences in symbol period t . The sets $\mathcal{B}_{t,k} = \{b_{t,k,m} : \text{for all } m\}$ and $\mathcal{X}_{t,k} = \{x_{t,k,m} : \text{for all } m\}$ represent the data and pilot symbols for user k in symbol period t , respectively. All data and pilot symbols in symbol period t are denoted by $\mathcal{B}_t = \{\mathcal{B}_{t,k} : \text{for all } k\}$ and $\mathcal{X}_t = \{\mathcal{X}_{t,k} : \text{for all } k\}$. The set $\mathcal{U}_t = \{u_{t,k,m} : \text{for all } k, m\}$ represents the input symbols in symbol period t . The channel vectors for user k are denoted by $\mathcal{H}_k = \{\mathbf{h}_{k,m} : \text{for all } m\}$. The set $\mathcal{I}_t = \{\mathcal{Y}_t, \mathcal{S}_t, \mathcal{U}_t\}$ denotes the information about the received vectors \mathcal{Y}_t , the spreading sequences \mathcal{S}_t , and the input symbols \mathcal{U}_t in symbol period t . The set $\bar{\mathcal{I}}_t = \{\mathcal{Y}_t, \mathcal{S}_t\}$ is obtained by eliminating the input symbols \mathcal{U}_t from \mathcal{I}_t . The training phase in stage t of successive decoding, introduced in the next section, is denoted by $\mathcal{T}_{t-1} = \{1, \dots, t-1\}$, while the following stages are denoted by $\mathcal{C}_{t+1} = \{t+1, \dots, T_c\}$. The set $\mathcal{C}_{\tau+1}$ is also used to represent the communication phase. Note that the same index t as for symbol periods is used for the indices of stages in successive decoding. A list for several sets used in this paper is summarized in Appendix G.

III. JOINT CE-MUDD

A. Joint CE-MUDD Based on LMMSE Channel Estimation

In order to define joint CE-MUDD based on LMMSE channel estimation, we shall derive a lower bound of the constrained capacity based on LMMSE channel estimation. The definition of joint CE-MUDD considered in this paper will be presented in the next subsection.

We start by the constrained capacity of the MIMO DS-CDMA channel (2) with no CSI. Let $\mathcal{Y}_{\mathcal{T}_\tau} = \{\mathcal{Y}_t : t \in \mathcal{T}_\tau\}$ and $\mathcal{Y}_{\mathcal{C}_{\tau+1}} = \{\mathcal{Y}_t : t \in \mathcal{C}_{\tau+1}\}$ denote the received vectors in the training and communication phases, respectively. Furthermore, we write all data symbols \mathcal{B} and all pilot symbols \mathcal{X} as $\mathcal{B} = \{\mathcal{B}_t : \text{for all } t \in \mathcal{C}_{\tau+1}\}$ and $\mathcal{X} = \{\mathcal{X}_t : \text{for all } t \in \mathcal{T}_\tau\}$. The constrained capacity for the no-CSI case is given by the mutual information per chip between all data symbols \mathcal{B} and $\{\mathcal{Y}_{\mathcal{C}_{\tau+1}}, \mathcal{Y}_{\mathcal{T}_\tau}, \mathcal{S}, \mathcal{X}\}$ known to the receiver [51], with $\mathcal{S} = \{\mathcal{S}_t : \text{for all } t\}$ denoting all spreading sequences,

$$C_{\text{opt}} = \frac{1}{LT_c} I(\mathcal{B}; \mathcal{Y}_{\mathcal{C}_{\tau+1}}, \mathcal{Y}_{\mathcal{T}_\tau}, \mathcal{S}, \mathcal{X}). \quad (4)$$

Using the chain rule for mutual information, we obtain

$$\begin{aligned} C_{\text{opt}} &= \frac{1}{LT_c} I(\mathcal{B}; \mathcal{Y}_{\mathcal{C}_{\tau+1}} | \mathcal{Y}_{\mathcal{T}_\tau}, \mathcal{S}, \mathcal{X}) + \frac{1}{LT_c} I(\mathcal{B}; \mathcal{Y}_{\mathcal{T}_\tau}, \mathcal{S}, \mathcal{X}) \\ &= \frac{1}{LT_c} I(\mathcal{B}; \mathcal{Y}_{\mathcal{C}_{\tau+1}} | \mathcal{Y}_{\mathcal{T}_\tau}, \mathcal{S}, \mathcal{X}), \end{aligned} \quad (5)$$

where the last equality holds since the data symbols \mathcal{B} are independent of $\{\mathcal{Y}_{\mathcal{T}_\tau}, \mathcal{S}, \mathcal{X}\}$. For notational convenience, we hereafter omit conditioning with respect to $\mathcal{Y}_{\mathcal{T}_\tau}$, \mathcal{S} , and \mathcal{X} .

It is well known that the constrained capacity can be achieved by successive decoding. In order to obtain a lower bound for the constrained capacity, a successive decoding strategy has been considered in [52], [53]. In this strategy, channel estimation and MUD in successive decoding are replaced by suboptimal ones that allow us to evaluate the performance analytically. We present joint CE-MUDD based on LMMSE channel estimation,

following the successive decoding strategy. In successive decoding with $\tau' = T_c - \tau$ stages, the data symbols $\{\mathcal{B}_t\}$ are decoded in the order $t = \tau + 1, \dots, T_c$. Stage $t \in \mathcal{C}_{\tau+1}$ consists of K substages, in which the data symbols $\{\mathcal{B}_{t,k}\}$ in symbol period t are decoded in the order $k = 1, \dots, K$. We focus on substage k within stage t . Let $\mathcal{B}_{(\tau,t)} = \{\mathcal{B}_{t'} : t' = \tau + 1, \dots, t - 1\}$ and $\mathcal{Y}_{\mathcal{C}_{\tau+1} \setminus \{t\}} = \{\mathcal{Y}_{t'} : t' \in \mathcal{C}_{\tau+1}, t' \neq t\}$ denote the data symbols decoded successfully in the preceding stages and the received vectors in the communication phase except for \mathcal{Y}_t , respectively. The independency of $\{\mathcal{B}_t\}$ for all t implies that \mathcal{B}_t is independent of the received vectors $\{\mathcal{Y}_{t'}\}$ in different symbol periods $t' \neq t$. By using the chain rule for mutual information repeatedly, (5) yields

$$\begin{aligned} I(\mathcal{B}; \mathcal{Y}_{\mathcal{C}_{\tau+1}}) &= \sum_{t=\tau+1}^{T_c} I(\mathcal{B}_t; \mathcal{Y}_{\mathcal{C}_{\tau+1}} | \mathcal{B}_{(\tau,t)}) \\ &= \sum_{t=\tau+1}^{T_c} [I(\mathcal{B}_t; \mathcal{Y}_{\mathcal{C}_{\tau+1} \setminus \{t\}} | \mathcal{B}_{(\tau,t)}) + I(\mathcal{B}_t; \mathcal{Y}_t | \mathcal{B}_{(\tau,t)}, \mathcal{Y}_{\mathcal{C}_{\tau+1} \setminus \{t\}})] \\ &= \sum_{t=\tau+1}^{T_c} I(\mathcal{B}_t; \mathcal{Y}_t | \mathcal{B}_{(\tau,t)}, \mathcal{Y}_{\mathcal{C}_{\tau+1} \setminus \{t\}}), \end{aligned} \quad (6)$$

where the last equality holds since \mathcal{B}_t is independent of $\mathcal{Y}_{\mathcal{C}_{\tau+1} \setminus \{t\}}$. If there were dependencies between the data symbols in different symbol periods, the equality would not hold. Applying the chain rule for mutual information to (6) gives

$$C_{\text{opt}} = \frac{1}{LT_c} \sum_{t=\tau+1}^{T_c} \sum_{k=1}^K C_{t,k}^{\text{opt}}, \quad (7)$$

with

$$C_{t,k}^{\text{opt}} = I(\mathcal{B}_{t,k}; \mathcal{Y}_t | \mathcal{B}_{t,[1,k]}, \mathcal{B}_{(\tau,t)}, \mathcal{Y}_{\mathcal{C}_{\tau+1} \setminus \{t\}}), \quad (8)$$

where $\mathcal{B}_{t,[1,k]} = \{\mathcal{B}_{t,k'} : k' = 1, \dots, k - 1\}$ denotes the data symbols decoded in the preceding substages.

We focus on each mutual information (8). In estimating $\mathcal{B}_{t,k}$, the data symbols $\mathcal{B}_{(\tau,t)}$ decoded in the preceding stages are available for channel estimation, while the data symbols $\mathcal{B}_{t,[1,k]}$ decoded in the preceding substages are used in MUD. The optimal receiver achieving the mutual information (8) consists of the optimal channel estimator, the optimal detector, and per-user decoders. The optimal channel estimator uses the information $\mathcal{I}_{\mathcal{T}_{t-1}} = \{\mathcal{I}_{t'} : t' \in \mathcal{T}_{t-1}\}$ in the preceding stages and the information $\bar{\mathcal{I}}_{\mathcal{C}_{t+1}} = \{\bar{\mathcal{I}}_{t'} : t' \in \mathcal{C}_{t+1}\}$ in the following stages to construct the posterior pdf $p(\mathcal{H} | \mathcal{I}_{\mathcal{T}_{t-1}}, \bar{\mathcal{I}}_{\mathcal{C}_{t+1}})$ of all channel vectors $\mathcal{H} = \{\mathcal{H}_k : \text{for all } k\}$, which is sent to the optimal detector. Note that $p(\mathcal{H} | \mathcal{I}_{\mathcal{T}_{t-1}}, \bar{\mathcal{I}}_{\mathcal{C}_{t+1}})$ is non-Gaussian, since $\bar{\mathcal{I}}_{\mathcal{C}_{t+1}} = \{\mathcal{Y}_{t'}, \mathcal{S}_{t'} : t' \in \mathcal{C}_{t+1}\}$ is an incomplete data set, i.e, it does not contain the data symbols $\{\mathcal{B}_{t'}\}$. Consequently, the optimal channel estimator is nonlinear. In the optimal detector, the posterior pdf $p(\mathcal{B}_{t,k} | \mathcal{Y}_t, \mathcal{S}_t, \mathcal{B}_{t,[1,k]}, \mathcal{I}_{\mathcal{T}_{t-1}}, \bar{\mathcal{I}}_{\mathcal{C}_{t+1}})$ is constructed and fed to the corresponding decoder, by utilizing the information about the received vector \mathcal{Y}_t , the spreading sequences \mathcal{S}_t , the data symbols $\mathcal{B}_{t,[1,k]}$ in the preceding substages, and the posterior pdf $p(\mathcal{H} | \mathcal{I}_{\mathcal{T}_{t-1}}, \bar{\mathcal{I}}_{\mathcal{C}_{t+1}})$ provided by the channel estimator.

It is difficult to obtain an analytical expression for the constrained capacity (7), since the optimal channel estimator is nonlinear. In order to obtain a lower bound based on LMMSE channel estimation, we consider a lower bound for (8),

$$C_{t,k}^{\text{opt}} \geq I(\mathcal{B}_{t,k}; \mathcal{Y}_t | \mathcal{B}_{t,[1,k]}, \mathcal{B}_{(\tau,t)}, \mathcal{Y}_{(\tau,t)}), \quad (9)$$

with $\mathcal{Y}_{(\tau,t)} = \{\mathcal{Y}_{t'} : t' = \tau + 1, \dots, t - 1\}$ denoting the received vectors in the preceding stages. In the derivation of (9), we have used the assumption of independent data symbols and the fact that conditioning does not increase (differential) entropy. Recall that conditioning with respect to $\mathcal{Y}_{\mathcal{T}_\tau}$, \mathcal{S} , and \mathcal{X} in the mutual information is omitted. Substituting (9) to (7) yields the lower bound $C_{\text{opt}} > C$, with

$$C = \frac{1}{LT_c} \sum_{t=\tau+1}^{T_c} \sum_{k=1}^K I(\mathcal{B}_{t,k}; \mathcal{Y}_t | \mathcal{B}_{t,[1,k]}, \mathcal{I}_{\mathcal{T}_{t-1}}, S_t), \quad (10)$$

where we have re-written the conditioning random variables as $\{\mathcal{B}_{t,[1,k]}, \mathcal{I}_{\mathcal{T}_{t-1}}, S_t\}$, using the fact that the lower bound (9) is independent of the spreading sequences $\mathcal{S}_{\mathcal{C}_{t+1}} = \{\mathcal{S}_{t'} : t' \in \mathcal{C}_{t+1}\}$ in the following stages anymore.

The receiver achieving the lower bound (10) is obtained by replacing the optimal channel estimator by a channel estimator that sends the posterior pdf $p(\mathcal{H} | \mathcal{I}_{\mathcal{T}_{t-1}})$, instead of $p(\mathcal{H} | \mathcal{I}_{\mathcal{T}_{t-1}}, \bar{\mathcal{I}}_{\mathcal{C}_{t+1}})$. It is straightforward to find that this channel estimator is equivalent to the LMMSE channel estimator, as shown in the following remark. Thus, we refer to the lower bound (10) as the spectral efficiency of the joint CE-MUDD based on LMMSE channel estimation.

Remark 1. *We shall show that the channel estimator corresponding to the lower bound (9) is the LMMSE channel estimator. We first confirm that the channel estimator is linear. The information $\mathcal{I}_{\mathcal{T}_{t-1}}$ in the training phase is a complete data set for estimating the channel vectors \mathcal{H} , i.e., $\mathcal{I}_{\mathcal{T}_{t-1}}$ contains the received vectors, the spreading sequences, and the input symbols in each symbol period. The Gaussian assumption of the channel vectors $\mathbf{h}_k \sim \mathcal{CN}(\mathbf{0}, \mathbf{I}_N)$ implies that the posterior pdf $p(\mathcal{H} | \mathcal{I}_{\mathcal{T}_{t-1}})$ is a proper complex Gaussian pdf whose mean is given by a linear transform of the received vectors. Thus, the channel estimator based on the posterior mean estimator is linear.*

We next show that the channel estimator is equal to the LMMSE channel estimator. See Appendix A for derivations of the LMMSE estimator. Following [32], [33], we replace the term $\mathbf{h}_{k,m} s_{l,t',k,m} b_{t',k,m}$ in (2) for the following stages $t' = t + 1, \dots, T_c$ by a proper complex Gaussian random vector whose mean and covariance are given by $\mathbf{h}_{k,m} s_{l,t',k,m} \mathbb{E}[b_{t',k,m}]$ and $|s_{l,t',k,m}|^2 \mathbb{E}[\mathbf{h}_{k,m} b_{t',k,m} (\mathbf{h}_{k,m} b_{t',k,m})^H]$, respectively. However, the mean is equal to zero, because of $\mathbb{E}[b_{t',k,m}] = 0$. As a result, the received vectors in the following stages is independent of the channel vectors anymore. In other words, the LMMSE channel estimator does not utilize the information $\mathcal{Y}_{\mathcal{C}_{t+1}} = \{\mathcal{Y}_{t'} : t' \in \mathcal{C}_{t+1}\}$ in the following stages, since the LMMSE channel estimator postulates that the received vector $\mathbf{y}_{l,t'}$ in (2) is independent of the channel vectors for $t' \in \mathcal{C}_{t+1}$. Therefore, the lower bound (9) corresponds to the spectral efficiency of the receiver based on the LMMSE channel estimation.

B. Joint CE-MUDD Based on Suboptimal LMMSE Channel Estimation

It is still hard to evaluate the spectral efficiency (10) of the joint CE-MUDD based on LMMSE channel estimation, since the posterior pdf $p(\mathcal{H} | \mathcal{I}_{\mathcal{T}_{t-1}})$ sent by the LMMSE channel estimator is not factorized into the product of the marginal posterior pdfs $\prod_{k=1}^K p(\mathcal{H}_k | \mathcal{I}_{\mathcal{T}_{t-1}})$. Instead, we consider a suboptimal receiver in which the LMMSE channel estimator is replaced by a suboptimal LMMSE channel estimator that sends the product $\prod_{k=1}^K p(\mathcal{H}_k | \mathcal{I}_{\mathcal{T}_{t-1}})$. The spectral efficiency for the suboptimal receiver provides a lower bound for the spectral efficiency (10) based

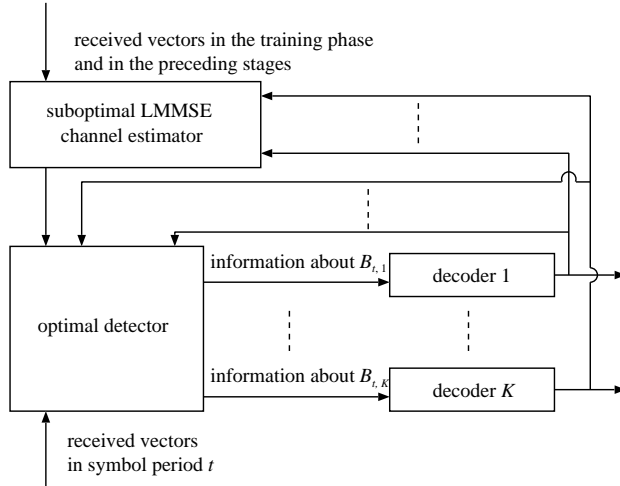


Fig. 1. Joint CE-MUDD based on suboptimal LMMSE channel estimation.

on LMMSE channel estimation. Since the LMMSE detector uses no covariances of the channel estimation errors between different users [34], as noted in Section IV-D, no performance loss due to this replacement occurs for the LMMSE receiver. On the other hand, the optimal detector utilizes all information about the channel vectors, i.e., the joint posterior pdf $p(\mathcal{H}|\mathcal{I}_{\mathcal{T}_{t-1}})$. It is unclear whether the performance loss caused by using the suboptimal LMMSE channel estimator is negligible in the large-system limit for the optimal detector.

Let us focus on substage k within stage t . The suboptimal receiver consists of a suboptimal LMMSE channel estimator, the optimal detector, and the per-user decoders (See Fig. 1). The channel estimator uses the pilot symbols and the data symbols decoded in the preceding stages to estimate the channel vectors. More precisely, the channel estimator constructs the posterior pdf $p(\mathcal{H}_k|\mathcal{I}_{\mathcal{T}_{t-1}})$ of the channel vectors \mathcal{H}_k for each user by utilizing the known information $\mathcal{I}_{\mathcal{T}_{t-1}} = \{\mathcal{Y}_{t'}, \mathcal{S}_{t'}, \mathcal{U}_{t'} : t' \in \mathcal{T}_{t-1}\}$,

$$p(\mathcal{H}_k|\mathcal{I}_{\mathcal{T}_{t-1}}) = \frac{\int \prod_{t'=1}^{t-1} p(\mathcal{Y}_{t'}|\mathcal{H}, \mathcal{S}_{t'}, \mathcal{U}_{t'}) p(\mathcal{H}) d\mathcal{H}_{\setminus\{k\}}}{\int \prod_{t'=1}^{t-1} p(\mathcal{Y}_{t'}|\mathcal{H}, \mathcal{S}_{t'}, \mathcal{U}_{t'}) p(\mathcal{H}) d\mathcal{H}}, \quad (11)$$

with $\mathcal{H}_{\setminus\{k\}} = \{\mathcal{H}_{k'} : \text{for all } k' \neq k\}$ denoting the channel vectors except for \mathcal{H}_k . In (11), the pdf $p(\mathcal{Y}_{t'}|\mathcal{H}, \mathcal{S}_{t'}, \mathcal{U}_{t'})$ represents the MIMO DS-CDMA channel (2) in symbol period t' . Then, the marginal posterior pdfs $\{p(\mathcal{H}_k|\mathcal{I}_{\mathcal{T}_{t-1}}) : \text{for all } k\}$ are sent towards the optimal detector. Sending $p(\mathcal{H}_k|\mathcal{I}_{\mathcal{T}_{t-1}})$ is equivalent to feeding the LMMSE estimates $\hat{\mathbf{h}}_{k,m}^{\mathcal{T}_{t-1}} = \int \mathbf{h}_{k,m} p(\mathcal{H}_k|\mathcal{I}_{\mathcal{T}_{t-1}}) d\mathcal{H}_k$ and the covariances of the estimation errors $\Delta \mathbf{h}_{k,m}^{\mathcal{T}_{t-1}} = \mathbf{h}_{k,m} - \hat{\mathbf{h}}_{k,m}^{\mathcal{T}_{t-1}}$ for all m , since the posterior pdf $p(\mathcal{H}_k|\mathcal{I}_{\mathcal{T}_{t-1}})$ is CSCG.

The optimal detector uses the information about the received vectors \mathcal{Y}_t , the data symbols $\mathcal{B}_{t,[1,k]}$ decoded in the preceding substages, the spreading sequences \mathcal{S}_t , and the posterior pdfs $\{p(\mathcal{H}_k|\mathcal{I}_{\mathcal{T}_{t-1}})\}$ provided by the channel estimator to detect the data symbols $\mathcal{B}_{t,k}$. The term ‘‘optimal detector’’ indicates that the detector is optimal among all detectors that regard the product $\prod_{k=1}^K p(\mathcal{H}_k|\mathcal{I}_{\mathcal{T}_{t-1}})$ of the marginal posterior pdfs as the true joint posterior pdf. The optimal detector constructs a posterior pdf $p(\tilde{\mathcal{B}}_{t,k}|\mathcal{Y}_t, \mathcal{B}_{t,[1,k]}, \mathcal{S}_t, \mathcal{I}_{\mathcal{T}_{t-1}})$ and subsequently forwards it to

the corresponding per-user decoder. In the posterior pdf, the data symbols $\tilde{\mathcal{B}}_{t,k} = \{\tilde{b}_{t,k,m} \in \mathbb{C} : \text{for all } m\} \sim \prod_{m=1}^M p(b_{t,k,m})$ denotes the data symbols in the MIMO DS-CDMA channel postulated by the optimal detector

$$\tilde{\mathbf{y}}_{l,t} = \frac{1}{\sqrt{L}} \sum_{k=1}^K \sum_{m=1}^M \tilde{\mathbf{h}}_{k,m} s_{l,t,k,m} \tilde{b}_{t,k,m} + \tilde{\mathbf{n}}_{l,t}, \quad (12)$$

with $\tilde{\mathbf{n}}_{l,t} \sim \mathcal{CN}(\mathbf{0}, N_0 \mathbf{I}_N)$. In (12), $\tilde{\mathcal{H}}_k = \{\tilde{\mathbf{h}}_{k,m} \in \mathbb{C}^N : \text{for all } m\}$ denotes random vectors representing the information about \mathcal{H}_k provided by the channel estimator. The joint posterior pdf of $\tilde{\mathcal{H}} = \{\tilde{\mathcal{H}}_k : \text{for all } k\}$ satisfies

$$p(\tilde{\mathcal{H}}|\mathcal{I}_{\mathcal{T}_{t-1}}) = \prod_{k=1}^K p(\mathcal{H}_k = \tilde{\mathcal{H}}_k|\mathcal{I}_{\mathcal{T}_{t-1}}). \quad (13)$$

Note that $p(\tilde{\mathcal{H}}|\mathcal{I}_{\mathcal{T}_{t-1}}) \neq p(\mathcal{H}|\mathcal{I}_{\mathcal{T}_{t-1}})$ since $p(\mathcal{H}|\mathcal{I}_{\mathcal{T}_{t-1}})$ is not decomposed into the product of the marginal pdfs. The posterior pdf $p(\tilde{\mathcal{B}}_{t,k}|\mathcal{Y}_t, \mathcal{B}_{t,[1,k]}, \mathcal{S}_t, \mathcal{I}_{\mathcal{T}_{t-1}})$ is an abbreviation of $p(\tilde{\mathcal{B}}_{t,k}|\tilde{\mathcal{Y}}_t = \mathcal{Y}_t, \tilde{\mathcal{B}}_{t,[1,k]} = \mathcal{B}_{t,[1,k]}, \mathcal{S}_t, \mathcal{I}_{\mathcal{T}_{t-1}})$, with $\tilde{\mathcal{Y}}_t = \{\tilde{\mathbf{y}}_{l,t} \in \mathbb{C}^N : \text{for all } l\}$ and $\tilde{\mathcal{B}}_{t,[1,k]} = \{\tilde{\mathcal{B}}_{t,k'} : k' = 1, \dots, k-1\}$ denoting the received vectors in (12) and the postulated data symbols in the preceding substages, respectively, given by

$$p(\tilde{\mathcal{B}}_{t,k}|\tilde{\mathcal{Y}}_t, \tilde{\mathcal{B}}_{t,[1,k]}, \mathcal{S}_t, \mathcal{I}_{\mathcal{T}_{t-1}}) = \frac{\int p(\tilde{\mathcal{Y}}_t|\tilde{\mathcal{B}}_t, \mathcal{S}_t, \mathcal{I}_{\mathcal{T}_{t-1}}) p(\tilde{\mathcal{B}}_t) d\tilde{\mathcal{B}}_{t,(k,K)}}{\int p(\tilde{\mathcal{Y}}_t|\tilde{\mathcal{B}}_t, \mathcal{S}_t, \mathcal{I}_{\mathcal{T}_{t-1}}) p(\tilde{\mathcal{B}}_t) d\tilde{\mathcal{B}}_{t,[k,K]}}, \quad (14)$$

with $\tilde{\mathcal{B}}_{t,(k,K)} = \{\tilde{\mathcal{B}}_{t,k'} : k' = k+1, \dots, K\}$ and $\tilde{\mathcal{B}}_{t,[k,K]} = \{\tilde{\mathcal{B}}_{t,k'} : k' = k, \dots, K\}$. In (14), $p(\tilde{\mathcal{Y}}_t|\tilde{\mathcal{B}}_t, \mathcal{S}_t, \mathcal{I}_{\mathcal{T}_{t-1}})$ is given by

$$p(\tilde{\mathcal{Y}}_t|\tilde{\mathcal{B}}_t, \mathcal{S}_t, \mathcal{I}_{\mathcal{T}_{t-1}}) = \int p(\tilde{\mathcal{Y}}_t|\tilde{\mathcal{H}}, \mathcal{S}_t, \tilde{\mathcal{B}}_t) p(\tilde{\mathcal{H}}|\mathcal{I}_{\mathcal{T}_{t-1}}) d\tilde{\mathcal{H}}, \quad (15)$$

where $p(\tilde{\mathcal{Y}}_t|\tilde{\mathcal{H}}, \mathcal{S}_t, \tilde{\mathcal{B}}_t)$ represents the MIMO DS-CDMA channel (12) postulated by the optimal detector in symbol period t . The marginal posterior pdf (14) would reduce to the true one $p(\mathcal{B}_{t,k}|\mathcal{Y}_t, \mathcal{B}_{t,[1,k]}, \mathcal{S}_t, \mathcal{I}_{\mathcal{T}_{t-1}})$ if the channel estimator sent the joint posterior pdf $p(\mathcal{H}|\mathcal{I}_{\mathcal{T}_{t-1}})$.

The spectral efficiency C_{joint} of the joint CE-MUDD based on the suboptimal LMMSE channel estimation is given by,

$$C_{\text{joint}} = \frac{1}{LT_c} \sum_{t=\tau+1}^{T_c} \sum_{k=1}^K C_{t,k}, \quad (16)$$

with

$$C_{t,k} = I(\mathcal{B}_{t,k}; \tilde{\mathcal{B}}_{t,k}|\mathcal{B}_{t,[1,k]}, \mathcal{I}_{\mathcal{T}_{t-1}}, \mathcal{S}_t). \quad (17)$$

The conditional mutual information (17) is characterized by the equivalent channel between user k and the corresponding decoder, given by

$$p(\tilde{\mathcal{B}}_{t,k}|\mathcal{B}_{t,k}, \mathcal{B}_{t,[1,k]}, \mathcal{I}_{\mathcal{T}_{t-1}}, \mathcal{S}_t) = \int p(\tilde{\mathcal{B}}_{t,k}|\mathcal{Y}_t, \mathcal{B}_{t,[1,k]}, \mathcal{S}_t, \mathcal{I}_{\mathcal{T}_{t-1}}) p(\mathcal{Y}_t|\mathcal{B}_{t,[1,k]}, \mathcal{S}_t, \mathcal{I}_{\mathcal{T}_{t-1}}) d\mathcal{Y}_t, \quad (18)$$

where

$$p(\mathcal{Y}_t|\mathcal{B}_{t,[1,k]}, \mathcal{S}_t, \mathcal{I}_{\mathcal{T}_{t-1}}) = \int p(\mathcal{Y}_t|\mathcal{H}, \mathcal{S}_t, \mathcal{B}_t) p(\mathcal{B}_{t,(k,K)}) p(\mathcal{H}|\mathcal{I}_{\mathcal{T}_{t-1}}) d\mathcal{H} d\mathcal{B}_{t,(k,K)}, \quad (19)$$

with $\mathcal{B}_{t,[1,k]} = \{\mathcal{B}_{t,k'} : k' = 1, \dots, k\}$ and $\mathcal{B}_{t,(k,K)} = \{\mathcal{B}_{t,k'} : k' = k+1, \dots, K\}$. In (19), $p(\mathcal{Y}_t|\mathcal{H}, \mathcal{S}_t, \mathcal{B}_t)$ represents the MIMO DS-CDMA channel (2) in symbol period t . Note that $\tilde{\mathcal{B}}_{t,k}$ in (17) plays the role of random

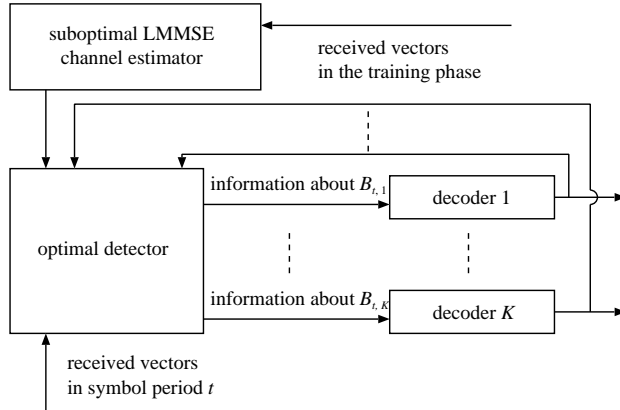


Fig. 2. One-shot CE-MUDD based on suboptimal LMMSE channel estimation.

variables representing the information about $\mathcal{B}_{t,k}$ provided to the per-user decoder, although we have introduced $\tilde{\mathcal{B}}_{t,k}$ as random variables representing the data symbols postulated by the optimal detector in (12).

The spectral efficiency (16) of the joint CE-MUDD based on the suboptimal LMMSE channel estimation is a lower bound for the spectral efficiency (10) based on the LMMSE channel estimation. We hereafter focus on the lower bound (16). Thus, the joint CE-MUDD based on the suboptimal LMMSE channel estimation is simply referred to as the joint CE-MUDD. The spectral efficiency (16) of the joint CE-MUDD should not be confused with the spectral efficiency (10) based on the LMMSE channel estimation or with the constraint capacity (6).

IV. RECEIVERS BASED ON ONE-SHOT CHANNEL ESTIMATION

A. One-Shot Channel Estimation

For comparison with the joint CE-MUDD, we consider three receivers based on one-shot channel estimation, in which the decoded data symbols are not used to refine the channel estimates. A first receiver performs joint MUDD based on one-shot LMMSE channel estimation, called one-shot CE-MUDD. This receiver is obtained by eliminating the feedback from the per-user decoders to the suboptimal LMMSE channel estimator in Fig. 1. A second receiver performs separated decoding based on one-shot LMMSE channel estimation, called the optimum separated receiver. The receiver is obtained by eliminating the feedback from the per-user decoders to the channel estimator and to the optimal detector. The last receiver is an LMMSE receiver in which the detector in the optimum separated receiver is replaced by an LMMSE detector. The four receivers considered in this paper are listed in Table I.

B. One-Shot CE-MUDD

We define the one-shot CE-MUDD based on the suboptimal LMMSE channel estimation (See Fig. 2). In stage t of the joint CE-MUDD, the channel estimator has used the information $\mathcal{I}_{\mathcal{T}_{t-1}} = \{\mathcal{Y}_{t'}, \mathcal{S}_{t'}, \mathcal{U}_{t'} : t' \in \mathcal{T}_{t-1}\}$

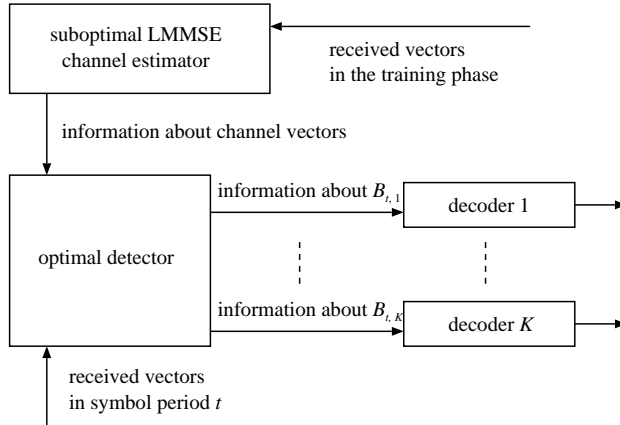


Fig. 3. Optimum separated receiver based on suboptimal LMMSE channel estimation.

about the received vectors $\{\mathcal{Y}_{t'}\}$, the spreading sequences $\{\mathcal{S}_{t'}\}$, and the transmitted symbols $\mathcal{U}_{t'}$ in symbol periods $t' \in \mathcal{T}_{t-1}$. On the other hand, the LMMSE channel estimation in the one-shot CE-MUDD cannot utilize the data symbols $\{\mathcal{B}_{t'} : t' = \tau + 1, \dots, t - 1\}$ decoded in the preceding stages. This restriction is equivalent to assuming that the information $\mathcal{I}_{(\tau,t)} = \{\mathcal{Y}_{t'}, \mathcal{S}_{t'}, \mathcal{U}_{t'} : t' = \tau + 1, \dots, t - 1\}$ in the preceding stages is not used for channel estimation, as discussed in Remark 1. In other words, the information $\mathcal{I}_{\mathcal{T}_\tau} = \{\mathcal{Y}_{t'}, \mathcal{S}_{t'}, \mathcal{X}_{t'} : \text{for all } t' \in \mathcal{T}_\tau\}$ in the training phase is utilized for channel estimation. Thus, the suboptimal LMMSE channel estimator in the one-shot CE-MUDD provides the marginal posterior pdfs $\{p(\mathcal{H}_k | \mathcal{I}_{\mathcal{T}_\tau})\}$ to the optimal detector. Note that sending the joint posterior pdf $p(\mathcal{H} | \mathcal{I}_{\mathcal{T}_\tau})$ is of course optimal. Strictly speaking, the one-shot CE-MUDD should be referred to as the one-shot CE-MUDD based on the suboptimal LMMSE channel estimation. However, we simply call it the one-shot CE-MUDD, since the true LMMSE channel estimator is not analyzed in this paper.

The marginal posterior pdf $p(\mathcal{H}_k | \mathcal{I}_{\mathcal{T}_\tau})$ is equal to the one constructed in the first stage of the joint CE-MUDD. Thus, the spectral efficiency of the one-shot CE-MUDD is given by

$$C_{\text{one}} = \left(1 - \frac{\tau}{T_c}\right) L^{-1} \sum_{k=1}^K C_{\tau+1,k}, \quad (20)$$

where the mutual information $C_{\tau+1,k}$ is defined as (17).

C. Optimum Separated Receiver

We define the optimum separate receiver based on the suboptimal LMMSE channel estimation (See Fig. 3). In substage k of the joint CE-MUDD, the optimal detector has used the data symbols $\mathcal{B}_{t,[1,k]}$ in the preceding substages to mitigate MAI. In the optimum separated receiver, on the other hand, the information $\mathcal{B}_{t,[1,k]}$ is not utilized for MUD. The posterior pdf $p(\tilde{\mathcal{B}}_{t,k} | \mathcal{Y}_t, \mathcal{S}_t, \mathcal{I}_{\mathcal{T}_\tau})$ is constructed and sent to the corresponding per-user decoder. The posterior pdf is equal to the one constructed in the first substage of the joint CE-MUDD. Thus, the

spectral efficiency of the optimum separated receiver is given by

$$C_{\text{sep}} = \frac{K}{L} \left(1 - \frac{\tau}{T_c} \right) C_{\tau+1,1}, \quad (21)$$

where the mutual information $C_{\tau+1,1}$ is defined as (17).

D. LMMSE Receiver

The LMMSE receiver is obtained by replacing the optimal detector in the optimum separated receiver by the LMMSE detector. We first derive the LMMSE estimator of the data symbols $\mathcal{B}_{t,k}$, after which we define the information about $\mathcal{B}_{t,k}$ provided from the LMMSE detector to the corresponding decoder. The LMMSE estimator of $\mathcal{B}_{t,k}$ would be obtained by regarding $\mathcal{B}_{t,k}$ as CSCG random variables $\tilde{\mathcal{B}}_{t,k}^{(L)} = \{\tilde{b}_{t,k,m}^{(L)} \in \mathbb{C} : \text{for all } m\}$ with $\mathbb{E}[\tilde{b}_{t,k,m}^{(L)} (\tilde{b}_{t,k,m'}^{(L)})^*] = (P/M)\delta_{m,m'}$ if the receiver had perfect CSI [20]. However, the posterior mean of $\tilde{\mathcal{B}}_{t,k}^{(L)}$ is nonlinear in the received vectors \mathcal{Y}_t since the channel model (12) includes multiplicative noise due to the influence of channel estimation errors. We approximate the channel model (12) by a channel model without multiplicative noise. We extract the term including channel estimation errors from the first term on the right-hand side of (12), and subsequently approximate the extracted one by an AWGN term with the same covariance. Therefore, the MIMO DS-CDMA channel in symbol period t postulated by the LMMSE detector is given as

$$\tilde{\mathbf{y}}_{l,t}^{(L)} = \frac{1}{\sqrt{L}} \sum_{k=1}^K \sum_{m=1}^M s_{l,t,k,m} \left(\hat{\mathbf{h}}_{k,m}^{\mathcal{I}_\tau} \tilde{b}_{t,k,m}^{(L)} + \tilde{\mathbf{w}}_{t,k,m}^{(L)} \right) + \tilde{\mathbf{n}}_{l,t}^{(L)}, \quad (22)$$

with $\tilde{\mathbf{n}}_{l,t}^{(L)} \sim \mathcal{CN}(\mathbf{0}, N_0 \mathbf{I}_N)$. In (22), $\hat{\mathbf{h}}_{k,m}^{\mathcal{I}_\tau}$ denotes the LMMSE channel estimates $\hat{\mathbf{h}}_{k,m}^{\mathcal{I}_\tau} = \int \mathbf{h}_{k,m} p(\mathcal{H}_k | \mathcal{I}_\tau) d\mathcal{H}_k$. The vectors $\{\tilde{\mathbf{w}}_{t,k,m}^{(L)} \in \mathbb{C}^N\}$ are independent CSCG random vectors with the covariance matrix $(P/M)\boldsymbol{\Sigma}_{k,m}$ for all t, k , and m , in which $\boldsymbol{\Sigma}_{k,m}$ denotes the covariance matrix of the channel estimation errors $\Delta \mathbf{h}_{k,m}^{\mathcal{I}_\tau} = \mathbf{h}_{k,m} - \hat{\mathbf{h}}_{k,m}^{\mathcal{I}_\tau}$, i.e., $\boldsymbol{\Sigma}_{k,m} = \mathbb{E}[\Delta \mathbf{h}_{k,m}^{\mathcal{I}_\tau} (\Delta \mathbf{h}_{k,m}^{\mathcal{I}_\tau})^H | \mathcal{I}_{\mathcal{T}_\tau}]$. Note that $\mathbb{E}[\Delta \mathbf{h}_{k,m}^{\mathcal{I}_\tau} b_{t,k,m} (\Delta \mathbf{h}_{k',m}^{\mathcal{I}_\tau} b_{t,k',m})^H | \mathcal{I}_{\mathcal{T}_\tau}] = \mathbf{O}$ for $k \neq k'$, since the data symbols $\{b_{t,k,m}\}$ are independent unbiased random variables. Thus, the same detector would be obtained even if the true LMMSE channel estimator was used instead of the suboptimal one.

Let $\tilde{\mathcal{Y}}_t^{(L)} = \{\tilde{\mathbf{y}}_{l,t}^{(L)} \in \mathbb{C}^N : \text{for all } l\}$ denote the received vectors postulated by the LMMSE detector in symbol period t . Furthermore, we write the postulated data symbols in symbol period t and the postulated data symbols except for $\tilde{\mathcal{B}}_{t,k}$ as $\tilde{\mathcal{B}}_t^{(L)} = \{\tilde{\mathcal{B}}_{t,k}^{(L)} : \text{for all } k\}$ and $\tilde{\mathcal{B}}_{t,\setminus\{k\}}^{(L)} = \{\tilde{\mathcal{B}}_{t,k'}^{(L)} : \text{for all } k' \neq k\}$, respectively. The linear estimator of $\mathcal{B}_{t,k}$ is given by the mean of $\tilde{\mathcal{B}}_{t,k}^{(L)}$ with respect to the posterior pdf

$$p(\tilde{\mathcal{B}}_{t,k}^{(L)} | \tilde{\mathcal{Y}}_t^{(L)}) = \mathcal{Y}_t, \mathcal{S}_t, \mathcal{I}_{\mathcal{T}_\tau} = \frac{\int p(\tilde{\mathcal{Y}}_t^{(L)} = \mathcal{Y}_t | \tilde{\mathcal{B}}_t^{(L)}, \mathcal{S}_t, \mathcal{I}_{\mathcal{T}_\tau}) p(\tilde{\mathcal{B}}_t^{(L)}) d\tilde{\mathcal{B}}_{t,\setminus\{k\}}^{(L)}}{\int p(\tilde{\mathcal{Y}}_t^{(L)} = \mathcal{Y}_t | \tilde{\mathcal{B}}_t^{(L)}, \mathcal{S}_t, \mathcal{I}_{\mathcal{T}_\tau}) p(\tilde{\mathcal{B}}_t^{(L)}) d\tilde{\mathcal{B}}_t^{(L)}}, \quad (23)$$

with

$$p(\tilde{\mathcal{Y}}_t^{(L)} | \tilde{\mathcal{B}}_t^{(L)}, \mathcal{S}_t, \mathcal{I}_{\text{tr}}) = \int p(\tilde{\mathcal{Y}}_t^{(L)} | \tilde{\mathcal{B}}_t^{(L)}, \mathcal{S}_t, \{\tilde{\mathbf{w}}_{t,k,m}^{(L)}\}, \{\hat{\mathbf{h}}_{k,m}^{\mathcal{I}_\tau}\}) \prod_{k=1}^K \prod_{m=1}^M \left\{ p(\tilde{\mathbf{w}}_{t,k,m}^{(L)}) d\tilde{\mathbf{w}}_{t,k,m}^{(L)} \right\}, \quad (24)$$

where $p(\tilde{\mathcal{Y}}_t^{(L)} | \tilde{\mathcal{B}}_t^{(L)}, \mathcal{S}_t, \{\tilde{\mathbf{w}}_{t,k,m}^{(L)}\}, \{\hat{\mathbf{h}}_{k,m}^{\mathcal{I}_\tau}\})$ represents the MIMO DS-CDMA channel (22) in the $t(> \tau)$ th symbol period postulated by the LMMSE detector.

The LMMSE detector provides the posterior pdf (23) to the decoder of the k th user. The transfer of (23) is equivalent to feeding the LMMSE estimate of $\mathcal{B}_{t,k}$ and the covariance matrix of its estimation errors. We remark that our LMMSE receiver is equivalent to the one proposed by Evans and Tse [34] for $N = M = 1$.

The spectral efficiency of the LMMSE receiver is given by

$$C_L = \frac{K}{L} \left(1 - \frac{\tau}{T_c}\right) \sum_{k=1}^K I(\mathcal{B}_{t,k}; \tilde{\mathcal{B}}_{t,k}^{(L)} | \mathcal{I}_{\mathcal{T}}, \mathcal{S}_t). \quad (25)$$

In (25), the mutual information $I(\mathcal{B}_{t,k}; \tilde{\mathcal{B}}_{t,k}^{(L)} | \mathcal{I}_{\mathcal{T}}, \mathcal{S}_t)$ is characterized by the equivalent channel between user k and the corresponding decoder for the LMMSE receiver,

$$p(\tilde{\mathcal{B}}_{t,k}^{(L)} | \mathcal{B}_{t,k}, \mathcal{S}_t, \mathcal{I}_{\mathcal{T}_\tau}) = \int p(\tilde{\mathcal{B}}_{t,k}^{(L)} | \tilde{\mathcal{Y}}_t^{(L)} = \mathcal{Y}_t, \mathcal{S}_t, \mathcal{I}_{\mathcal{T}_\tau}) p(\mathcal{Y}_t | \mathcal{B}_{t,k}, \mathcal{S}_t, \mathcal{I}_{\mathcal{T}_\tau}) d\mathcal{Y}_t, \quad (26)$$

where $p(\mathcal{Y}_t | \mathcal{B}_{t,k}, \mathcal{S}_t, \mathcal{I}_{\mathcal{T}_\tau})$ is defined in the same manner as in (19).

V. MAIN RESULTS

A. Large-System Analysis

In order to evaluate the spectral efficiencies of the four receivers listed in Table I, we consider the large-system limit, in which the number of users K and the spreading factor L tend to infinity while the system load $\beta = K/L$ and the number of transmit and receive antennas are kept constant. More precisely, we evaluate the spectral efficiencies by analyzing asymptotic properties of the equivalent channel between a finite number of users and their decoders. We write a finite number of users as \mathcal{K} , which is a finite subset of $\{1, \dots, K\}$, and consider the large-system limit $\lim_{K,L \rightarrow \infty}$ in which K and L tend to infinity with β and \mathcal{K} fixed.

We focus on substage k within stage t of the joint CE-MUDD. A finite subset of users \mathcal{K} is chosen from the set $\{k, \dots, K\}$ of users decoded in the current and following substages, i.e., $\mathcal{K} \cap \{1, \dots, k-1\} = \emptyset$. Let $\mathcal{B}_{t,\mathcal{K}} = \{\mathcal{B}_{t,k} : k \in \mathcal{K}\}$ and $\tilde{\mathcal{B}}_{t,\mathcal{K}} = \{\tilde{\mathcal{B}}_{t,k} : k \in \mathcal{K}\}$ denote the data symbols and the postulated data symbols for a finite subset \mathcal{K} of users in symbol period t , respectively. The equivalent channel $p(\tilde{\mathcal{B}}_{t,\mathcal{K}} | \mathcal{B}_{t,\mathcal{K}}, \mathcal{B}_{t,[1,k]}, \mathcal{I}_{\mathcal{T}_{t-1}}, \mathcal{S}_t, \mathcal{H})$ between the users in \mathcal{K} and their decoders, defined in the same manner as in (18), is expected to be self-averaging with respect to the spreading sequences \mathcal{S}_t in the large-system limit: The equivalent channel converges to the one averaged over the spreading sequences for almost all realizations of the data symbols $\mathcal{B}_{t,\mathcal{K}}$, the data symbols $\mathcal{B}_{t,[1,k]}$ decoded in the preceding substages, the known information $\mathcal{I}_{\mathcal{T}_{t-1}}$ in symbol periods $t' \in \mathcal{T}_{t-1}$, and the channel vectors \mathcal{H} in the large-system limit. The self-averaging property has been proved for linear receivers [15], [34] and for the constrained capacity of CDMA systems with perfect CSI at the receiver [47], [54]. However, it is an open challenging problem to show whether the self-averaging property holds for general receivers. Therefore, we postulate the self-averaging property.

Assumption 1. *The conditional distribution of $\tilde{\mathcal{B}}_{t,\mathcal{K}}$ given $\mathcal{B}_{t,\mathcal{K}}$, $\mathcal{B}_{t,[1,k]}$, $\mathcal{I}_{\mathcal{T}_{t-1}}$, \mathcal{S}_t , and \mathcal{H} converges in law to a conditional distribution that is independent of \mathcal{S}_t in the large-system limit.*

Another crucial assumption is replica symmetry (RS) [18]. See Appendix C for a formal definition of the RS assumption. In order to present an intuitive understanding of the RS assumption, let us consider an iterative MUD algorithm based on belief propagation (BP) [55]. Roughly speaking, the algorithm iteratively calculates a local minimum solution of an object function, called free energy, in the large-system limit. The global minimum solution of the free energy corresponds to the optimal one. The RS assumption implies that the free energy has the unique stable solution or at most two stable solutions. If the free energy has many stable solutions, replica-symmetry breaking (RSB) should be assumed [39].

Two necessary conditions for checking the RS assumption are known: de Almeida-Thouless (AT) stability [56] and the non-negative-entropy condition [39]. The AT condition is a necessary condition for the stability of RS solutions. The non-negative-entropy condition is a necessary condition under which the entropy for the posterior distribution of replicated random variables is non-negative when the random variables are discrete. Note that the non-negative-entropy condition is not defined for the no-CSI case, since the channel vectors are not discrete. See Appendix D for details. The RS solution for the individually-optimal (IO) receiver with perfect CSI, which corresponds to the optimum separated receiver in this paper, has been proved to satisfy the AT stability condition [18], [57]. Furthermore, that solution satisfies the non-negative-entropy condition derived in [18, Equation (69)] for CDMA systems with perfect CSI². These results may imply that the RS assumption is valid for the IO receiver. In fact, several rigorous studies have shown that this statement is partially correct: Nishimori [57] has used a gauge theory to show that the free energy has no complicated structure for the IO receiver. See Appendix C for the precise statement. Korada and Montanari [47] have proved that the RS assumption is correct if the free energy under the RS assumption has the unique stable solution. Thus, we postulate the RS assumption in this paper.

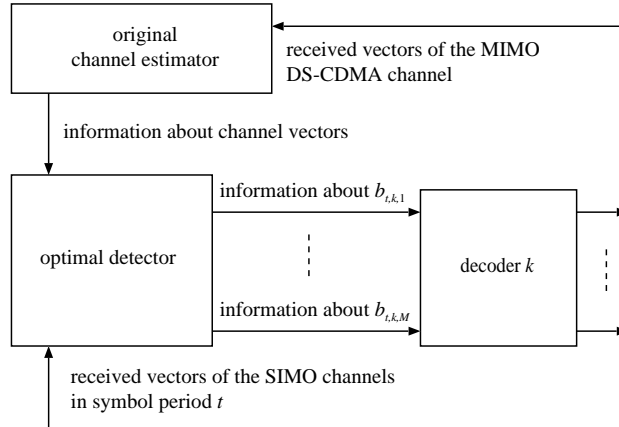
We show under these assumptions that the randomly-spread MIMO DS-CDMA channel with no CSI is decoupled into a bank of single-user single-input multiple-output (SIMO) channels with no CSI

$$\underline{\mathbf{y}}_{t,k,m} = \mathbf{h}_{k,m} u_{t,k,m} + \underline{\mathbf{n}}_{t,k,m}, \quad (27)$$

where $\underline{\mathbf{n}}_{t,k,m} \sim \mathcal{CN}(0, \sigma_t^2 \mathbf{I}_N)$ denotes AWGN with variance σ_t^2 . The equivalent channel between the users in \mathcal{K} and their decoders looks like a bundle of the single-user SIMO channels (27) with the *original* channel estimator (11). Furthermore, MAI to the users in \mathcal{K} converges towards MAI from the single-user SIMO channels (27) with no CSI in the large-system limit. Our result is an extension of the decoupling results for randomly-spread MIMO DS-CDMA channels with perfect CSI at the receiver [11], [20] to the no-CSI case at the receiver. The difference from the previous decoupling results appears in the receiver structure for the SIMO channel (27), which depends on the receiver structure of the original MIMO DS-CDMA systems.

The equivalent channel between the users in \mathcal{K} and the corresponding decoders is characterized by two receivers for the decoupled SIMO channels (27), i.e., a receiver for the users in \mathcal{K} and another receiver for the users who interfere to the users in \mathcal{K} . In the former receiver joint decoding of all data streams for each user is performed. The

² It is straightforward to prove that the non-negative-entropy condition [18, Equation (69)] is satisfied for the IO receiver, although the proof was not presented in [18].


 Fig. 4. Receiver for the users in \mathcal{K} .

receiver consists of the original LMMSE channel estimator providing the marginal posterior pdfs (11), an optimal detector, and the decoder of user k (See Fig. 4). The latter receiver performs per-stream decoding, and is to be used in the decoupled expression for quantifying the strength of MAI from outside \mathcal{K} . The receiver consists of another LMMSE channel estimator, the optimal detector, and the per-stream decoders (See Fig. 5). Note that the information $\mathcal{B}_{t,[1,k]}$ in the preceding substages does not appear explicitly in the two receivers. It affects the decoupling results via the noise variance σ_t^2 .

Definition 1 (Receiver for the users in \mathcal{K}). *In symbol period $t (> \tau)$, the optimal detector uses the information about the received vectors $\underline{\mathbf{y}}_{t,k} = \{\mathbf{y}_{t,k,m} : \text{for all } m\}$ of the single-user SIMO channel (27) in symbol period t and about the posterior pdf (11) provided by the original channel estimator to construct the posterior pdf*

$$p(\mathcal{B}_{t,k} | \underline{\mathbf{y}}_{t,k}, \mathcal{I}_{\mathcal{T}_{t-1}}) = \frac{\prod_{m=1}^M p(\mathbf{y}_{t,k,m} | \mathbf{h}_{k,m}, b_{t,k,m}) p(\mathcal{H}_k | \mathcal{I}_{\mathcal{T}_{t-1}}) p(\mathcal{B}_{t,k})}{\int \prod_{m=1}^M p(\mathbf{y}_{t,k,m} | \mathbf{h}_{k,m}, b_{t,k,m}) p(\mathcal{H}_k | \mathcal{I}_{\mathcal{T}_{t-1}}) p(\mathcal{B}_{t,k}) d\mathcal{H}_k d\mathcal{B}_{t,k}}, \quad (28)$$

where $p(\mathbf{y}_{t,k,m} | \mathbf{h}_{k,m}, b_{t,k,m})$ represents the single-user SIMO channel (27). Subsequently, the optimal detector sends the posterior pdf (28) towards the decoder of user k .

Definition 2 (Receiver for the interfering users). *The LMMSE channel estimator constructs the posterior pdf $p(\mathbf{h}_{k,m} | \underline{\mathcal{I}}_{\mathcal{T}_{t-1},k,m})$ of $\mathbf{h}_{k,m}$ by utilizing the information $\underline{\mathcal{I}}_{\mathcal{T}_{t-1},k,m} = \{\underline{\mathcal{I}}_{t',k,m} : t' \in \mathcal{T}_{t-1}\}$ in the preceding stages, in which $\underline{\mathcal{I}}_{t',k,m} = \{u_{t',k,m}, \mathbf{y}_{t',k,m}\}$ denotes the information about the input symbol $u_{t',k,m}$ and the received vector $\mathbf{y}_{t',k,m}$ in the single-user SIMO channel (27). Subsequently, the posterior pdf $p(\mathbf{h}_{k,m} | \underline{\mathcal{I}}_{\mathcal{T}_{t-1},k,m})$ is sent towards the optimal detector.*

In symbol period $t (> \tau)$, the optimal detector utilizes the information about the received vector $\underline{\mathbf{y}}_{t,k,m}$ and $p(\mathbf{h}_{k,m} | \underline{\mathcal{I}}_{\mathcal{T}_{t-1},k,m})$ provided by the channel estimator for the SIMO channel (27), and constructs the posterior pdf

$$p(b_{t,k,m} | \underline{\mathbf{y}}_{t,k,m}, \underline{\mathcal{I}}_{\mathcal{T}_{t-1},k,m}) = \int p(b_{t,k,m}, \mathbf{h}_{k,m} | \underline{\mathbf{y}}_{t,k,m}, \underline{\mathcal{I}}_{\mathcal{T}_{t-1},k,m}) d\mathbf{h}_{k,m}, \quad (29)$$

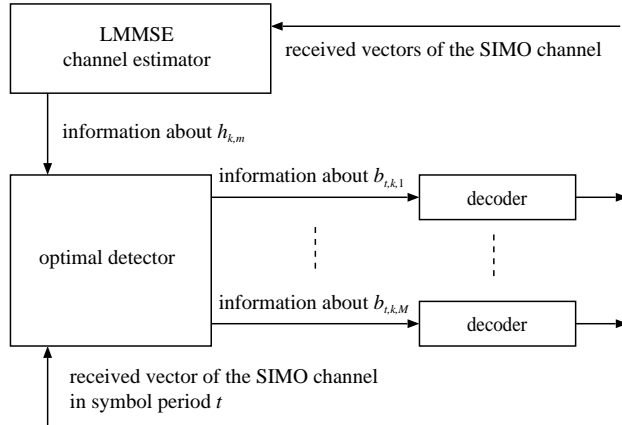


Fig. 5. Receiver for the users interfering to the users in \mathcal{K} .

with

$$p(b_{t,k,m}, \mathbf{h}_{k,m} | \underline{\mathbf{y}}_{t,k,m}, \underline{\mathcal{I}}_{\mathcal{T}_{t-1},k,m}) = \frac{p(\underline{\mathbf{y}}_{t,k,m} | \mathbf{h}_{k,m}, b_{t,k,m}) p(b_{t,k,m}) p(\mathbf{h}_{k,m} | \underline{\mathcal{I}}_{\mathcal{T}_{t-1},k,m})}{\int p(\underline{\mathbf{y}}_{t,k,m} | \mathbf{h}_{k,m}, b_{t,k,m}) p(b_{t,k,m}) p(\mathbf{h}_{k,m} | \underline{\mathcal{I}}_{\mathcal{T}_{t-1},k,m}) db_{t,k,m} d\mathbf{h}_{k,m}}. \quad (30)$$

Subsequently, the optimal detector sends the posterior pdf (29) towards the corresponding per-stream decoder.

We summarize several symbols used for claiming the main results. The LMMSE estimate of $\mathbf{h}_{k,m}$ for the single-user SIMO channel (27) is denoted by

$$\hat{\underline{\mathbf{h}}}_{k,m}^{\mathcal{T}_{t-1}} = \int \mathbf{h}_{k,m} p(\mathbf{h}_{k,m} | \underline{\mathcal{I}}_{\mathcal{T}_{t-1},k,m}) d\mathbf{h}_{k,m}. \quad (31)$$

When $\sigma_{t'}^2 = \sigma_{\text{tr}}^2$ for $t' \in \mathcal{T}_{t-1}$, the covariance matrix of the LMMSE estimation error $\Delta \hat{\underline{\mathbf{h}}}_{k,m}^{\mathcal{T}_{t-1}} = \mathbf{h}_{k,m} - \hat{\underline{\mathbf{h}}}_{k,m}^{\mathcal{T}_{t-1}}$ is given by $\xi^2(\sigma_{\text{tr}}^2, t-1) \mathbf{I}_N$ [58], with

$$\xi^2(\sigma_{\text{tr}}^2, t-1) = \frac{\sigma_{\text{tr}}^2}{(t-1)(P/M) + \sigma_{\text{tr}}^2}, \quad (32)$$

where $(t-1)$ corresponds to the length of the *training* phase in stage t . The estimate $\hat{\underline{\mathbf{h}}}_{k,m}^{\mathcal{T}_{t-1}}$ is a CSCG random vector with the covariance matrix $(1 - \xi^2(\sigma_{\text{tr}}^2, t-1)) \mathbf{I}_N$, since $\hat{\underline{\mathbf{h}}}_{k,m}^{\mathcal{T}_{t-1}}$ and $\Delta \hat{\underline{\mathbf{h}}}_{k,m}^{\mathcal{T}_{t-1}}$ are uncorrelated. Furthermore, we write the posterior mean of $b_{t,k,m}$ given $\underline{\mathbf{y}}_{t,k,m}$ and $\underline{\mathcal{I}}_{\mathcal{T}_{t-1},k,m}$ as

$$\langle b_{t,k,m} \rangle = \int b_{t,k,m} p(b_{t,k,m}, \mathbf{h}_{k,m} | \underline{\mathbf{y}}_{t,k,m}, \underline{\mathcal{I}}_{\mathcal{T}_{t-1},k,m}) db_{t,k,m} d\mathbf{h}_{k,m}. \quad (33)$$

Finally, let $\underline{C}_t(\sigma_{\text{tr}}^2(t-1), \sigma_t^2)$ denote the conditional mutual information between the data symbol $b_{t,1,1}$ and the received vector $\underline{\mathbf{y}}_{t,1,1}$ for the SIMO channel (27) given the information $\underline{\mathcal{I}}_{\mathcal{T}_{t-1},1,1}$, i.e.,

$$\underline{C}_t(\sigma_{\text{tr}}^2(t-1), \sigma_t^2) = I(b_{t,1,1}; \underline{\mathbf{y}}_{t,1,1} | \underline{\mathcal{I}}_{\mathcal{T}_{t-1},1,1}), \quad (34)$$

with $\sigma_{t'}^2 = \sigma_{\text{tr}}^2(t-1)$ for $t' \in \mathcal{T}_{t-1}$. The conditional mutual information corresponds to the spectral efficiency of the receiver defined in Definition 2 for the single-user SIMO channel (27).

Remark 2. We shall discuss the relationship between the RSB assumption and the decoupling result. Under the RSB assumption, the equivalent channel would still be decoupled into single-user channels. However, the noise in the SIMO channel (27) would be non-Gaussian. This implies that if the RS assumption is not correct a naive intuition is wrong: MAI should converge to Gaussian noise due to the central limit theorem. In fact, the RSB assumption should be considered if the jointly-optimal (JO) receiver is used [18], [59].

B. Optimum Separated Receiver

It is the main part in our derivation to analyze the spectral efficiency (21) of the optimum separated receiver in the large-system limit. The spectral efficiencies of the one-shot CE-MUDD and the joint CE-MUDD can be straightforwardly derived from the result for the optimum separated receiver. Thus, we first present an analytical expression for the spectral efficiency of the optimum separated receiver. Analytical formulas for the spectral efficiencies of the one-shot CE-MUDD and the joint CE-MUDD will be presented in Section V-C and Section V-D.

Let $\tilde{\mathcal{B}}_{t,k} = \{\tilde{b}_{t,k,m} \in \mathbb{C} : \text{for all } m\} \sim p(\mathcal{B}_{t,k} | \mathcal{Y}_{t,k}, \mathcal{I}_{\mathcal{T}_\tau})$, defined by (28), denote random variables representing the information about $\mathcal{B}_{t,k}$, provided by the optimal detector. The equivalent channel between user k and the corresponding decoder is given by

$$p(\tilde{\mathcal{B}}_{t,k} | \mathcal{B}_{t,k}, \mathcal{H}_k, \mathcal{I}_{\mathcal{T}_\tau}) = \int p(\mathcal{B}_{t,k} = \tilde{\mathcal{B}}_{t,k} | \mathcal{Y}_{t,k}, \mathcal{I}_{\mathcal{T}_\tau}) \prod_{m=1}^M \left\{ p(\underline{\mathbf{y}}_{t,k,m} | \mathbf{h}_{k,m}, b_{t,k,m}) d\underline{\mathbf{y}}_{t,k,m} \right\}. \quad (35)$$

Proposition 1. Assume that Assumption 1 and the RS assumption hold. Then,

$$\lim_{K, L \rightarrow \infty} p(\tilde{\mathcal{B}}_{t,\mathcal{K}} | \mathcal{B}_{t,\mathcal{K}}, \mathcal{I}_{\mathcal{T}_\tau}, \mathcal{S}_t, \mathcal{H}) = \prod_{k \in \mathcal{K}} p(\tilde{\mathcal{B}}_{t,k} = \tilde{\mathcal{B}}_{t,k} | \mathcal{B}_{t,k}, \mathcal{H}_k, \mathcal{I}_{\mathcal{T}_\tau}) \quad \text{in law}, \quad (36)$$

where $\sigma_t^2 = \sigma_c^2$ for $t \in \mathcal{C}_{\tau+1}$ is given by a solution to the fixed-point equation

$$\sigma_c^2 = N_0 + \lim_{K \rightarrow \infty} \frac{\beta}{K} \sum_{k \notin \mathcal{K}} \left\{ \frac{P \xi^2 \sigma_c^2}{(P/M) \xi^2 + \sigma_c^2} + \frac{M}{N} \left(\frac{\sigma_c^2}{(P/M) \xi^2 + \sigma_c^2} \right)^2 \mathbb{E} \left[\|\hat{\underline{\mathbf{h}}}_{k,1}^{\mathcal{T}_\tau}\|^2 | b_{t,k,1} - \langle b_{t,k,1} \rangle|^2 \right] \right\}, \quad (37)$$

with $\hat{\underline{\mathbf{h}}}_{k,1}^{\mathcal{T}_\tau}$ and $\xi^2 = \xi^2(\sigma_{\text{tr}}^2(\tau), \tau)$ give by (31) and (32), respectively. In evaluating (37), $\sigma_{t'}^2 = \sigma_{\text{tr}}^2(\tau)$ for $t' \in \mathcal{T}_\tau$ is given as the unique solution to the fixed-point equation

$$\sigma_{\text{tr}}^2(\tau) = N_0 + \beta P \xi^2(\sigma_{\text{tr}}^2(\tau), \tau). \quad (38)$$

If (37) has multiple solutions, one should choose the solution minimizing the following quantity

$$\lim_{K \rightarrow \infty} \frac{\beta M}{K} \sum_{k \notin \mathcal{K}} I(b_{t,k,1}, \mathbf{h}_{k,1}; \underline{\mathbf{y}}_{t,k,1} | \underline{\mathcal{I}}_{\mathcal{T}_\tau, k, 1}) + ND(N_0 | \sigma_c^2). \quad (39)$$

The derivation of Proposition 1 is deferred to the end of this section. The fixed-point equation (38) was originally derived in [34] by using *rigorous* random matrix theory, while we have used the replica method. The second term of the right-hand side of (37) corresponds to MAI from the users who do not belong to the users in \mathcal{K} . This expression implies that the asymptotic MAI becomes the sum of interference from $(K - |\mathcal{K}|)M$ independent SIMO channels (27). Furthermore, each interference is represented by two effects: The first term within the curly brackets

in (37) corresponds to contribution from channel estimation errors, and the second term corresponds to MAI from the single-user SIMO channel with perfect CSI at the receiver,

$$\underline{z}_{t,k,m} = \hat{\underline{h}}_{k,m}^{\mathcal{T}_\tau} b_{t,k,m} + \underline{v}_{t,k,m}, \quad (40)$$

with $\underline{v}_{t,k,m} \sim \mathcal{CN}(\mathbf{0}, [(P/M)\xi^2 + \sigma_c^2]\mathbf{I}_N)$. The received vector $\underline{z}_{t,k,m}$ conditioned on $\underline{\mathcal{I}}_{\mathcal{T}_\tau, k, m}$ and $b_{t,k,m}$ is statistically equivalent to $\underline{y}_{t,k,m}$ in (27) under the same conditions, due to $|b_{t,k,m}|^2 = P/M$ with probability one. We remark that this interpretation holds only for phase-shift keying modulations.

The fixed-point equation (37) can have multiple solutions. The criterion (39) to select the correct solution corresponds to the conditional mutual information $L^{-1}I(\mathcal{B}_t, \mathcal{H}; \mathcal{Y}_t | \mathcal{S}_t, \mathcal{I}_{\mathcal{T}_\tau})$ in the large-system limit, although its proof is omitted. This phenomenon is related to the so-called phase coexistence in statistical mechanics. For the details in the context of wireless communications, see [18], [20]. The existence of multiple solutions implies that the asymptotic performance discontinuously changes at a critical point. This asymptotic result predicts that the performance sharply changes in the neighborhood of the critical point for finite-sized systems.

Proposition 1 implies that the equivalent channel between the users in \mathcal{K} and their decoders is not fully decoupled into single-user channels, since the channel estimator in Definition 1 utilizes the information $\mathcal{I}_{\mathcal{T}_\tau}$ depending on all users. This is the main difference between the cases of perfect CSI and of no CSI. The following proposition indicates that the equivalent channel is decomposed in terms of the spectral efficiency.

Proposition 2. *Assume that Assumption 1 and the RS assumption hold. Then, the spectral efficiency (21) of the optimum separated receiver converges to the spectral efficiency of the optimum separated receiver for the single-user SIMO channel (27) in the large-system limit,*

$$\lim_{K, L \rightarrow \infty} C_{\text{sep}} = \beta M \left(1 - \frac{\tau}{T_c}\right) \underline{C}_{\tau+1}(\sigma_{\text{tr}}^2(\tau), \sigma_c^2), \quad (41)$$

where $\underline{C}_{\tau+1}(\sigma_{\text{tr}}^2(\tau), \sigma_c^2)$ is given by (34). In evaluating the right-hand side, $\sigma_{\text{tr}}^2(\tau)$ is given as the solution to the fixed-point equation (38). On the other hand, σ_c^2 is given as a solution to the fixed-point equation (37). If (37) has multiple solutions, the solution minimizing (39) should be chosen.

Proof of Proposition 2: We use a technical lemma, presented in the end of this section, to prove Proposition 2. See Appendix F for the details. ■

This result implies that the asymptotic equivalent channel between user k and the associated decoder looks like the SIMO channel (27) in terms of the spectral efficiency. In other words, the performance loss caused by coding the data streams for each user separately vanishes in the large-system limit, as shown in [11] for the perfect-CSI case. We remark that it is relatively easy to evaluate (41) numerically, by using $\underline{y}_{t,k,m} \sim \underline{z}_{t,k,m}$ in (40) conditioned on $\underline{\mathcal{I}}_{\mathcal{T}_\tau, k, m}$ and $b_{t,k,m}$.

The prefactor $(1 - \tau/T_c)$ corresponds to the rate loss due to the transmission of pilot symbols. The spectral efficiency $\underline{C}_{\tau+1}(\sigma_{\text{tr}}^2(\tau), \sigma_c^2)$ grows with the increase of τ since the channel estimation improves, while the prefactor decreases. Thus, there is the optimal length of the training phase to maximize the spectral efficiency of the optimum separated receiver, as shown in Section VI.

We shall present a sketch of the derivation of Proposition 1. The derivation of Proposition 1 consists of two parts: the analysis of the channel estimator and the analysis of the optimal detector. The goal in the analysis of the channel estimator is to prove the following lemma.

Lemma 1. *Let $\mathcal{H}_k^{\{a\}} = \{\mathbf{h}_{k,m}^{\{a\}} : \text{for all } m\}$ be replicas of the channel vectors \mathcal{H}_k for $a \in \{1, \dots, n\}$, with a natural number n : $\{\mathcal{H}_k^{\{a\}}\}$ are independently drawn from $p(\mathcal{H}_k)$ for all k . Suppose that $\{\mathcal{A}_k\}$ are mutually disjoint subsets of $\{2, 3, \dots, n\}$ for all $k \in \mathcal{K}$. We define a random variable $X_k(\mathcal{H}_k^{\{1\}}, \mathcal{I}_{\mathcal{T}_\tau}; \Theta) \in \mathbb{R}$ with a set Θ of fixed parameters as*

$$X_k(\mathcal{H}_k^{\{1\}}, \mathcal{I}_{\mathcal{T}_\tau}; \Theta) = \int f_k(\mathcal{H}_k^{\{1\}}, \mathcal{H}_k^{\mathcal{A}_k}; \Theta) \prod_{a \in \mathcal{A}_k} \left\{ p(\mathcal{H}_k^{\{a\}} | \mathcal{I}_{\mathcal{T}_\tau}) d\mathcal{H}_k^{\{a\}} \right\}, \quad (42)$$

with $\mathcal{H}_k^{\mathcal{A}_k} = \{\mathcal{H}_k^{\{a\}} : a \in \mathcal{A}_k\}$ denoting the set of the replicated channel vectors associated with indices \mathcal{A}_k . In (42), $f_k(\mathcal{H}_k^{\{1\}}, \mathcal{H}_k^{\mathcal{A}_k}; \Theta) \in \mathbb{R}$ is a deterministic function of $\mathcal{H}_k^{\{1\}}$, $\mathcal{H}_k^{\mathcal{A}_k}$, and Θ . Suppose that the joint moment generating function of $\{X_k(\mathcal{H}_k^{\{1\}}, \mathcal{I}_{\mathcal{T}_\tau}; \Theta) : k \in \mathcal{K}\}$ exists in the neighborhood of the origin. Then,

$$\lim_{K, L \rightarrow \infty} p(\{X_k : k \in \mathcal{K}\}) = \prod_{k \in \mathcal{K}} p(\underline{X}_k = X_k), \quad (43)$$

in which

$$\underline{X}_k(\mathcal{H}_k^{\{1\}}, \underline{\mathcal{I}}_{\mathcal{T}_\tau, k}; \Theta) = \int f_k(\mathcal{H}_k^{\{1\}}, \mathcal{H}_k^{\mathcal{A}_k}; \Theta) \prod_{a \in \mathcal{A}_k} \prod_{m=1}^M \left\{ p(\mathbf{h}_{k,m}^{\{a\}} | \underline{\mathcal{I}}_{\mathcal{T}_\tau, k, m}) d\mathbf{h}_{k,m}^{\{a\}} \right\}, \quad (44)$$

with $\underline{\mathcal{I}}_{\mathcal{T}_\tau, k} = \{\underline{\mathcal{I}}_{\mathcal{T}_\tau, k, m} : \text{for all } m\}$. In (43), X_k and \underline{X}_k are abbreviations of (42) and (44). In evaluating (44), $\sigma_t^2 = \sigma_{\text{tr}}^2(\tau)$ for $t \in \mathcal{T}_\tau$ is given by the solution to the fixed-point equation (38).

Proof of Lemma 1: See Appendix B. ■

Lemma 1 is used to prove that MAI to the users in \mathcal{K} is self-averaging with respect to $\mathcal{I}_{\mathcal{T}_\tau}$ under Assumption 1. The natural number n corresponds to the number of replicas introduced in the analysis of the optimal detector. The details of the derivation of Proposition 1 are summarized in Appendix D.

C. One-Shot CE-MUDD

We present an analytical expression for the spectral efficiency (20) of the one-shot CE-MUDD. The expression is straightforwardly obtained from Proposition 2.

Proposition 3. *Suppose that Assumption 1 and the RS assumption hold. Then, the spectral efficiency (20) of the one-shot CE-MUDD is given by*

$$\lim_{K, L \rightarrow \infty} C_{\text{one}} = \beta M \left(1 - \frac{\tau}{T_c} \right) \int_0^1 \underline{C}_{\tau+1}(\sigma_{\text{tr}}^2(\tau), \sigma_c^2(\kappa)) d\kappa, \quad (45)$$

in the large-system limit, in which $\underline{C}_{\tau+1}(\sigma_{\text{tr}}^2(\tau), \sigma_c^2(\kappa))$ is defined as (34). In evaluating the integrand, $\sigma_t^2 = \sigma_{\text{tr}}^2(\tau)$ for $t \in \mathcal{T}_\tau$ is given as the solution to the fixed-point equation (38). On the other hand, $\sigma_c^2(\kappa)$ satisfies the fixed-point equation

$$\sigma_c^2(\kappa) = N_0 + \frac{\beta P \xi^2 \sigma_c^2(\kappa)}{(P/M)\xi^2 + \sigma_c^2(\kappa)} + \frac{\beta(1-\kappa)M}{N} \left(\frac{\sigma_c^2(\kappa)}{(P/M)\xi^2 + \sigma_c^2(\kappa)} \right)^2 \mathbb{E} \left[\|\hat{\mathbf{h}}_{1,1}\|^2 |b_{\tau+1,1,1} - \langle b_{\tau+1,1,1} \rangle|^2 \right], \quad (46)$$

with $\hat{\mathbf{h}}_{1,1} = \hat{\mathbf{h}}_{1,1}^{\mathcal{T}_\tau}$ and $\xi^2 = \xi^2(\sigma_{\text{tr}}^2(\tau), \tau)$ given by (31) and (32), respectively. If the fixed-point equation (46) has multiple solutions, one should choose the solution minimizing the following quantity

$$\beta M \left[\kappa I(\mathbf{h}_{1,1}; \mathbf{y}_{\tau+1,1,1} | b_{\tau+1,1,1}, \underline{\mathcal{I}}_{\mathcal{T}_\tau,1,1}) + (1 - \kappa) I(b_{\tau+1,1,1}, \mathbf{h}_{1,1}; \mathbf{y}_{\tau+1,1,1} | \underline{\mathcal{I}}_{\mathcal{T}_\tau,1,1}) \right] + ND(N_0 \| \sigma_c^2(\kappa)). \quad (47)$$

The integrand in (45) is equal to the asymptotic spectral efficiency of the optimum separated receiver for a MIMO DS-CDMA system in which $(1 - \kappa)K$ users send data symbols and κK users transmit symbols known to the receiver in symbol period $\tau + 1$. The symbols known to the receiver corresponds to the data symbols decoded successfully in the preceding substages. The factor $1 - \kappa$ appears in the last term of the right-hand side of (46), since the system load decreases effectively as successive decoding proceeds.

Proof of Proposition 3: The quantity $C_{\tau+1,k}$ in the spectral efficiency (20) of the one-shot CE-MUDD corresponds to the spectral efficiency of the optimum separated receiver for a MIMO DS-CDMA system in which the first $(k - 1)$ users transmit known symbols $\{p_{t,k',m}\}$ for $k' = 1, \dots, k - 1$ in symbol period $t (> \tau)$. We have already evaluated the spectral efficiency in Proposition 2 when all users transmit data symbols in symbol period t . We do not use the statistical property of each data symbol $b_{t,k,m}$ in the derivation of Proposition 2. Furthermore, the derivation still holds even if the noise variance σ_t^2 for the single-user SIMO channel (27) depends on k . For some natural number K_0 , consider the large-system limit in which K , L , and K_0 tend to infinity while $\beta = K/L$ and $\kappa_0 = K_0/K$ are kept constant. Replacing the prior of $b_{t,k',m}$ for $k' = 1, \dots, k - 1$ by $\text{Prob}(b_{t,k',m} = p_{t,k',m}) = 1$ and $\text{Prob}(b_{t,k',m} \neq p_{t,k',m}) = 0$ in substage $k \geq K_0$, we find that the fixed-point equation (37) reduces to (46) with $\kappa = k/K$, since $\mathbb{E}[\|\mathbf{h}_{k',1}^{\mathcal{T}_\tau}\|^2 | b_{t,k',1} - \langle b_{t,k',1} \rangle]^2] = 0$ for $k' = 1, \dots, k - 1$. Similarly, the quantity (39) for $t = \tau + 1$ reduces to (47). These results imply

$$C_{\text{one}} = \beta \left(1 - \frac{\tau}{T_c} \right) \left[\frac{1}{K} \sum_{k=1}^{K_0-1} C_{t,k} + \frac{M}{K} \sum_{k=K_0}^K \underline{C}_{\tau+1}(\sigma_{\text{tr}}^2(\tau), \sigma_c^2(\kappa)) \right], \quad (48)$$

in the large-system limit. In evaluating the second term, $\sigma_{\text{tr}}^2(\tau)$ is given as the solution to the fixed-point equation (38). On the other hand, $\sigma_c^2(\kappa)$ satisfies the fixed-point equation (46). If the latter fixed-point equation has multiple solutions, the solution minimizing (47) should be chosen.

The definition of the Riemann integral implies that $K^{-1} \sum_{k=K_0}^K$ in the second term of (48) becomes $\int_{\kappa_0}^1 d\kappa$ in the large-system limit. Therefore, we arrive at Proposition 3 by taking $\kappa_0 \rightarrow 0$, since the first term in (48) vanishes in that limit. ■

D. Joint CE-MUDD

We evaluate the spectral efficiency (16) of the joint CE-MUDD in the large-system limit. An analytical expression of the spectral efficiency (16) is immediately obtained from Proposition 3.

Proposition 4. *Suppose that Assumption 1 and the RS assumption hold. Then, the spectral efficiency (16) of the joint CE-MUDD is given by*

$$\lim_{K,L \rightarrow \infty} C_{\text{joint}} = \frac{\beta M}{T_c} \sum_{t=\tau+1}^{T_c} \int_0^1 \underline{C}_t(\sigma_{\text{tr}}^2(t-1), \sigma_c^2(\kappa)) d\kappa, \quad (49)$$

in the large-system limit, in which $\underline{C}_t(\sigma_{\text{tr}}^2(t-1), \sigma_c^2(\kappa))$ is defined as (34). In evaluating the integrand, $\sigma_{\text{tr}}^2(t-1)$ is given as the solution to the fixed point equation (38) with $\tau = t-1$. On the other hand, $\sigma_c^2(\kappa)$ satisfies the fixed-point equation (46) with $\hat{\mathbf{h}}_{1,1} = \hat{\mathbf{h}}_{1,1}^{\mathcal{T}_{t-1}}$ and $\xi^2 = \xi^2(\sigma_{\text{tr}}^2(t-1), t-1)$ given by (31) and (32), respectively. If the fixed-point equation (46) has multiple solutions, the solution minimizing (47) should be chosen.

Derivation of Proposition 4: The quantity $C_{t,k}$ in (16) corresponds to the spectral efficiency of the one-shot CE-MUDD for the MIMO DS-CDMA channel (2) with the first $t-1$ symbol periods as a training phase. Applying Proposition 3 with $\tau = t-1$ to (16), we obtain (49). ■

The spectral efficiency (49) does not decrease with each increase of τ . Furthermore, the integral in (49) is equal to zero for $t=1$, since $t=1$ implies no pilots. Therefore, the spectral efficiency (49) is maximized at $\tau=0$ and $\tau=1$ if the integral in (49) is strictly positive for $t \geq 2$. This observation implies that the joint CE-MUDD can reduce the training overhead significantly.

Remark 3. We have so far considered the equal power case. One interesting issue would be temporal power allocation. It is straightforward to extend Proposition 4 to the temporally unequal power case. Intuitively, allocating much power to around the beginning of one fading block improves the accuracy of the channel estimates, while power used for transmission of data symbols around the end decreases. Thus, it is not straightforward to find the temporally optimal power allocation. This power allocation issue is left as future work.

Remark 4. It is possible in principle to evaluate the spectral efficiency of joint CE-MUDD based on nonlinear channel estimation in the large-system limit, in which the channel estimator sends the marginal posterior pdfs $\{p(\mathcal{H}_k | \mathcal{I}_{\mathcal{T}_{t-1}}, \bar{\mathcal{I}}_{\mathcal{C}_{t+1}})\}$ to the optimal detector in stage t , instead of (11). The spectral efficiency would be given as that of a receiver with the optimal nonlinear channel estimator for the single-user SIMO channel (27). However, the obtained spectral efficiency is difficult to calculate in terms of the computational complexity. In this sense, the bound based on nonlinear channel estimation is not an analytical one, while the formula itself is simple.

E. LMMSE Receiver

The LMMSE receiver for $M=N=1$ has been analyzed rigorously in [34] by using random matrix theory. In this section, we show that the replica method can derive the same result as the rigorous one.

The spectral efficiency (25) of the LMMSE receiver is given via the spectral efficiency of a bank of the single-user SIMO channels (27) with an LMMSE receiver. We first define the LMMSE receiver for the SIMO channel (27), after which we present an analytical expression for the spectral efficiency (25) of the LMMSE receiver in the large-system limit. The LMMSE receiver is obtained by replacing the optimal detector in Fig. 5 by the LMMSE detector.

Definition 3. The LMMSE detector estimates the data symbol $b_{t,k,m}$ from the received vector $\underline{\mathbf{y}}_{t,k,m}$ for the single-user SIMO channel (27) in the same symbol period t and the information about $\mathbf{h}_{k,m}$ provided by the LMMSE channel estimator defined in Definition 2, and feeds the information about $b_{t,k,m}$ to the per-stream decoders. In

order to define the information about $b_{t,k,m}$, we consider the single-user SIMO channel in the t th symbol period postulated by the LMMSE detector,

$$\tilde{\mathbf{y}}_{t,k,m}^{(L)} = \hat{\mathbf{h}}_{k,m}^{\mathcal{T}_\tau} \tilde{b}_{t,k,m}^{(L)} + \tilde{\mathbf{w}}_{t,k,m}^{(L)} + \tilde{\mathbf{n}}_{t,k,m}^{(L)}, \quad (50)$$

with $\tilde{\mathbf{n}}_{t,k,m}^{(L)} \sim \mathcal{CN}(\mathbf{0}, \sigma_n^2 \mathbf{I}_N)$. In (50), $\hat{\mathbf{h}}_{k,m}^{\mathcal{T}_\tau}$ denotes the LMMSE channel estimate (31) for the single-user SIMO channel (27). The vector $\tilde{\mathbf{w}}_{t,k,m}^{(L)} \in \mathbb{C}^N$ conditioned on $\mathcal{I}_{\mathcal{T}_\tau, k, m}$ is a CSCG random vector with the covariance matrix $(P/M)\underline{\Sigma}_{t,k,m}$, in which $\underline{\Sigma}_{t,k,m}$ denotes the covariance matrix of the channel estimation errors $\Delta \hat{\mathbf{h}}_{k,m}^{\mathcal{T}_\tau} = \mathbf{h}_{k,m} - \hat{\mathbf{h}}_{k,m}^{\mathcal{T}_\tau}$, i.e., $\underline{\Sigma}_{t,k,m} = \mathbb{E}[\Delta \hat{\mathbf{h}}_{k,m}^{\mathcal{T}_\tau} (\Delta \hat{\mathbf{h}}_{k,m}^{\mathcal{T}_\tau})^H | \mathcal{I}_{\mathcal{T}_\tau, k, m}]$. The information about $b_{t,k,m}$ is defined as

$$p(\tilde{b}_{t,k,m}^{(L)} | \mathbf{y}_{t,k,m}^{(L)}, \mathcal{I}_{\mathcal{T}_\tau, k, m}) = \int p(\tilde{b}_{t,k,m}^{(L)}, \tilde{\mathbf{w}}_{t,k,m}^{(L)} | \mathbf{y}_{t,k,m}^{(L)}, \mathcal{I}_{\mathcal{T}_\tau, k, m}) d\tilde{\mathbf{w}}_{t,k,m}^{(L)}, \quad (51)$$

with

$$p(\tilde{b}_{t,k,m}^{(L)}, \tilde{\mathbf{w}}_{t,k,m}^{(L)} | \mathbf{y}_{t,k,m}^{(L)}, \mathcal{I}_{\mathcal{T}_\tau, k, m}) = \frac{p(\mathbf{y}_{t,k,m}^{(L)} | \tilde{b}_{t,k,m}^{(L)}, \tilde{\mathbf{w}}_{t,k,m}^{(L)}, \hat{\mathbf{h}}_{k,m}^{\mathcal{T}_\tau}) p(\tilde{\mathbf{w}}_{t,k,m}^{(L)}) p(\tilde{b}_{t,k,m}^{(L)})}{\int \int p(\mathbf{y}_{t,k,m}^{(L)} | \tilde{b}_{t,k,m}^{(L)}, \tilde{\mathbf{w}}_{t,k,m}^{(L)}, \hat{\mathbf{h}}_{k,m}^{\mathcal{T}_\tau}) p(\tilde{\mathbf{w}}_{t,k,m}^{(L)}) p(\tilde{b}_{t,k,m}^{(L)}) d\tilde{\mathbf{w}}_{t,k,m}^{(L)} d\tilde{b}_{t,k,m}^{(L)}}, \quad (52)$$

where $p(\mathbf{y}_{t,k,m}^{(L)} | \tilde{b}_{t,k,m}^{(L)}, \tilde{\mathbf{w}}_{t,k,m}^{(L)}, \hat{\mathbf{h}}_{k,m}^{\mathcal{T}_\tau})$ denotes the single-user SIMO channel (50) postulated by the LMMSE detector.

Proposition 5. Under the RS assumption, the spectral efficiency (25) of the LMMSE receiver converges to the spectral efficiency of the LMMSE receiver for the single-user SIMO channel (27) with in the large-system limit:

$$\lim_{K, L \rightarrow \infty} C_L = \beta M \left(1 - \frac{\tau}{T_c} \right) \underline{C}_{\tau+1}(\sigma_{\text{tr}}^2(\tau), \sigma_L^2), \quad (53)$$

where $\underline{C}_{\tau+1}(\sigma_{\text{tr}}^2(\tau), \sigma_L^2)$ is given by (34). In evaluating (53), $\sigma_{\text{tr}}^2(\tau)$ for $t \in \mathcal{T}_\tau$ is given as the solution to the fixed-point equation (38). On the other hand, σ_L^2 satisfies the fixed-point equation

$$\sigma_L^2 = N_0 + \frac{\beta P \xi^2 \sigma_L^2}{(P/M)\xi^2 + \sigma_L^2} + \frac{\beta M}{N} \left(\frac{\sigma_L^2}{(P/M)\xi^2 + \sigma_L^2} \right)^2 \mathbb{E} \left[\|\hat{\mathbf{h}}_{k,m}^{\mathcal{T}_\tau}\|^2 |b_{t,k,m} - \langle \tilde{b}_{t,k,m}^{(L)} \rangle_L|^2 \right], \quad (54)$$

with $\xi^2 = \xi^2(\sigma_{\text{tr}}^2(\tau), \tau)$ and $\langle \cdots \rangle_L = \int \cdots p(\tilde{b}_{t,k,m}^{(L)}, \tilde{\mathbf{w}}_{t,k,m}^{(L)} | \mathbf{y}_{t,k,m}^{(L)}, \mathcal{I}_{\mathcal{T}_\tau, k, m}) d\tilde{b}_{t,k,m}^{(L)} d\tilde{\mathbf{w}}_{t,k,m}^{(L)}$.

Note that the LMMSE receiver can achieve the constrained capacity of the single-user SIMO channel (27). The fixed-point equation (54) coincides with that in [34] for $M = N = 1$. This implies that the result obtained by using the replica method is correct for the LMMSE receiver. The difference between the fixed-point equations (37) and (54) appears in the last terms of their respective right-hand sides. The last term of the right-hand side of (54) corresponds to the mean-squared error (MSE) of the *linear* MMSE estimate of $b_{t,k,m}$ for the single-user SIMO channel (40) with perfect CSI at the receiver, whereas the last term of the right-hand side of (37) corresponds to the MSE of the minimum mean-squared error (MMSE) estimate of $b_{t,k,m}$ for the same SIMO channel.

VI. NUMERICAL RESULTS

The spectral efficiency of the joint CE-MUDD is compared to the spectral efficiencies of the one-shot CE-MUDD, the optimum separated receiver, and the LMMSE receiver, on the basis of Propositions 2–5. See Table I for the differences between the four receivers. The performance gap between the joint CE-MUDD and the one-shot CE-MUDD corresponds to the gains obtained by using the decoded data symbols to refine the channel estimates. The

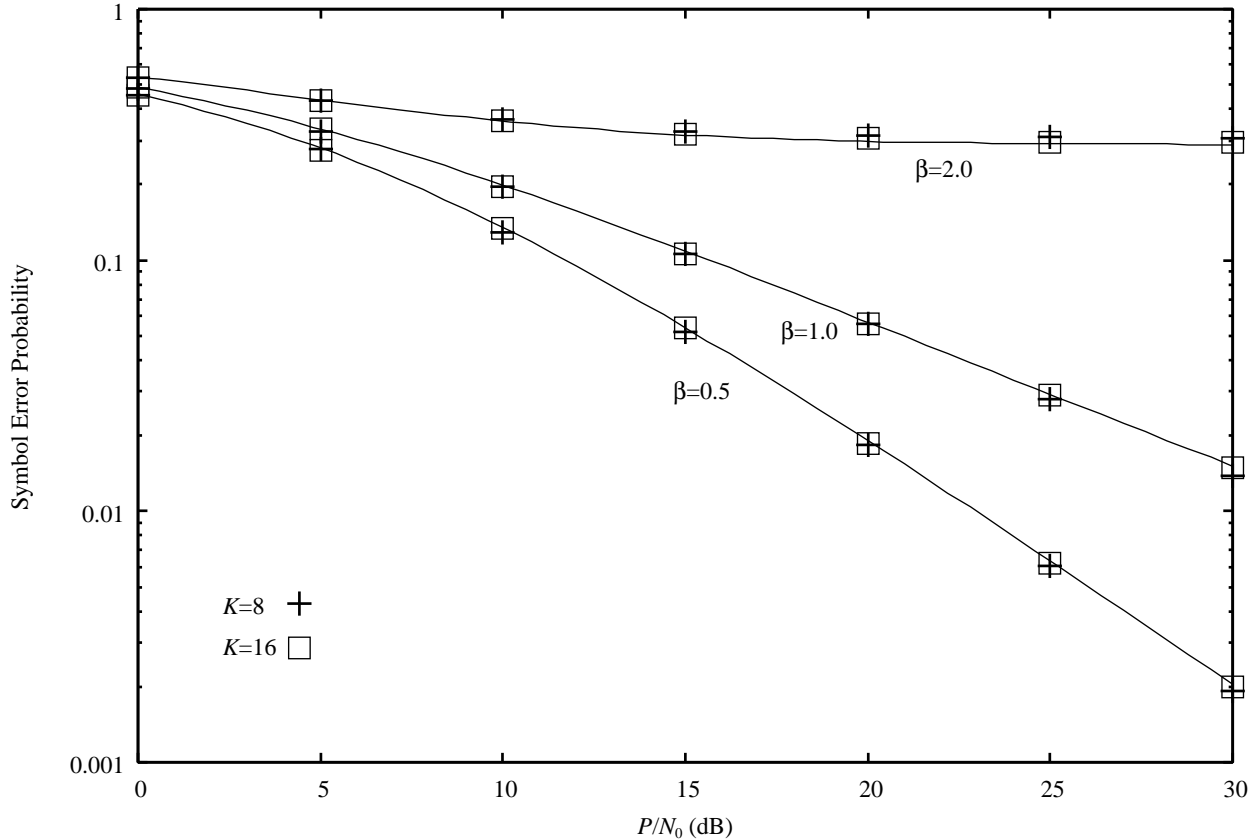


Fig. 6. Symbol error probability of $b_{1,t,1}$ versus P/N_0 for the LMMSE receiver. From top to bottom, $\{+\}$ denote the symbol error probabilities of the LMMSE receiver for $(K, L) = (8, 4), (8, 8), (8, 16)$. $\{\square\}$ represent the symbol error probabilities of the LMMSE receiver for $(K, L) = (16, 8), (16, 16), (16, 32)$ from top to bottom. The solid lines represent the symbol error probabilities of the LMMSE receiver in the large-system limit for $\beta = 2.0, 1.0, 0.5$ from top to bottom. $\tau = 4$ and $M = N = 1$.

gap between the one-shot CE-MUDD and the optimum separated receiver is related to the gains obtained by using the decoded data symbols to mitigate MAI. The performance gap between the optimum separated receiver and the LMMSE receiver corresponds to the gains obtained by performing the optimal MUD, instead of the LMMSE MUD. The spectral efficiencies of the three receivers based on the one-shot channel estimation are well-defined for $\tau \geq 0$. For clarity, these spectral efficiencies are calculated for $\tau \geq 0$, while the spectral efficiency (49) of the joint CE-MUDD is evaluated for $\tau = 0, 1, \dots, T_c$. In all numerical results, unbiased QPSK input symbols are used.

We first present Monte Carlo simulation results for finite-sized systems and compare them with the analytical predictions derived in the large-system limit. In the Monte Carlo simulations we assume QPSK spreading, which is performed by using two mutually independent binary-antipodal random spreading sequences for in-phase and quadrature-phase channels. We only consider the LMMSE receiver since the computational complexity of the optimal detector is high. Figure 6 plots the symbol error probability of $b_{1,t,1}$ for $M = N = 1$ and $\tau = 4$. The solid lines represent the symbol error probability of the LMMSE receiver for the single-user SIMO channel (27)

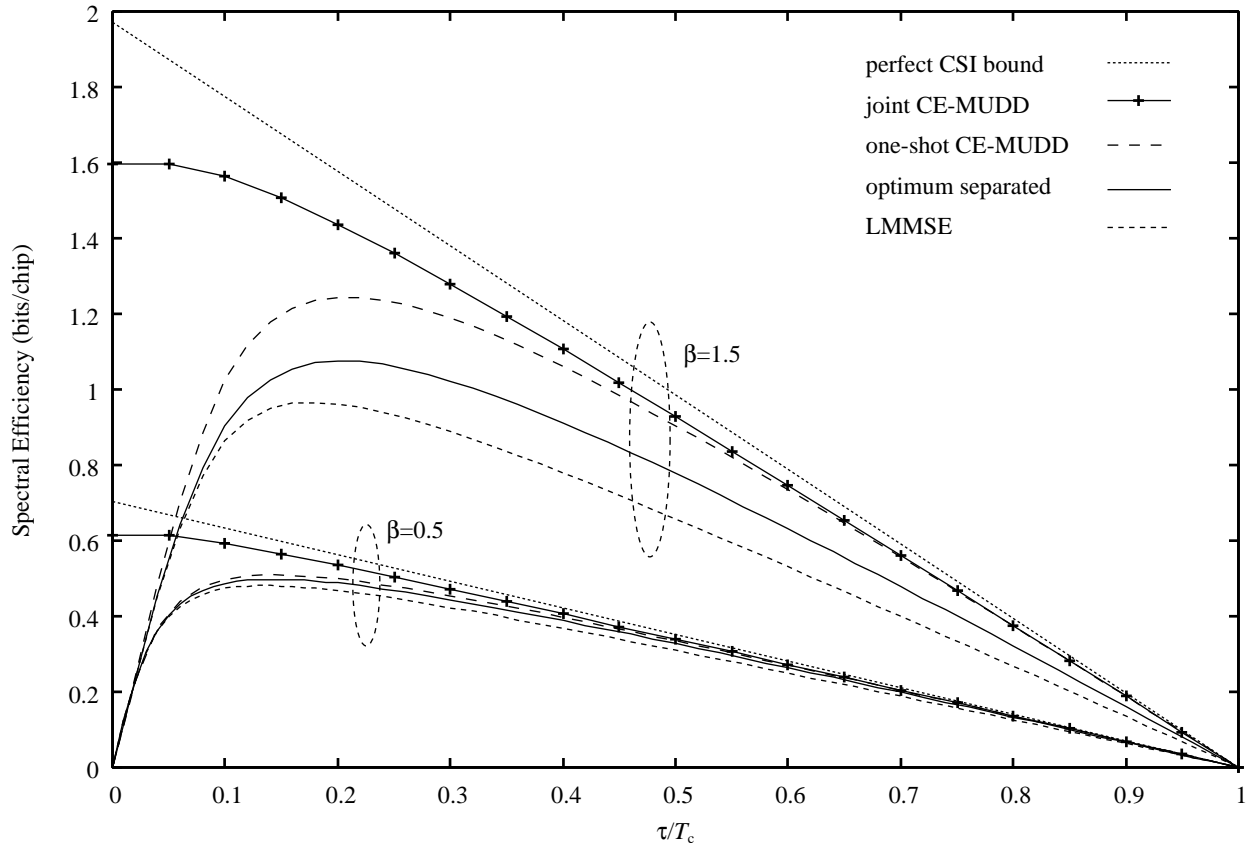


Fig. 7. Spectral efficiency versus τ/T_c in the large-system limit. The pluses connected by straight lines display the spectral efficiency of the joint CE-MUDD. The dashed lines, the solid lines, and the dotted lines represent the spectral efficiencies of the one-shot CE-MUDD, the optimum separated receiver, and the LMMSE receiver, respectively. The fine dotted straight lines shows an upper bound of the constrained capacity (5) based on the optimal receiver with perfect CSI. $P/N_0 = 6$ dB, $M = N = 1$, and $T_c = 20$.

in which $\sigma_{t'}^2$ for $t' \in \mathcal{T}_\tau$ is given by the solution to the fixed-point equation (38) and in which σ_t^2 is given as the solution to the fixed-point equation (54). We find that the analytical predictions are in agreement with the Monte Carlo simulation results for $K = 16$, while they are slightly different from the simulation results for $K = 8$. This result has two consequences: One is that the asymptotic results for the LMMSE receiver are applicable to a non-Gaussian distribution of $s_{l,t,k,m}$, as noted in [34]. The other is that the convergence of spectral efficiency to its asymptotic value is so fast that our analytical results, especially for the LMMSE receiver, provide reasonably good approximations of the true spectral efficiencies even for small-sized systems. The latter observation has also been made in [42], [60].

We next focus on the asymptotic spectral efficiencies for single-antenna systems. Figure 7 displays the spectral efficiencies of the four receivers for $P/N_0 = 6$ dB. An upper bound $(1 - \tau/T_c)C_{\text{opt}}^{(\text{per})}$ of the constrained capacity (5) is also shown, which is based on the asymptotic spectral efficiency $C_{\text{opt}}^{(\text{per})}$ of the optimal receiver with perfect CSI [11]. We find that the spectral efficiencies of the one-shot CE-MUDD and the two separated receivers are maximized

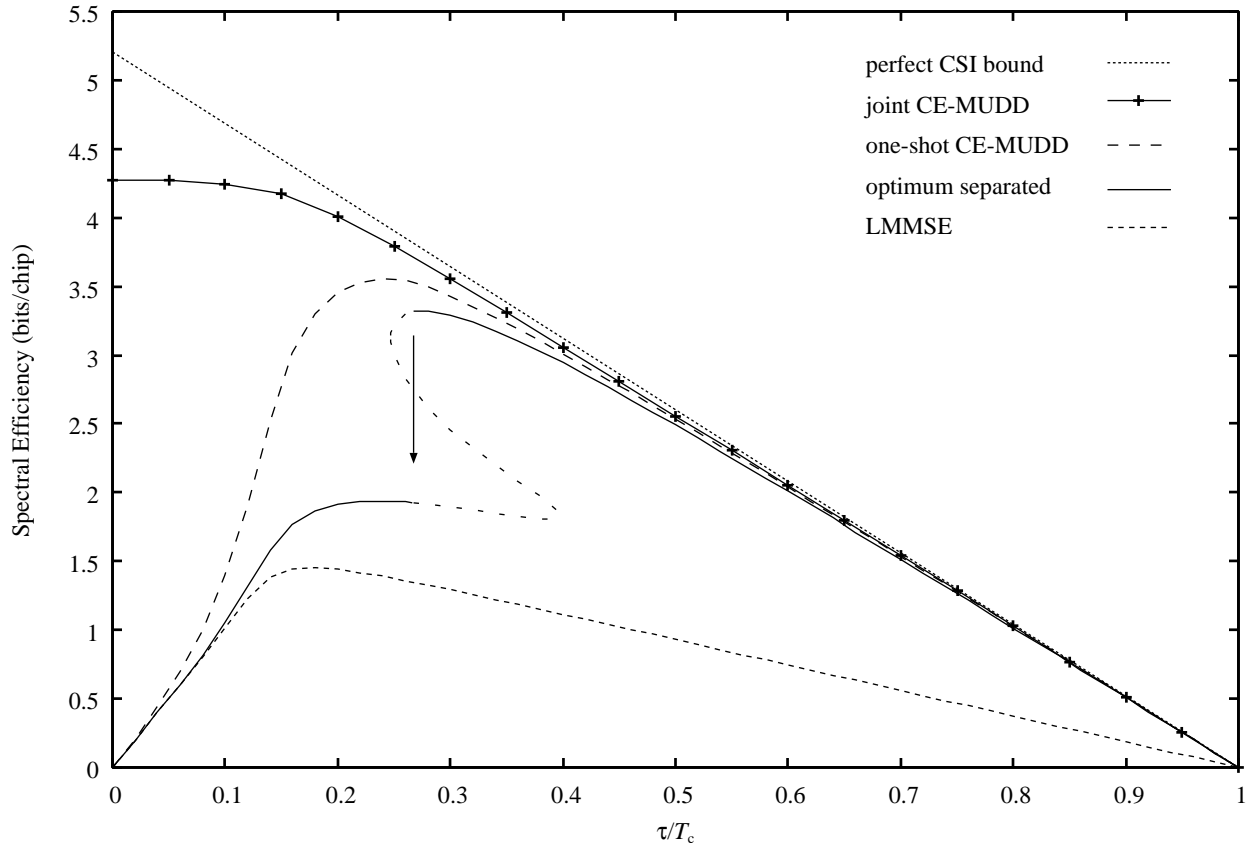


Fig. 8. Spectral efficiency versus τ/T_c in the large-system limit. The pluses connected by straight lines display the spectral efficiency of the joint CE-MUDD. The dashed lines, the solid lines, and the dotted lines represent the spectral efficiencies of the one-shot CE-MUDD, the optimum separated receiver, and the LMMSE receiver, respectively. The fine dotted straight lines shows an upper bound of the constrained capacity (5) based on the optimal receiver with perfect CSI. The widely-spaced dotted lines denotes solutions for the optimum separated receivers which are not selected by the criterion (39). $\beta = 2.75$, $P/N_0 = 15$ dB, $M = N = 1$, and $T_c = 20$.

at optimal $\tau = \tau_{\text{opt}}$. This observation results from two effects: the improvement of the accuracy of the channel estimation and the decrease of the number of transmitted data symbols, both caused by the increase of τ . The spectral efficiency (49) of the joint CE-MUDD is maximized at $\tau = 0$ and $\tau = 1$. These results imply that the training overhead can be significantly reduced by using joint CE-MUDD.

The performance gaps between the one-shot CE-MUDD and the two separated receivers are negligibly small for $\beta = 0.5$, while there is a noticeable gap between the spectral efficiencies of the joint CE-MUDD and the one-shot CE-MUDD. We found by numerical evaluation that $P/N_0 \approx 8.2$ dB is required for $\beta = 0.5$ in order for the one-shot CE-MUDD to achieve the same spectral efficiency as that of the joint CE-MUDD for $P/N_0 = 6$ dB. In other words, the joint CE-MUDD provides a performance gain of 2.2 dB. For $\beta = 1.5$, the performance gaps between the optimal one-shot CE-MUDD, the optimum separated receiver, and the LMMSE receiver are large. This result implies that performance gains can be obtained by using an MUDD scheme with higher performance

than the LMMSE receiver. Furthermore, there is a large performance gap between the joint CE-MUDD and the one-shot CE-MUDD. More precisely, we found that $P/N_0 \approx 8.5$ dB is needed for $\beta = 1.5$ in order for the one-shot CE-MUDD to achieve the same spectral efficiency as that of the joint CE-MUDD for $P/N_0 = 6$ dB. These observations indicate that joint CE-MUDD can provide significant performance gains regardless of β , compared to one-shot CE-MUDD.

Figure 8 shows the spectral efficiencies of the four receivers for $P/N_0 = 15$ dB and $\beta = 2.75$. The upper bound $(1 - \tau/T_c)C_{\text{opt}}^{(\text{per})}$ is also shown. One interesting observation is that the spectral efficiency of the optimum separated receiver is discontinuous. This result predicts that the spectral efficiency of the optimum separated receiver exhibits a waterfall behavior: The spectral efficiency rapidly degrades in the neighborhood of the discontinuous point $\tau = \tau_c$, shown by the arrow, which corresponds to the threshold between interference-limited and non-limited regions. The system is not *interference-limited* for $\tau > \tau_c$, i.e., the asymptotic multiuser efficiency N_0/σ_c^2 is close to one. On the other hand, the system is *interference-limited* for $\tau < \tau_c$, i.e., the asymptotic multiuser efficiency is small.

The spectral efficiency of the one-shot CE-MUDD seems to be continuous. This observation is explained as follows: Users decoded in the initial substages of successive decoding are interference-limited, while the remaining users are not interference-limited. Therefore, the achievable rate of each user changes discontinuously for the one-shot CE-MUDD. However, the achievable sum rate of the one-shot CE-MUDD changes continuously since the threshold κ_c between the two groups of interference-limited users and non-limited users should move continuously with the change of τ . We remark that it might be possible to cancel out MAI successfully by optimizing the power allocation and the rate of each user, as discussed in [26].

Finally, we investigate multiple-antenna systems. Figure 9 shows the spectral efficiencies of the four receivers for $M = N = 8$. The upper bound $(1 - \tau/T_c)C_{\text{opt}}^{(\text{per})}$ is also shown. We find that the optimal number τ_{opt} of pilot symbols is larger than that for $M = N = 1$ (Compare Figs. 7 and 9), since the number of unknown channel coefficients increases. On the other hand, the spectral efficiency of the joint CE-MUDD is maximized at $\tau = 0$ and $\tau = 1$ even for $M = N = 8$. Consequently, the performance gap between the joint CE-MUDD and the one-shot CE-MUDD becomes larger than that for single-antenna systems. When $\beta = 0.5$, the performance gap between the joint CE-MUDD and the one-shot CE-MUDD is approximately 1.47 bits/chip for $M = N = 8$ (0.18 bits/chip per the number of antennas), while the performance gap is approximately 0.10 bits/chip for $M = N = 1$. We found by numerical evaluation that a performance gain of 1.47 bits/chip corresponds to that of approximately 3.4 dB. For $\beta = 1.5$, the performance gain increases up to approximately 2.88 bits/chip for $M = N = 8$ (0.36 bits/chip per the number of antennas), while it is 0.35 bits/chip for $M = N = 1$. Interestingly, a performance gain of 2.88 bits/chip corresponds to a gain of 7.2 dB. These results imply that joint CE-MUDD can provide a significant performance gain for multiple-antenna systems.

Figure 10 shows the optimal training overhead τ_{opt}/T_c for $M = N$, maximizing the spectral efficiencies of the one-shot CE-MUDD and the two separated receivers. Note that the optimal training overhead for the joint CE-MUDD corresponds to $1/T_c = 0.05$. We find that the optimal training overheads increase logarithmically with the increase of the number of antennas for small M , while they tend towards around 0.5 for large M . This observation

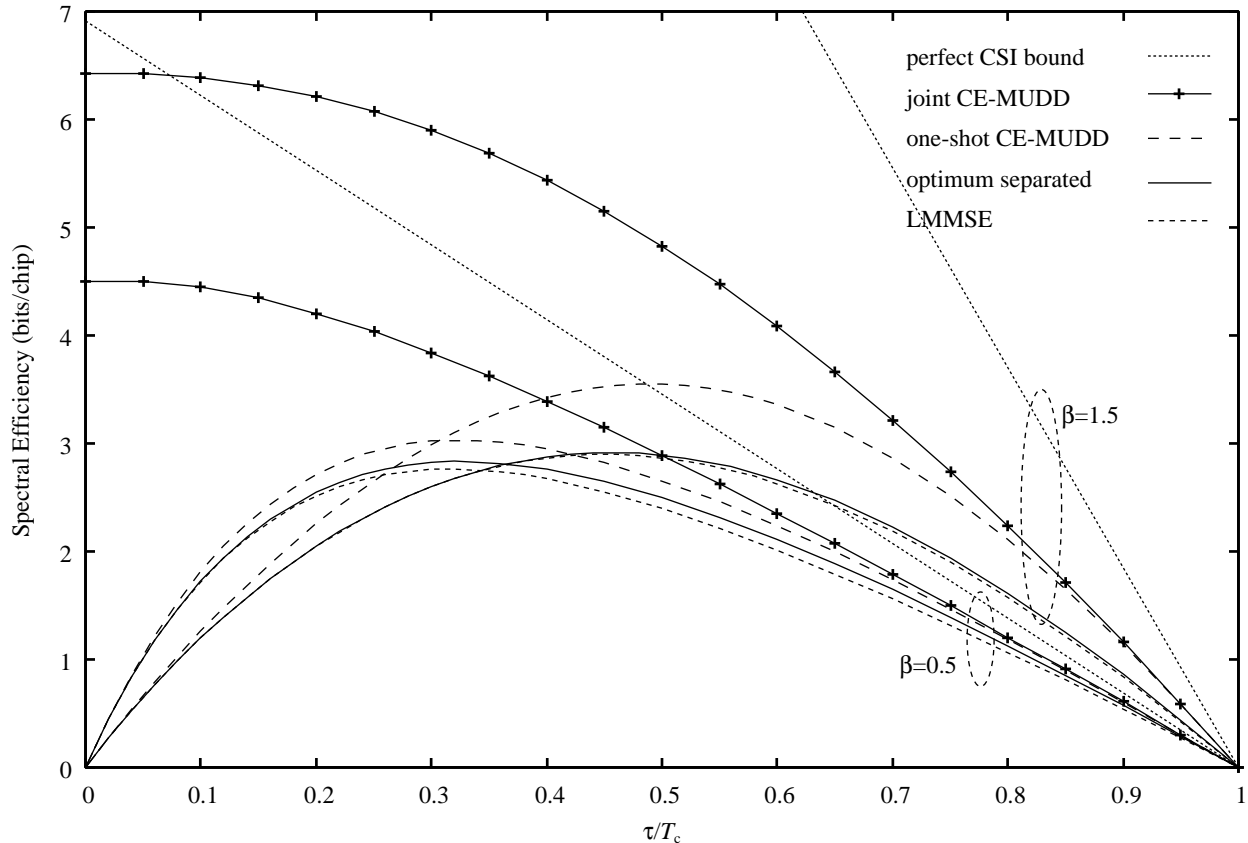


Fig. 9. Spectral efficiency versus τ/T_c in the large-system limit. The pluses connected by straight lines display the spectral efficiency of the joint CE-MUDD. The dashed lines, the solid lines, and the dotted lines represent the spectral efficiencies of the one-shot CE-MUDD, the optimum separated receiver, and the LMMSE receiver, respectively. The fine dotted straight lines shows an upper bound of the constrained capacity (5) based on the optimal receiver with perfect CSI. $P/N_0 = 6$ dB, $M = N = 8$, and $T_c = 20$.

implies that the performance gains obtained by using joint CE-MUDD increase as the number of antennas grows.

VII. CONCLUSIONS

We have analyzed the asymptotic performance of joint CE-MUDD for randomly-spread MIMO DS-CDMA systems with no CSI. The main contribution of this paper from a theoretical point of view is to derive a lower bound for the spectral efficiency of the optimal joint CE-MUDD on the basis of successive decoding with suboptimal LMMSE channel estimation, along with the spectral efficiencies of the one-shot CE-MUDD and the optimum separated receiver. The asymptotic performance of MIMO DS-CDMA systems with no CSI is characterized via the performance of a bank of single-user SIMO channels with no CSI. This decoupling result is an extension of previous studies [11], [20] for the case of perfect CSI at the receiver to the no-CSI case.

The main contribution of this paper from a practical point of view is to demonstrate that joint CE-MUDD can significantly reduce the training overhead due to transmission of pilot signals, compared to receivers based on

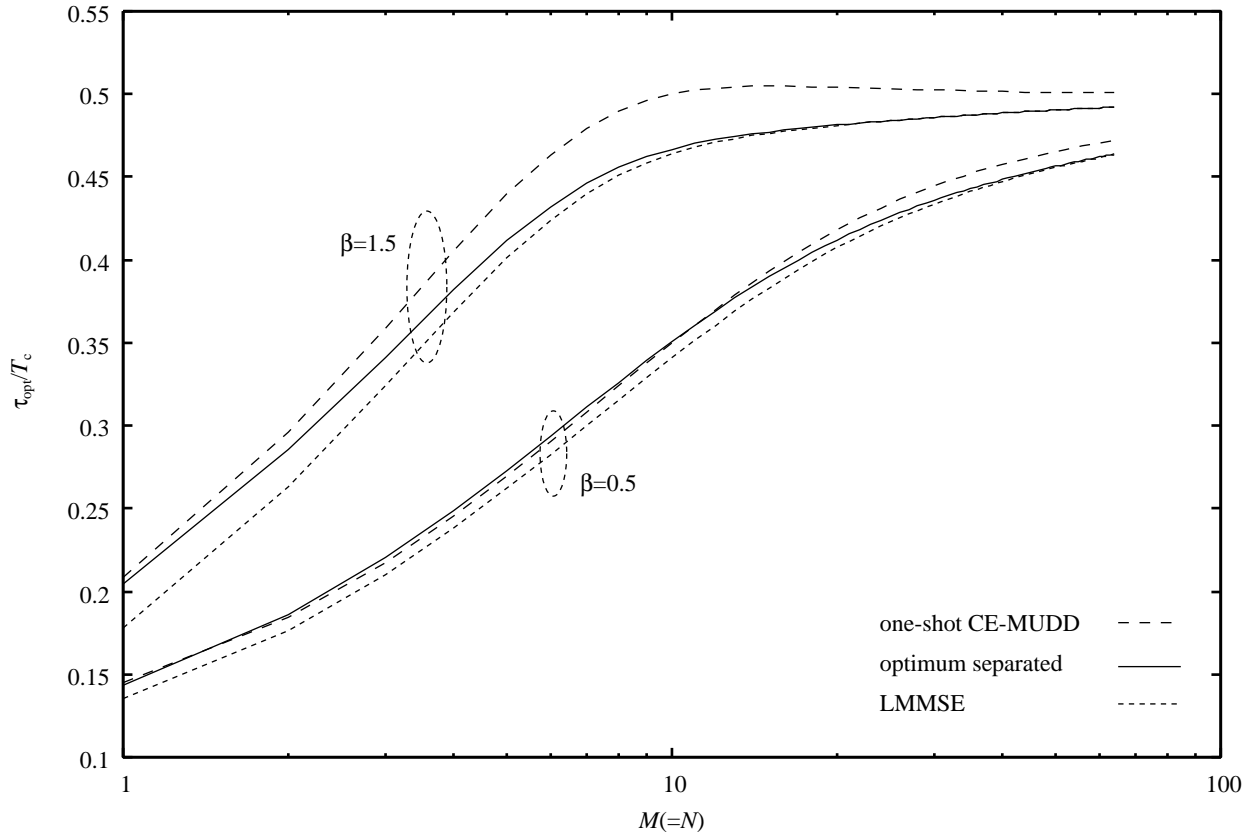


Fig. 10. τ_{opt}/T_c versus $M(=N)$ in the large-system limit. The dashed lines, the solid lines, and the dotted lines represent the optimal training overhead of the one-shot CE-MUDD, the optimum separated receiver, and the LMMSE receiver, respectively. $P/N_0 = 6$ dB and $T_c = 20$.

one-shot channel estimation. The results imply that joint CE-MUDD can provide significant performance gains for systems which require large training overhead for attaining accurate CSI. We conclude that the iterative refinement of channel estimates by utilizing soft feedback from per-user decoders may lead to substantial reduction of the rate loss due to transmission of pilot signals for MIMO DS-CDMA systems.

APPENDIX A

DERIVATIONS OF LMMSE ESTIMATORS

A. Perfect-CSI Case

We shall present two derivations of the LMMSE estimator for vector channels with perfect CSI. One is based on the minimization of the MSE, and the other on Bayesian inference. Let us consider the $N \times K$ vector channel with perfect CSI

$$\mathbf{y} = \mathbf{H}\mathbf{x} + \mathbf{n} \in \mathbb{C}^N. \quad (55)$$

In (55), $\mathbf{x} \in \mathbb{C}^K$ denotes a zero-mean transmitted vector with covariance matrix $\mathbb{E}[\mathbf{x}\mathbf{x}^H] = P\mathbf{I}_K$. The noise vector $\mathbf{n} \in \mathbb{C}^N$ is a zero-mean random vector with covariance matrix $\mathbf{\Sigma}$. Furthermore, $\mathbf{H} \in \mathbb{C}^{N \times K}$ denotes a random channel matrix with mean $\bar{\mathbf{H}} \in \mathbb{C}^{N \times K}$. The three random variables \mathbf{H} , \mathbf{x} , and \mathbf{n} are independent of each other.

The goal is to find the LMMSE estimator, i.e., a linear estimator $\hat{\mathbf{x}} = \mathbf{F}_{\text{per}}^H \mathbf{y}$ of the transmitted vector that minimizes the MSE $\mathbb{E}[\|\mathbf{x} - \hat{\mathbf{x}}\|^2 | \mathbf{H}]$. Substituting $\hat{\mathbf{x}} = \mathbf{F}_{\text{per}}^H \mathbf{y}$ into the MSE $\mathbb{E}[\|\mathbf{x} - \hat{\mathbf{x}}\|^2 | \mathbf{H}]$ yields

$$\mathbb{E}[\|\mathbf{x} - \hat{\mathbf{x}}\|^2 | \mathbf{H}] = P\|\mathbf{I}_K - \mathbf{F}_{\text{per}}^H \mathbf{H}\|^2 + \text{Tr} \left(\mathbf{F}_{\text{per}}^H \mathbf{\Sigma} \mathbf{F}_{\text{per}} \right). \quad (56)$$

It is well known that \mathbf{F}_{per} to minimize the MSE (56) is given by

$$\mathbf{F}_{\text{per}} = \mathbf{\Sigma}^{-1} \mathbf{H} (P^{-1} \mathbf{I}_K + \mathbf{H}^H \mathbf{\Sigma}^{-1} \mathbf{H})^{-1}. \quad (57)$$

In the derivation of (57), we have minimized the MSE (56) among all possible *linear* estimators $\hat{\mathbf{x}} = \mathbf{F}_{\text{per}}^H \mathbf{y}$. The MSE (56) for the LMMSE estimator is larger than the MMSE in general, which is the minimum of the MSE for all possible estimators. However, it is known that the two MSEs coincides with each other when the transmitted vector \mathbf{x} and the noise vector \mathbf{n} are CSCG. This observation implies that the LMMSE estimator can be derived as the posterior mean estimator for a Gaussian vector channel. Let us define the vector channel postulated by the receiver as

$$\tilde{\mathbf{y}}_{\text{per}} = \mathbf{H} \tilde{\mathbf{x}}_{\text{per}} + \tilde{\mathbf{n}}_{\text{per}}, \quad (58)$$

with $\tilde{\mathbf{x}}_{\text{per}} \sim \mathcal{CN}(\mathbf{0}, P\mathbf{I}_K)$ and $\tilde{\mathbf{n}}_{\text{per}} \sim \mathcal{CN}(\mathbf{0}, \mathbf{\Sigma})$. It is straightforward to confirm that the posterior mean estimator $\mathbb{E}[\tilde{\mathbf{x}}_{\text{per}} | \tilde{\mathbf{y}}_{\text{per}} = \mathbf{y}, \mathbf{H}]$ for the postulated vector channel is equal to the LMMSE estimator.

B. No-CSI Case

We consider the no-CSI case: The channel matrix \mathbf{H} is assumed to be unknown to the receiver, while the statistical properties of \mathbf{x} , \mathbf{H} , and \mathbf{n} are known. The LMMSE estimator is defined as the linear estimator $\hat{\mathbf{x}} = \mathbf{F}^H \mathbf{y}$ to minimize the MSE $\mathbb{E}[\|\mathbf{x} - \hat{\mathbf{x}}\|^2]$ averaged over the channel matrix \mathbf{H} . Substituting $\hat{\mathbf{x}} = \mathbf{F}^H \mathbf{y}$ into this MSE gives

$$\mathbb{E}[\|\mathbf{x} - \hat{\mathbf{x}}\|^2] = P\|\mathbf{I}_K - \mathbf{F}^H \bar{\mathbf{H}}\|^2 + \text{Tr} \left\{ \mathbf{F}^H \left(P\mathbb{E}[\Delta\mathbf{H}\Delta\mathbf{H}^H] + \mathbf{\Sigma} \right) \mathbf{F} \right\}, \quad (59)$$

with $\Delta\mathbf{H} = \mathbf{H} - \bar{\mathbf{H}}$. Comparing this expression with (56), we find that the optimal filter \mathbf{F} is given by

$$\mathbf{F} = \mathbf{\Sigma}_{\text{ef}}^{-1} \bar{\mathbf{H}} (P^{-1} \mathbf{I}_K + \bar{\mathbf{H}}^H \mathbf{\Sigma}_{\text{ef}}^{-1} \bar{\mathbf{H}})^{-1}, \quad (60)$$

with $\mathbf{\Sigma}_{\text{ef}} = P\mathbb{E}[\Delta\mathbf{H}\Delta\mathbf{H}^H] + \mathbf{\Sigma}$.

In order to interpret the meaning of the effective covariance matrix $\mathbf{\Sigma}_{\text{ef}}$, we re-write the vector channel (55) as

$$\mathbf{y} = \bar{\mathbf{H}}\mathbf{x} + \Delta\mathbf{H}\mathbf{x} + \mathbf{n}. \quad (61)$$

The effective covariance matrix $\mathbf{\Sigma}_{\text{ef}}$ is equal to the covariance matrix of the channel estimator error plus the noise vector, i.e., $\Delta\mathbf{H}\mathbf{x} + \mathbf{n}$. This observation implies that the LMMSE estimator is equal to the posterior mean estimator $\mathbb{E}[\tilde{\mathbf{x}} | \tilde{\mathbf{y}} = \mathbf{y}]$ for the postulated vector channel,

$$\tilde{\mathbf{y}} = \bar{\mathbf{H}}\tilde{\mathbf{x}} + \tilde{\mathbf{w}} + \tilde{\mathbf{n}}, \quad (62)$$

where $\tilde{\mathbf{x}} \in \mathbb{C}^K$, $\tilde{\mathbf{w}} \in \mathbb{C}^N$, and $\tilde{\mathbf{n}} \in \mathbb{C}^N$ are independent CSCG random vectors with covariance matrices $P\mathbf{I}_K$, $P\mathbb{E}[\Delta\mathbf{H}\Delta\mathbf{H}^H]$, and Σ , respectively. If $\bar{\mathbf{H}} = \mathbf{O}$, the LMMSE estimator is obviously independent of the received vector \mathbf{y} .

APPENDIX B
PROOF OF LEMMA 1

In order to prove Lemma 1 we need the following lemma, which is derived by extending the replica analysis in [11].

Lemma 2. *Suppose that $\{\mathcal{A}_k\}$ are mutually disjoint subsets of $\{2, 3, \dots, n\}$ for $k \in \mathcal{K}$. Then,*

$$\lim_{K, L \rightarrow \infty} \mathbb{E}_{\mathcal{I}_{\mathcal{T}_\tau} \tau} \left[p(\mathcal{H}_{\mathcal{K}}^{\{1\}} | \mathcal{I}_{\mathcal{T}_\tau}) \prod_{k \in \mathcal{K}} \prod_{a \in \mathcal{A}_k} p(\mathcal{H}_k^{\{a\}} | \mathcal{I}_{\mathcal{T}_\tau}) \right] = \prod_{k \in \mathcal{K}} \prod_{m=1}^M \mathbb{E}_{\underline{\mathcal{I}}_{\mathcal{T}_\tau, k, m}} \left[\prod_{a \in \{1\} \cup \mathcal{A}_k} p(\mathbf{h}_{k, m} = \mathbf{h}_{k, m}^{\{a\}} | \underline{\mathcal{I}}_{\mathcal{T}_\tau, k, m}) \right], \quad (63)$$

with $\mathcal{H}_{\mathcal{K}}^{\{a\}} = \{\mathcal{H}_k^{\{a\}} : k \in \mathcal{K}\}$ denoting the a th replicas of the channel vectors for the users in \mathcal{K} . In evaluating the right-hand side of (63), $\sigma_t^2 = \sigma_{\text{tr}}^2(\tau)$ for $t \in \mathcal{T}_\tau$ is given by the solution to the fixed-point equation (38).

Derivation of Lemma 2: See Appendix C. ■

Lemma 2 implies that the information about $\{\mathbf{h}_{k, m}\}$ obtained by utilizing the information $\mathcal{I}_{\mathcal{T}_\tau}$ is mutually independent in the large-system limit for all $k \in \mathcal{K}$ and m , and that the information about each $\mathbf{h}_{k, m}$ looks like that provided by the LMMSE channel estimator for the single-user SIMO channel (27). A result equivalent to Lemma 2 was proved in [34] for $M = N = 1$, by using random matrix theory. Lemma 2 is used to evaluate the joint moment sequence of $\{X_k : k \in \mathcal{K}\}$, defined by (42), in the following proof of Lemma 1.

Proof of Lemma 1: It is sufficient to prove that the joint moment sequence of $\{X_k : k \in \mathcal{K}\}$ converges to that for the distribution defined by the right-hand side of (43) in the large-system limit, since we have assumed the existence of the joint moment generating function.

For non-negative integers $\{\tilde{n}_k\}$, a joint moment of $\{X_k : k \in \mathcal{K}\}$ is given by

$$\mathbb{E} \left[\prod_{k \in \mathcal{K}} X_k^{\tilde{n}_k} \right] = \mathbb{E} \left[\prod_{k \in \mathcal{K}} \prod_{i=1}^{\tilde{n}_k} \int f_k(\mathcal{H}_k^{\{1\}}, \mathcal{H}_k^{\mathcal{A}_k^{(i)}}; \Theta) \prod_{a \in \mathcal{A}_k^{(i)}} \left\{ p(\mathcal{H}_k^{\{a\}} | \mathcal{I}_{\mathcal{T}_\tau}) d\mathcal{H}_k^{\{a\}} \right\} \right], \quad (64)$$

where $\{\mathcal{A}_k^{(i)} : \text{for all } k \in \mathcal{K}, i\}$ are mutually disjoint subsets of $\{2, 3, \dots, n\}$ satisfying $|\mathcal{A}_k^{(i)}| = |\mathcal{A}_k|$. The right-hand side of (64) is defined as the integration of $\prod_{k \in \mathcal{K}} \prod_{i=1}^{\tilde{n}_k} f_k(\mathcal{H}_k^{\{1\}}, \mathcal{H}_k^{\mathcal{A}_k^{(i)}}; \Theta)$ with respect to the measure

$$\mathbb{E}_{\mathcal{I}_{\mathcal{T}_\tau} \tau} \left[p(\mathcal{H}_{\mathcal{K}}^{\{1\}} | \mathcal{I}_{\mathcal{T}_\tau}) \prod_{k \in \mathcal{K}} \prod_{a \in \mathcal{A}_k} p(\mathcal{H}_k^{\{a\}} | \mathcal{I}_{\mathcal{T}_\tau}) \right] d\mathcal{H}_{\mathcal{K}}^{\{1\}} \prod_{k \in \mathcal{K}} \prod_{a \in \mathcal{A}_k} d\mathcal{H}_k^{\{a\}}, \quad (65)$$

with $\tilde{\mathcal{A}}_k = \cup_{i=1}^{\tilde{n}_k} \mathcal{A}_k^{(i)}$. Applying Lemma 2 to (65), we obtain

$$\lim_{K, L \rightarrow \infty} \mathbb{E} \left[\prod_{k \in \mathcal{K}} X_k^{\tilde{n}_k} \right] = \prod_{k \in \mathcal{K}} \mathbb{E} \left[\prod_{i=1}^{\tilde{n}_k} \int f_k(\mathcal{H}_k^{\{1\}}, \mathcal{H}_k^{\mathcal{A}_k^{(i)}}; \Theta) \prod_{m=1}^M \prod_{a \in \mathcal{A}_k^{(i)}} \left\{ p(\mathbf{h}_{k, m} = \mathbf{h}_{k, m}^{\{a\}} | \underline{\mathcal{I}}_{\mathcal{T}_\tau, k, m}) d\mathbf{h}_{k, m}^{\{a\}} \right\} \right], \quad (66)$$

in the large-system limit, which is equal to the corresponding joint moment $\prod_{k \in \mathcal{K}} \mathbb{E}[X_k^{\tilde{n}_k}]$ for the distribution defined as the right-hand side of (43). \blacksquare

APPENDIX C

DERIVATION OF LEMMA 2

A. Replica Method

We present a brief introduction of the replica method. For details of the replica method, see [37]–[39]. Let $f(X, Y; N) > 0$ denote a deterministic function of two random variables X and Y with a parameter N . Our goal is to evaluate the expectation $\mathbb{E}_Y[Z(Y; N)^{-1}]$ for the so-called partition function $Z(Y; N) = \mathbb{E}_X[f(X, Y; N)]$ in the limit $N \rightarrow \infty$. For that purpose, we first evaluate $\lim_{N \rightarrow \infty} \mathbb{E}_Y[Z(Y; N)^{\tilde{n}-1}]$ for any natural number $\tilde{n} \in \mathbb{N}$, by utilizing the following expression

$$\mathbb{E}_Y [Z(Y; N)^{\tilde{n}-1}] = \mathbb{E} \left[\prod_{a=1}^{\tilde{n}-1} f(X_a, Y; N) \right], \quad (67)$$

where $\{X_a : a = 1, \dots, \tilde{n} - 1\}$ are i.i.d. replicated random variables following $p(X)$. Suppose that the analytical expression obtained via (67) is well-defined even for $\tilde{n} \in \mathbb{R}$. We take $\tilde{n} \rightarrow +0$ to obtain an analytical expression of $\lim_{N \rightarrow \infty} \mathbb{E}_Y[Z(Y; N)^{-1}]$, assuming that the obtained expression coincides with the correct one. It is a challenging problem to prove whether this assumption holds.

B. Formulation

In order to show Lemma 2 by using the replica method, we transform the left-hand side of (63) into a formula corresponding to $\mathbb{E}_Y[Z(Y; N)^{\tilde{n}-1}]$. The posterior pdf of the replicated channel vectors $\mathcal{H}_{\mathcal{K}}^{\{a\}}$ for the users in \mathcal{K} , defined in the same manner as in (11), is given by

$$p(\mathcal{H}_{\mathcal{K}}^{\{a\}} | \mathcal{I}_{\mathcal{T}_\tau}) = \frac{\int \prod_{t=1}^{\tau} p(\mathcal{Y}_t | \mathcal{H}^{\{a\}}, \mathcal{S}_t, \mathcal{U}_t) p(\mathcal{H}^{\{a\}}) d\mathcal{H}_{\mathcal{K}}^{\{a\}}}{\int \prod_{t=1}^{\tau} p(\mathcal{Y}_t | \mathcal{H}, \mathcal{S}_t, \mathcal{U}_t) p(\mathcal{H}) d\mathcal{H}}, \quad (68)$$

with $\mathcal{H}^{\{a\}} = \{\mathcal{H}_k^{\{a\}} : \text{for all } k\}$ and $\mathcal{H}_{\mathcal{K}}^{\{a\}} = \{\mathcal{H}_k^{\{a\}} : \text{for all } k \notin \mathcal{K}\}$. In (68), the pdf $p(\mathcal{Y}_t | \mathcal{H}^{\{a\}}, \mathcal{S}_t, \mathcal{U}_t)$ is an abbreviation of $p(\mathcal{Y}_t | \mathcal{H} = \mathcal{H}^{\{a\}}, \mathcal{S}_t, \mathcal{U}_t)$. Let $\mathcal{H}_{\mathcal{K}}^{\mathcal{A}} = \{\mathcal{H}_k^{\mathcal{A}_k} : k \in \mathcal{K}\}$ denote the replicas of the channel vectors for $\mathcal{A} = \cup_{k \in \mathcal{K}} \mathcal{A}_k$, with $\mathcal{H}_k^{\mathcal{A}_k} = \{\mathcal{H}_k^{\{a\}} : a \in \mathcal{A}_k\}$. Applying (68) to the left-hand side of (63) and subsequently introducing a real number $\tilde{n} \in \mathbb{R}$, we obtain

$$\lim_{K, L \rightarrow \infty} \mathbb{E}_{\mathcal{I}_{\mathcal{T}_\tau}} \left[p(\mathcal{H}_{\mathcal{K}}^{\{1\}} | \mathcal{I}_{\mathcal{T}_\tau}) \prod_{k \in \mathcal{K}} \prod_{a \in \mathcal{A}_k} p(\mathcal{H}_k^{\{a\}} | \mathcal{I}_{\mathcal{T}_\tau}) \right] = \lim_{K, L \rightarrow \infty} \lim_{\tilde{n} \rightarrow +0} \Xi_{\tilde{n}}(\mathcal{H}_{\mathcal{K}}^{\{1\}}, \mathcal{H}_{\mathcal{K}}^{\mathcal{A}}), \quad (69)$$

where $\Xi_{\tilde{n}}(\mathcal{H}_{\mathcal{K}}^{\{1\}}, \mathcal{H}_{\mathcal{K}}^{\mathcal{A}})$ is given by

$$\begin{aligned} \Xi_{\tilde{n}}(\mathcal{H}_{\mathcal{K}}^{\{1\}}, \mathcal{H}_{\mathcal{K}}^{\mathcal{A}}) &= \mathbb{E} \left[\int \left\{ \int \prod_{t=1}^{\tau} p(\mathcal{Y}_t | \mathcal{H}, \mathcal{S}_t, \mathcal{U}_t) p(\mathcal{H}) d\mathcal{H} \right\}^{\tilde{n}-1-|\mathcal{A}|} \right. \\ &\times \left. \prod_{a \in \{0,1\} \cup \mathcal{A}} \left\{ \prod_{t=1}^{\tau} p(\mathcal{Y}_t | \mathcal{H}^{\{a\}}, \mathcal{S}_t, \mathcal{U}_t) p(\mathcal{H}^{\{a\}}) \right\} \prod_{t=1}^{\tau} d\mathcal{Y}_t d\mathcal{H}^{\{0\}} d\mathcal{H}_{\mathcal{K}}^{\{1\}} d\mathcal{H}_{\mathcal{K}}^{\mathcal{A}} \right] \mathcal{H}_{\mathcal{K}}^{\{1\}}, \mathcal{H}_{\mathcal{K}}^{\mathcal{A}}. \end{aligned} \quad (70)$$

In (70), we have written \mathcal{H} as $\mathcal{H}^{\{0\}}$. Furthermore, the set $\setminus \mathcal{H}_{\mathcal{K}}^A$ denotes all replicas of the channel vectors for $a \geq 2$ except for $\mathcal{H}_{\mathcal{K}}^A$. The expression (70) implies that $\prod_{t=1}^{\tau} p(\mathcal{Y}_t | \mathcal{H}, \mathcal{S}_t, \mathcal{U}_t)$ corresponds to the function $f(X, Y; N)$ with $X = \mathcal{H}$.

C. Average over Quenched Randomness

We evaluate (70) up to $O(1)$ in the large-system limit for any natural number \tilde{n} , satisfying $\mathcal{A} \subset \{1, 2, \dots, \tilde{n}\}$. We first calculate the expectations in (70) with respect to $\{\mathcal{Y}_t\}$ and $\{\mathcal{S}_t\}$. For $\tilde{n} \in \mathbb{N}$, we have a special expression of (70)

$$\Xi_{\tilde{n}}(\mathcal{H}_{\mathcal{K}}^{\{1\}}, \mathcal{H}_{\mathcal{K}}^A) = \mathbb{E} \left[\int \prod_{a=0}^{\tilde{n}} \left\{ \prod_{t=1}^{\tau} p(\mathcal{Y}_t | \mathcal{H}^{\{a\}}, \mathcal{S}_t, \mathcal{U}_t) p(\mathcal{H}^{\{a\}}) \right\} \prod_{t=1}^{\tau} d\mathcal{Y}_t d\mathcal{H}^{\{0\}} d\mathcal{H}_{\setminus \mathcal{K}}^{\{1\}} d\setminus \mathcal{H}_{\mathcal{K}}^A \middle| \mathcal{H}_{\mathcal{K}}^{\{1\}}, \mathcal{H}_{\mathcal{K}}^A \right]. \quad (71)$$

Let us re-write the MIMO DS-CDMA channel (2) in the training phase as

$$\mathbf{y}_l = \frac{1}{\sqrt{L}} \sum_{k=1}^K \sum_{t=1}^{\tau} \sum_{m=1}^M (\mathbf{e}_{\tau}^{(t)} \otimes \mathbf{h}_{k,m}) s_{l,t,k,m} x_{t,k,m} + \mathbf{n}_l, \quad (72)$$

with $\mathbf{y}_l = (\mathbf{y}_{l,1}^T, \dots, \mathbf{y}_{l,\tau}^T)^T \in \mathbb{C}^{N\tau}$ and $\mathbf{n}_l = (\mathbf{n}_{l,1}^T, \dots, \mathbf{n}_{l,\tau}^T)^T \in \mathbb{C}^{N\tau}$. By evaluating the expectation in (71) with respect to $\{\mathcal{S}_t\}$, from the independency of $\{s_{l,t,k,m}\}$ for all l , (71) yields

$$\Xi_{\tilde{n}}(\mathcal{H}_{\mathcal{K}}^{\{1\}}, \mathcal{H}_{\mathcal{K}}^A) = p(\mathcal{H}_{\mathcal{K}}^{\{1\}}) p(\mathcal{H}_{\mathcal{K}}^A) \mathbb{E} \left[\left\{ \mathbb{E} \left[\int \prod_{a=0}^{\tilde{n}} \left\{ \frac{1}{(\pi N_0)^{N\tau}} e^{-\frac{1}{N_0} \|\mathbf{y}_1 - \sqrt{\beta} \mathbf{v}^{\{a\}}\|^2} d\mathbf{y}_1 \right\} \right] \right\}^L \middle| \mathcal{H}_{\mathcal{K}}^{\{1\}}, \mathcal{H}_{\mathcal{K}}^A \right], \quad (73)$$

where the inner expectation is taken over $\{s_{1,t,k,m} : \text{for all } t, k, m\}$. In (73), $\mathbf{v}^{\{a\}} \in \mathbb{C}^{N\tau}$ is defined as

$$\mathbf{v}^{\{a\}} = \frac{1}{\sqrt{K}} \sum_{k=1}^K \sum_{t=1}^{\tau} \sum_{m=1}^M s_{1,t,k,m} \boldsymbol{\omega}_{t,k,m}^{\{a\}}, \quad (74)$$

where $\boldsymbol{\omega}_{t,k,m}^{\{a\}} \in \mathbb{C}^{N\tau}$ is given by

$$\boldsymbol{\omega}_{t,k,m}^{\{a\}} = (\mathbf{e}_{\tau}^{(t)} \otimes \mathbf{h}_{k,m}^{\{a\}}) x_{t,k,m}, \quad (75)$$

with $\mathbf{h}_{k,m}^{\{0\}} = \mathbf{h}_{k,m}$. Let us define $\mathbf{v} \in \mathbb{C}^{(\tilde{n}+1)N\tau}$ as $\mathbf{v} = ((\mathbf{v}^{\{0\}})^T, \dots, (\mathbf{v}^{\{\tilde{n}\}})^T)^T$. We perform the Gaussian integration in (73) with respect to \mathbf{y}_1 to obtain

$$\Xi_{\tilde{n}}(\mathcal{H}_{\mathcal{K}}^{\{1\}}, \mathcal{H}_{\mathcal{K}}^A) = p(\mathcal{H}_{\mathcal{K}}^{\{1\}}) p(\mathcal{H}_{\mathcal{K}}^A) \mathbb{E} \left[\left\{ \frac{\mathbb{E} \left[e^{-\mathbf{v}^H \mathbf{A}_{\tau}(\tilde{n}) \mathbf{v}} \right]}{(\pi N_0)^{\tilde{n}N\tau} (1 + \tilde{n})^{N\tau}} \right\}^L \middle| \mathcal{H}_{\mathcal{K}}^{\{1\}}, \mathcal{H}_{\mathcal{K}}^A \right], \quad (76)$$

with

$$\mathbf{A}_{\tau}(\tilde{n}) = \frac{\beta}{N_0 + \tilde{n}N_0} \begin{pmatrix} \tilde{n} & -\mathbf{1}_{\tilde{n}}^T \\ -\mathbf{1}_{\tilde{n}} & (1 + \tilde{n})\mathbf{I}_{\tilde{n}} - \mathbf{1}_{\tilde{n}}\mathbf{1}_{\tilde{n}}^T \end{pmatrix} \otimes \mathbf{I}_{N\tau}. \quad (77)$$

The CSCG assumption of $\{s_{l,t,k,m}\}$ implies that \mathbf{v} in (76) conditioned on $\{\mathcal{H}^{\{a\}} : \text{for all } a\}$ and \mathcal{X} is a CSCG random vector with the covariance matrix

$$\mathcal{Q} = \frac{1}{K} \sum_{k=1}^K \sum_{t=1}^{\tau} \sum_{m=1}^M \boldsymbol{\omega}_{k,t,m} \boldsymbol{\omega}_{k,t,m}^H, \quad (78)$$

with $\boldsymbol{\omega}_{k,t,m} = ((\boldsymbol{\omega}_{k,t,m}^{\{0\}})^T, \dots, (\boldsymbol{\omega}_{k,t,m}^{\{\tilde{n}\}})^T)^T$. Let us assume that \mathcal{Q} is non-singular. Then, (76) yields

$$\Xi_{\tilde{n}}(\mathcal{H}_{\mathcal{K}}^{\{1\}}, \mathcal{H}_{\mathcal{K}}^A) = p(\mathcal{H}_{\mathcal{K}}^{\{1\}})p(\mathcal{H}_{\mathcal{K}}^A)\mathbb{E}\left[e^{LG_{\tau}(\mathcal{Q};\tilde{n})}\middle|\mathcal{H}_{\mathcal{K}}^{\{1\}}, \mathcal{H}_{\mathcal{K}}^A\right], \quad (79)$$

with

$$G_{\tau}(\mathcal{Q}; \tilde{n}) = -\ln \det(\mathbf{I} + \mathbf{A}_{\tau}(\tilde{n})\mathcal{Q}) - \tilde{n}N\tau \ln(\pi N_0) - N\tau \ln(1 + \tilde{n}). \quad (80)$$

Note that (79) holds for any K and L . Without the assumption of $s_{l,t,k,m} \sim \mathcal{CN}(0, 1)$, it would be necessary to evaluate $\ln \mathbb{E}[\exp(-\mathbf{v}^H \mathbf{A}_{\tau}(\tilde{n})\mathbf{v})]$ up to $O(K^{-1})$ in the large-system limit by using the Edgeworth expansion, since (63) is a quantity of $O(1)$. The vector \mathbf{v} conditioned on $\{\mathcal{H}^{\{a\}} : \text{for all } a\}$ and \mathcal{X} converges in law to a CSCG random vector with the covariance matrix (78) in the large-system limit if one assumes that $\{\text{Re}[s_{l,t,k,m}], \text{Im}[s_{l,t,k,m}]\}$ are i.i.d. zero-mean random variables with variance $1/2$ and finite moments for all l, t, k , and m . Therefore, the expansion coefficient for $O(1)$ should coincide with (80). Furthermore, it was shown that the expansion coefficient for $O(K^{-1})$ does not affect the result in the large-system limit for conventional DS-CDMA channels [61]. Therefore, it is expected that the results in this paper holds for a general distribution of $s_{l,t,k,m}$.

D. Average over Replicated Randomness

The conditional expectation in (79) is given as the integration of $\exp[LG_{\tau}(\mathcal{Q}; \tilde{n})]$ with respect to the measure $\mu_K(\mathcal{Q}; \tilde{n})d\mathcal{Q}$ on the space $\mathcal{M}_{(\tilde{n}+1)N\tau}^+$ of all $(\tilde{n} + 1)N\tau \times (\tilde{n} + 1)N\tau$ positive definite Hermitian matrices:

$$\Xi_{\tilde{n}}(\mathcal{H}_{\mathcal{K}}^{\{1\}}, \mathcal{H}_{\mathcal{K}}^A) = p(\mathcal{H}_{\mathcal{K}}^{\{1\}})p(\mathcal{H}_{\mathcal{K}}^A) \int_{\mathcal{M}_{(\tilde{n}+1)N\tau}^+} e^{LG_{\tau}(\mathcal{Q};\tilde{n})} \mu_K(\mathcal{Q}; \tilde{n})d\mathcal{Q}, \quad (81)$$

where $\mu_K(\mathcal{Q}; \tilde{n})$ denotes the pdf of \mathcal{Q} conditioned on $\mathcal{H}_{\mathcal{K}}^{\{1\}}$ and $\mathcal{H}_{\mathcal{K}}^A$, induced from (78). We shall calculate $\mu_K(\mathcal{Q}; \tilde{n})$ up to $O(1)$ since our goal is to evaluate (70) up to $O(1)$ in the large-system limit.

We first evaluate the the moment generating function of (78), defined as

$$M_K(\tilde{\mathcal{Q}}; \tilde{n}) = \mathbb{E}\left[e^{K\text{Tr}(\tilde{\mathcal{Q}}\tilde{\mathcal{Q}})}\middle|\mathcal{H}_{\mathcal{K}}^{\{1\}}, \mathcal{H}_{\mathcal{K}}^A\right], \quad (82)$$

where an $(\tilde{n} + 1)N\tau \times (\tilde{n} + 1)N\tau$ non-singular Hermitian matrix $\tilde{\mathcal{Q}}$ is given by

$$\tilde{\mathcal{Q}} = \begin{pmatrix} \tilde{\mathcal{Q}}_{0,0} & \frac{1}{2}\tilde{\mathcal{Q}}_{0,1} & \cdots & \frac{1}{2}\tilde{\mathcal{Q}}_{0,\tilde{n}} \\ \frac{1}{2}\tilde{\mathcal{Q}}_{0,1}^H & \ddots & \ddots & \vdots \\ \vdots & \ddots & \ddots & \frac{1}{2}\tilde{\mathcal{Q}}_{\tilde{n}-1,\tilde{n}} \\ \frac{1}{2}\tilde{\mathcal{Q}}_{0,\tilde{n}}^H & \cdots & \frac{1}{2}\tilde{\mathcal{Q}}_{\tilde{n}-1,\tilde{n}}^H & \tilde{\mathcal{Q}}_{\tilde{n},\tilde{n}} \end{pmatrix}, \quad (83)$$

with $N\tau \times N\tau$ complex matrices $\{\tilde{\mathcal{Q}}_{a,b} : 0 \leq a < b \leq \tilde{n}\}$, in which the (j, k) -element of $\tilde{\mathcal{Q}}_{a,b}$ is given as $\tilde{q}_{a,b}^{j,k} \in \mathbb{C}$, and with $N\tau \times N\tau$ Hermitian matrices

$$\tilde{\mathcal{Q}}_{a,a} = \begin{pmatrix} \tilde{q}_{a,a}^{1,1} & \frac{1}{2}\tilde{q}_{a,a}^{1,2} & \cdots & \frac{1}{2}\tilde{q}_{a,a}^{1,N\tau} \\ \frac{1}{2}(\tilde{q}_{a,a}^{1,2})^* & \ddots & \ddots & \vdots \\ \vdots & \ddots & \ddots & \frac{1}{2}\tilde{q}_{a,a}^{N\tau-1,N\tau} \\ \frac{1}{2}(\tilde{q}_{a,a}^{1,N\tau})^* & \cdots & \frac{1}{2}(\tilde{q}_{a,a}^{N\tau-1,N\tau})^* & \tilde{q}_{a,a}^{N\tau,N\tau} \end{pmatrix} \quad \text{for all } a. \quad (84)$$

Since $\{\mathcal{X}_k = \{x_{t,k,m} : \text{for all } t, m\}\}$ and $\{\mathcal{H}_k^{\{a\}} : a = 0, \dots, \tilde{n}\}$ are mutually independent for all k , substituting (78) into (82) implies that (82) is decomposed into the product of K terms:

$$M_K(\tilde{\mathcal{Q}}; \tilde{n}) = \prod_{k \in \mathcal{K}} M_k(\tilde{\mathcal{Q}}; \tilde{n}) \prod_{k \notin \mathcal{K}} \mathbb{E} \left[e^{\Lambda_k(\tilde{\mathcal{Q}}; \tilde{n})} \right], \quad (85)$$

with

$$M_k(\tilde{\mathcal{Q}}; \tilde{n}) = \mathbb{E} \left[e^{\Lambda_k(\tilde{\mathcal{Q}}; \tilde{n})} \middle| \mathcal{H}_k^{\{1\}}, \mathcal{H}_k^{\mathcal{A}_k} \right]. \quad (86)$$

In these expressions, $\Lambda_k(\tilde{\mathcal{Q}}; \tilde{n})$ is given by

$$\Lambda_k(\tilde{\mathcal{Q}}; \tilde{n}) = \sum_{t=1}^{\tau} \sum_{m=1}^M \text{Tr}(\omega_{t,k,m} \omega_{t,k,m}^H \tilde{\mathcal{Q}}). \quad (87)$$

It will be shown later that the moment generating function (86) for the users in \mathcal{K} reduces to the right-hand side of (63).

We next calculate the pdf $\mu_K(\mathcal{Q}; \tilde{n})$ up to $O(1)$. The inversion formula of the moment generating function (85) implies

$$\mu_K(\mathcal{Q}; \tilde{n}) = \left(\frac{K}{2\pi i} \right)^{[(\tilde{n}+1)N\tau]^2} \int \left\{ \prod_{k \in \mathcal{K}} M_k(\tilde{\mathcal{Q}}; \tilde{n}) \right\} e^{-KI_K(\mathcal{Q}, \tilde{\mathcal{Q}}; \tilde{n})} d\tilde{\mathcal{Q}}, \quad (88)$$

where the integrations with respect to $d\text{Re}[\tilde{q}_{a,b}^{j,k}]$, $d\text{Im}[\tilde{q}_{a,b}^{j,k}]$, and $d\tilde{q}_{a,a}^{j,j}$ are taken along imaginary axes, respectively.

In (88), $I_K(\mathcal{Q}, \tilde{\mathcal{Q}}; \tilde{n})$ is defined as

$$I_K(\mathcal{Q}, \tilde{\mathcal{Q}}; \tilde{n}) = \text{Tr}(\mathcal{Q}\tilde{\mathcal{Q}}) - \frac{1}{K} \sum_{k \notin \mathcal{K}} \ln \mathbb{E} \left[e^{\Lambda_k(\tilde{\mathcal{Q}}; \tilde{n})} \right], \quad (89)$$

where $\Lambda_k(\tilde{\mathcal{Q}}; \tilde{n})$ is given by (87). Note that the limit $\lim_{K \rightarrow \infty} I_K(\mathcal{Q}, \tilde{\mathcal{Q}}; \tilde{n}) \equiv I(\mathcal{Q}, \tilde{\mathcal{Q}}; \tilde{n})$ exists obviously.

Applying the saddle-point method to (88) in the large-system limit, we obtain

$$\mu_K(\mathcal{Q}; \tilde{n}) = \left\{ \prod_{k \in \mathcal{K}} M_k(\tilde{\mathcal{Q}}_s; \tilde{n}) \right\} \left(\frac{K}{2\pi} \right)^{[(\tilde{n}+1)N\tau]^2/2} \left| \det \nabla_{\tilde{\mathcal{Q}}}^2 I(\mathcal{Q}, \tilde{\mathcal{Q}}_s; \tilde{n}) \right|^{-1/2} e^{-KI(\mathcal{Q}, \tilde{\mathcal{Q}}_s; \tilde{n})} [1 + o(K)], \quad (90)$$

where $\tilde{\mathcal{Q}}_s$ is implicitly given as the solution to the fixed-point equation

$$\mathcal{Q} = \lim_{K \rightarrow \infty} \frac{1}{K} \sum_{k \notin \mathcal{K}} \sum_{t=1}^{\tau} \sum_{m=1}^M \mathbb{E} \left\{ \frac{\mathbb{E} \left[\omega_{k,t,m} \omega_{k,t,m}^H e^{\Lambda_k(\tilde{\mathcal{Q}}; \tilde{n})} \right]}{\mathbb{E} \left[e^{\Lambda_k(\tilde{\mathcal{Q}}; \tilde{n})} \right]} \right\}. \quad (91)$$

In (90), $\nabla_{\tilde{\mathcal{Q}}}^2 I(\mathcal{Q}, \tilde{\mathcal{Q}}_s; \tilde{n})$ denotes the Hesse matrix of $I(\mathcal{Q}, \tilde{\mathcal{Q}}; \tilde{n})$ with respect to $\tilde{\mathcal{Q}}$ at the saddle point $\tilde{\mathcal{Q}}_s$. In the derivation of (90), we have used the fact that the Hesse matrix $\nabla_{\tilde{\mathcal{Q}}}^2 I(\mathcal{Q}, \tilde{\mathcal{Q}}_s; \tilde{n})$ is negative definite, due to the assumption of the non-singularity of \mathcal{Q} . Note that the concavity of (89) with respect to $\tilde{\mathcal{Q}}$ at $\tilde{\mathcal{Q}} = \tilde{\mathcal{Q}}_s$ is required for the use of the saddle-point method, since the integration in (88) is taken over imaginary axes.

Finally, we evaluate (81) up to $O(1)$ in the large-system limit. Substituting (90) into (81) and subsequently using the saddle-point method, we obtain

$$\Xi_{\tilde{n}}(\mathcal{H}_{\mathcal{K}}^{\{1\}}, \mathcal{H}_{\mathcal{K}}^{\mathcal{A}}) = D_{\tilde{n}} p(\mathcal{H}_{\mathcal{K}}^{\{1\}}) p(\mathcal{H}_{\mathcal{K}}^{\mathcal{A}}) \prod_{k \in \mathcal{K}} M_k(\tilde{\mathcal{Q}}_s; \tilde{n}) e^{-K\Phi(\mathcal{Q}_s; \tilde{n})} [1 + o(K)], \quad (92)$$

where \mathcal{Q}_s is a solution to satisfy

$$\mathcal{Q}_s = \underset{\mathcal{Q} \in \mathcal{M}_{(\tilde{n}+1)N\tau}^r}{\operatorname{arginf}} \Phi(\mathcal{Q}; \tilde{n}), \quad (93)$$

with

$$\Phi(\mathcal{Q}; \tilde{n}) = I(\mathcal{Q}, \tilde{\mathcal{Q}}_s; \tilde{n}) - \beta^{-1} G_\tau(\mathcal{Q}; \tilde{n}). \quad (94)$$

In (92), $D_{\tilde{n}} = [\det \nabla_{\mathcal{Q}}^2 \Phi(\mathcal{Q}_s; \tilde{n})]^{-1/2} |\det \nabla_{\mathcal{Q}}^2 I(\mathcal{Q}_s, \tilde{\mathcal{Q}}_s; \tilde{n})|^{-1/2}$, with $\nabla_{\mathcal{Q}}^2 \Phi(\mathcal{Q}_s; \tilde{n})$ denoting the Hesse matrix of $\Phi(\mathcal{Q}; \tilde{n})$ with respect to \mathcal{Q} at the saddle-point \mathcal{Q}_s . We have assumed that the Hesse matrix $\nabla_{\mathcal{Q}}^2 \Phi(\mathcal{Q}_s; \tilde{n})$ is positive definite. Calculating the solution (93) with (80) and (89), we find that \mathcal{Q}_s satisfies the stationarity condition

$$\tilde{\mathcal{Q}} = -\beta^{-1} (I + \mathbf{A}_\tau(\tilde{n})\mathcal{Q})^{-1} \mathbf{A}_\tau(\tilde{n}). \quad (95)$$

E. Evaluation of Fixed-Point Equations

It is generally difficult to solve the coupled fixed-point equations (91) and (95). At this point, we assume that the solution $(\mathcal{Q}_s, \tilde{\mathcal{Q}}_s)$ satisfies RS. Note that it depends on models whether the RS assumption holds. Fortunately, It is empirically known that the RS assumption is correct when replicated random variables are CSCG.

Assumption 2 (Replica Symmetry). $(\mathcal{Q}_s, \tilde{\mathcal{Q}}_s)$ is invariant under all permutations of replica indices:

$$\mathcal{Q}_s = \begin{pmatrix} \mathbf{Q}_0 & \mathbf{1}_{\tilde{n}}^T \otimes M \\ \mathbf{1}_{\tilde{n}} \otimes M^H & I_{\tilde{n}} \otimes (\mathbf{Q}_1 - \mathbf{Q}) + \mathbf{1}_{\tilde{n}} \mathbf{1}_{\tilde{n}}^T \otimes \mathbf{Q} \end{pmatrix}, \quad (96)$$

$$\tilde{\mathcal{Q}}_s = \begin{pmatrix} \tilde{\mathbf{Q}}_0 & \mathbf{1}_{\tilde{n}}^T \otimes \tilde{M} \\ \mathbf{1}_{\tilde{n}} \otimes \tilde{M}^H & I_{\tilde{n}} \otimes (\tilde{\mathbf{Q}}_1 - \tilde{\mathbf{Q}}) + \mathbf{1}_{\tilde{n}} \mathbf{1}_{\tilde{n}}^T \otimes \tilde{\mathbf{Q}} \end{pmatrix}, \quad (97)$$

with $M, \tilde{M} \in \mathbb{C}^{N\tau \times N\tau}$, and with $N\tau \times N\tau$ Hermitian matrices $\mathbf{Q}_0, \tilde{\mathbf{Q}}_0, \mathbf{Q}_1, \tilde{\mathbf{Q}}_1, \mathbf{Q}$, and $\tilde{\mathbf{Q}}$.

We first solve the fixed-point equation (95) under Assumption 2. Evaluating the right-hand side of (95) with (77) and subsequently comparing both sides, we obtain

$$\tilde{\mathbf{Q}}_0 = -\tilde{n}(\Sigma + \tilde{n}\Sigma_0)^{-1}, \quad \tilde{M} = (\Sigma + \tilde{n}\Sigma_0)^{-1}, \quad \tilde{\mathbf{Q}} = (\Sigma + \tilde{n}\Sigma_0)^{-1} \Sigma_0 \Sigma^{-1}, \quad \tilde{\mathbf{Q}}_1 = \tilde{\mathbf{Q}} - \Sigma^{-1}, \quad (98)$$

where Σ_0 and Σ are given by

$$\Sigma_0 = N_0 I_{N\tau} + \beta(\mathbf{Q}_0 - M - M^H + \mathbf{Q}), \quad (99)$$

$$\Sigma = N_0 I_{N\tau} + \beta(\mathbf{Q}_1 - \mathbf{Q}). \quad (100)$$

Note that Σ and $\Sigma + \tilde{n}\Sigma_0$ must be invertible since $(I + \mathbf{A}_\tau(\tilde{n})\mathcal{Q}_s)^{-1}$ exists due to the assumption of the positive definiteness of \mathcal{Q} . Nishimori [57] proved $\Sigma_0 = \Sigma$ for unfaded CDMA systems. The condition $\Sigma_0 = \Sigma$ implies that Σ_0 must be invertible, since Σ^{-1} exists. In this case we can re-write $\tilde{\mathbf{Q}}$ as $\tilde{\mathbf{Q}} = \Sigma^{-1}(\tilde{n}\Sigma^{-1} + \Sigma_0^{-1})^{-1} \Sigma^{-1}$.

We next evaluate $e^{\Lambda_k(\tilde{\mathcal{Q}}_s; \tilde{n})}$, assuming that Σ_0 is invertible. Substituting (87) and (98) into $e^{\Lambda_k(\tilde{\mathcal{Q}}_s; \tilde{n})}$ yields

$$e^{\Lambda_k(\tilde{\mathcal{Q}}_s; \tilde{n})} = \prod_{t=1}^{\tau} \prod_{m=1}^M e^{\mathbf{a}_{t,k,m}^H \tilde{\Sigma}_0 \mathbf{a}_{t,k,m} - \sum_{a=0}^{\tilde{n}} (\omega_{t,k,m}^{\{a\}})^H \Sigma_a^{-1} \omega_{t,k,m}^{\{a\}}}, \quad (101)$$

with $\tilde{\Sigma}_0 = (\tilde{n}\Sigma^{-1} + \Sigma_0^{-1})^{-1}$ and $\Sigma_a = \Sigma$ for $a = 1, \dots, \tilde{n}$. In (101), $\mathbf{a}_{t,k,m} \in \mathbb{C}^{N\tau}$ is defined as $\mathbf{a}_{t,k,m} = \sum_{a=0}^{\tilde{n}} \Sigma_a^{-1} \omega_{t,k,m}^{\{a\}}$. In order to linearize the quadratic form $\mathbf{a}_{t,k,m}^H \tilde{\Sigma}_0 \mathbf{a}_{t,k,m}$ in (101), we apply the identity

$$e^{\mathbf{a}_{t,k,m}^H \tilde{\Sigma}_0 \mathbf{a}_{t,k,m}} = \int \frac{1}{\pi^{N\tau} \det \tilde{\Sigma}_0} e^{-\tilde{\mathbf{y}}_{t,k,m}^H \tilde{\Sigma}_0^{-1} \tilde{\mathbf{y}}_{t,k,m} + \mathbf{a}_{t,k,m}^H \tilde{\mathbf{y}}_{t,k,m} + \tilde{\mathbf{y}}_{t,k,m}^H \mathbf{a}_{t,k,m}} d\tilde{\mathbf{y}}_{t,k,m}, \quad (102)$$

to (101), with $\tilde{\mathbf{y}}_{t,k,m} \in \mathbb{C}^{N\tau}$. Then, we obtain

$$e^{\Lambda_k(\tilde{\mathbf{Q}}_s; \tilde{n})} = C_{\tilde{n}}^{\tau M} \int \prod_{a=0}^{\tilde{n}} q(\tilde{\mathbf{Y}}_k | \Omega_k^{\{a\}}) d\tilde{\mathbf{Y}}_k, \quad (103)$$

with

$$C_{\tilde{n}} = [\pi^{\tilde{n}N\tau} \det\{\Sigma^{\tilde{n}-1}(\Sigma + \tilde{n}\Sigma_0)\}]. \quad (104)$$

In (103), $q(\tilde{\mathbf{Y}}_k | \Omega_k^{\{a\}})$, with $\tilde{\mathbf{Y}}_k = \{\tilde{\mathbf{y}}_{t,k,m} : \text{for all } t \in \mathcal{T}_\tau, m\}$ and $\Omega_k^{\{a\}} = \{\omega_{t,k,m}^{\{a\}} : \text{for all } t \in \mathcal{T}_\tau, m\}$, is defined as

$$q(\tilde{\mathbf{Y}}_k | \Omega_k^{\{a\}}) = \prod_{t=1}^{\tau} \prod_{m=1}^M g_{\tau N}(\tilde{\mathbf{y}}_{t,k,m} - \omega_{t,k,m}^{\{a\}}; \Sigma_a), \quad (105)$$

where $g_{\tau N}(\tilde{\mathbf{y}}_{t,k,m} - \omega_{t,k,m}^{\{a\}}; \Sigma_a)$ is given by (1), with $\omega_{t,k,m}^{\{a\}}$ defined as (75).

We solve the fixed-point equation (91) by substituting (103) into (91). It is sufficient to evaluate $\mathbf{Q}_0 - \mathbf{M} - \mathbf{M}^H + \mathbf{Q}$ and $\mathbf{Q}_1 - \mathbf{Q}$ owing to the fact that Σ_0 and Σ depend on $\tilde{\mathbf{Q}}_s$ only through them. Comparing both sides of (91), we have

$$\begin{aligned} \mathbf{Q}_0 - \mathbf{M} - \mathbf{M}^H + \mathbf{Q} &= \lim_{K \rightarrow \infty} \frac{1}{K} \sum_{k \notin \mathcal{K}} \sum_{t=1}^{\tau} \sum_{m=1}^M \mathbb{E} \left[\frac{C_{\tilde{n}}^{\tau M}}{\mathbb{E}\{e^{\Lambda_k(\tilde{\mathbf{Q}}_s; \tilde{n})}\}} \int \langle \omega_{t,k,m}^{\{0\}} - \omega_{t,k,m}^{\{1\}} \rangle \right. \\ &\quad \left. \times \langle \omega_{t,k,m}^{\{0\}} - \omega_{t,k,m}^{\{1\}} \rangle^H q(\tilde{\mathbf{Y}}_k | \Omega_k^{\{0\}}) \left\{ \mathbb{E}_{\mathcal{H}_k^{\{1\}}} \left[q(\tilde{\mathbf{Y}}_k | \Omega_k^{\{1\}}) | \mathcal{X}_k \right] \right\}^{\tilde{n}} d\tilde{\mathbf{Y}}_k \right], \quad (106) \end{aligned}$$

$$\begin{aligned} \mathbf{Q}_1 - \mathbf{Q} &= \lim_{K \rightarrow \infty} \frac{1}{K} \sum_{k \notin \mathcal{K}} \sum_{t=1}^{\tau} \sum_{m=1}^M \mathbb{E} \left[\frac{C_{\tilde{n}}^{\tau M}}{\mathbb{E}\{e^{\Lambda_k(\tilde{\mathbf{Q}}_s; \tilde{n})}\}} \int \langle \omega_{t,k,m}^{\{1\}} - \omega_{t,k,m}^{\{0\}} \rangle \right. \\ &\quad \left. \times \langle \omega_{t,k,m}^{\{1\}} - \omega_{t,k,m}^{\{0\}} \rangle^H q(\tilde{\mathbf{Y}}_k | \Omega_k^{\{0\}}) \left\{ \mathbb{E}_{\mathcal{H}_k^{\{1\}}} \left[q(\tilde{\mathbf{Y}}_k | \Omega_k^{\{1\}}) | \mathcal{X}_k \right] \right\}^{\tilde{n}} d\tilde{\mathbf{Y}}_k \right], \quad (107) \end{aligned}$$

In (106) and (107), $\mathbb{E}[\exp\{\Lambda_k(\tilde{\mathbf{Q}}_s; \tilde{n})\}]$ is explicitly given as

$$\mathbb{E} \left[e^{\Lambda_k(\tilde{\mathbf{Q}}_s; \tilde{n})} \right] = C_{\tilde{n}}^{\tau M} \mathbb{E} \left[\int q(\tilde{\mathbf{Y}}_k | \Omega_k^{\{0\}}) \left\{ \mathbb{E}_{\mathcal{H}_k^{\{1\}}} \left[q(\tilde{\mathbf{Y}}_k | \Omega_k^{\{1\}}) | \mathcal{X}_k \right] \right\}^{\tilde{n}} d\tilde{\mathbf{Y}}_k \right]. \quad (108)$$

Furthermore, $\langle f(\omega_{t,k,m}^{\{1\}}) \rangle$ for a function $f(\omega_{t,k,m}^{\{1\}})$ of (75) denotes the mean of $f(\omega_{t,k,m}^{\{1\}})$ with respect to the posterior measure $q(\mathcal{H}_k^{\{1\}} | \tilde{\mathbf{Y}}_k, \mathcal{X}_k) d\mathcal{H}_k^{\{1\}}$, defined as

$$q(\mathcal{H}_k^{\{a\}} | \tilde{\mathbf{Y}}_k, \mathcal{X}_k) = \frac{q(\tilde{\mathbf{Y}}_k | \Omega_k^{\{a\}}) p(\mathcal{H}_k^{\{a\}})}{\int q(\tilde{\mathbf{Y}}_k | \Omega_k^{\{a\}}) p(\mathcal{H}_k^{\{a\}}) d\mathcal{H}_k^{\{a\}}}, \quad (109)$$

where $q(\tilde{\mathbf{Y}}_k | \Omega_k^{\{a\}})$ is given by (105). Equations (99), (100), (106), and (107) form closed equations for Σ_0 and Σ , and are well-defined for $\tilde{n} \in \mathbb{R}$. Regarding \tilde{n} in these equations as a real number and taking $\tilde{n} \rightarrow +0$, we obtain

the coupled fixed-point equations

$$\mathbf{\Sigma}_0 = N_0 \mathbf{I}_{N\tau} + \lim_{K \rightarrow \infty} \frac{\beta}{K} \sum_{k \notin \mathcal{K}} \sum_{t=1}^{\tau} \sum_{m=1}^M \mathbb{E} \left[(\boldsymbol{\omega}_{t,k,m}^{\{0\}} - \langle \boldsymbol{\omega}_{t,k,m}^{\{1\}} \rangle) (\boldsymbol{\omega}_{t,k,m}^{\{0\}} - \langle \boldsymbol{\omega}_{t,k,m}^{\{1\}} \rangle)^H \right], \quad (110)$$

$$\mathbf{\Sigma} = N_0 \mathbf{I}_{N\tau} + \lim_{K \rightarrow \infty} \frac{\beta}{K} \sum_{k \notin \mathcal{K}} \sum_{t=1}^{\tau} \sum_{m=1}^M \mathbb{E} \left[\langle (\boldsymbol{\omega}_{t,k,m}^{\{1\}} - \langle \boldsymbol{\omega}_{t,k,m}^{\{1\}} \rangle) (\boldsymbol{\omega}_{t,k,m}^{\{1\}} - \langle \boldsymbol{\omega}_{t,k,m}^{\{1\}} \rangle)^H \rangle \right], \quad (111)$$

where the expectations in (110) and (111) are taken with respect to the measure $q(\vec{\mathcal{Y}}_k | \Omega_k^{\{0\}}) p(\mathcal{H}_k^{\{0\}}) p(\mathcal{X}_k) d\vec{\mathcal{Y}}_k d\mathcal{H}_k^{\{0\}} d\mathcal{X}_k$. Note that (110) and (111) are coupled since their second terms depend on both $\mathbf{\Sigma}_0$ and $\mathbf{\Sigma}$.

Let us assume $\mathbf{\Sigma}_0 = \mathbf{\Sigma}$. Then, it is straightforward to show that the coupled fixed-point equations (110) and (111) reduce to the single fixed-point equation

$$\mathbf{\Sigma}_0 = N_0 \mathbf{I}_{N\tau} + \lim_{K \rightarrow \infty} \frac{\beta}{K} \sum_{k \notin \mathcal{K}} \sum_{t=1}^{\tau} \sum_{m=1}^M \mathbb{E} \left[(\boldsymbol{\omega}_{t,k,m}^{\{0\}} - \langle \boldsymbol{\omega}_{t,k,m}^{\{0\}} \rangle) (\boldsymbol{\omega}_{t,k,m}^{\{0\}} - \langle \boldsymbol{\omega}_{t,k,m}^{\{0\}} \rangle)^H \right]. \quad (112)$$

In (112), the expectation is taken with respect to $q(\vec{\mathcal{Y}}_k | \Omega_k^{\{0\}}) p(\mathcal{H}_k^{\{0\}}) p(\mathcal{X}_k) d\vec{\mathcal{Y}}_k d\mathcal{H}_k^{\{0\}} d\mathcal{X}_k$. Furthermore, $\langle \boldsymbol{\omega}_{t,k,m}^{\{0\}} \rangle$ denotes the mean of $\boldsymbol{\omega}_{t,k,m}^{\{0\}}$ with respect to the posterior measure $q(\mathcal{H}_k^{\{0\}} | \vec{\mathcal{Y}}_k, \mathcal{X}_k) d\mathcal{H}_k^{\{0\}}$, given by (109). Substituting (75) into (112) after assuming $\mathbf{\Sigma}_0 = \sigma_{\text{tr}}^2(\tau) \mathbf{I}_{N\tau}$, we find that (112) reduces to (38).

F. Replica Continuity

We evaluate (80), (86), and (89) under Assumption 2. Substituting (77) and (96) into (80) and subsequently using (99) and (100), we obtain

$$G_\tau(\mathbf{Q}_s; \tilde{n}) = -(\tilde{n} - 1) \ln \det \mathbf{\Sigma} - \ln \det(\mathbf{\Sigma} + \tilde{n} \mathbf{\Sigma}_0) - \tilde{n} N \tau \ln \pi. \quad (113)$$

Next, from (103), the moment generating function (86) for the users in \mathcal{K} reduces to

$$M_k(\tilde{\mathbf{Q}}_s; \tilde{n}) = \frac{C_{\tilde{n}}^{\tau M}}{p(\mathcal{H}_k^{\{1\}} \cup \mathcal{A}_k)} \mathbb{E} \left[\int q(\vec{\mathcal{Y}}_k | \Omega_k^{\{0\}}) \prod_{a \in \{1\} \cup \mathcal{A}_k} q(\mathcal{H}_k^{\{a\}} | \vec{\mathcal{Y}}_k, \mathcal{X}_k) \left\{ \mathbb{E}_{\mathcal{H}_k^{\{1\}}} \left[q(\vec{\mathcal{Y}}_k | \Omega_k^{\{1\}}) | \mathcal{X}_k \right] \right\}^{\tilde{n}} d\vec{\mathcal{Y}}_k \right], \quad (114)$$

where $q(\mathcal{H}_k^{\{a\}} | \vec{\mathcal{Y}}_k, \mathcal{X}_k)$ is given by (109). Finally, calculating the first term on the right-hand side of (89), we have

$$\begin{aligned} I(\mathbf{Q}_s, \tilde{\mathbf{Q}}_s; \tilde{n}) = & -\frac{\tilde{n}}{\beta} \text{Tr} \left[\mathbf{I}_{N\tau} - N_0 (\mathbf{\Sigma} + \tilde{n} \mathbf{\Sigma}_0)^{-1} - N_0 \mathbf{\Sigma}^{-1} + N_0 (\mathbf{\Sigma} + \tilde{n} \mathbf{\Sigma}_0)^{-1} \mathbf{\Sigma}_0 \mathbf{\Sigma}^{-1} \right] \\ & - \lim_{K \rightarrow \infty} \frac{1}{K} \sum_{k \notin \mathcal{K}} \ln \mathbb{E} \left\{ e^{\Lambda_k(\tilde{\mathbf{Q}}_s; \tilde{n})} \right\}, \end{aligned} \quad (115)$$

in the limit $K \rightarrow \infty$, in which $\mathbb{E}[\exp\{\Lambda_k(\tilde{\mathbf{Q}}_s; \tilde{n})\}]$ is given by (108).

Equations (113), (114), and (115) are well-defined for $\tilde{n} \in \mathbb{R}$. Let us assume that they coincide with the true ones for $\tilde{n} \in [0, n_c)$ with some $n_c > 0$. Then, substituting (113), (114), and (115) into (92) and taking $\tilde{n} \rightarrow +0$, we arrive at

$$\lim_{\tilde{n} \rightarrow +0} \Xi_{\tilde{n}}(\mathcal{H}_{\mathcal{K}}^{\{1\}}, \mathcal{H}_{\mathcal{K}}^{\mathcal{A}}) = \left(\lim_{\tilde{n} \rightarrow +0} D_{\tilde{n}} \right) \prod_{k \in \mathcal{K}} \mathbb{E} \left[q(\mathcal{H}_k^{\{1\}} | \vec{\mathcal{Y}}_k, \mathcal{X}_k) \prod_{a \in \mathcal{A}_k} q(\mathcal{H}_k^{\{a\}} | \vec{\mathcal{Y}}_k, \mathcal{X}_k) \right] + o(K), \quad (116)$$

where the expectation is taken with respect to the measure $q(\vec{\mathcal{Y}}_k|\Omega_k^{\{0\}})p(\mathcal{H}_k^{\{0\}})p(\mathcal{X}_k)d\vec{\mathcal{Y}}_kd\mathcal{H}_k^{\{0\}}d\mathcal{X}_k$. We apply (116) to (69) to obtain

$$\lim_{K,L \rightarrow \infty} \mathbb{E}_{\mathcal{I}_{\mathcal{T}_\tau} } \left[p(\mathcal{H}_{\mathcal{K}}^{\{1\}}|\mathcal{I}_{\mathcal{T}_\tau}) \prod_{k \in \mathcal{K}} \prod_{a \in \mathcal{A}_k} p(\mathcal{H}_k^{\{a\}}|\mathcal{I}_{\mathcal{T}_\tau}) \right] = \prod_{k \in \mathcal{K}} \mathbb{E} \left[q(\mathcal{H}_k^{\{1\}}|\vec{\mathcal{Y}}_k, \mathcal{X}_k) \prod_{a \in \mathcal{A}_k} q(\mathcal{H}_k^{\{a\}}|\vec{\mathcal{Y}}_k, \mathcal{X}_k) \right], \quad (117)$$

where $q(\mathcal{H}_k^{\{a\}}|\vec{\mathcal{Y}}_k, \mathcal{X}_k)$ is given by (109). It is straightforward to find that the right-hand side of (117) is equal to that of (63). In the derivation of (117), we have used the fact that $\lim_{\tilde{n} \rightarrow +0} D_{\tilde{n}}$ should be equal to 1 due to the normalization of the pdf (117). We omit the proof of $\lim_{\tilde{n} \rightarrow +0} D_{\tilde{n}} = 1$ since it requires complicated calculations and is beyond the scope of this paper. Furthermore, the proof of the convexity of (94) at the saddle point is also omitted for the same reason. For details, see [18].

APPENDIX D

DERIVATION OF PROPOSITION 1

A. Formulation

We analyze the equivalent channel between the users in \mathcal{K} and their decoders in symbol period $t(> \tau)$ to derive Proposition 1. Our analysis is based on the replica method, which is basically the same as that for Lemma 2, presented in Appendix C. However, there are two differences between the two replica analyses. One is that we replicate not only the channel vectors but also the data symbols. The other is that the self-averaging property of MAI with respect to $\mathcal{I}_{\mathcal{T}_\tau}$ is shown by using Lemma 1.

It is sufficient from Assumption 1 to show that the distribution of $\tilde{\mathcal{B}}_{t,\mathcal{K}}$ conditioned on $\mathcal{B}_{t,\mathcal{K}}$, \mathcal{H} , and $\mathcal{I}_{\mathcal{T}_\tau}$ converges in law to the right-hand side of (36) in the large-system limit. We first transform $p(\tilde{\mathcal{B}}_{t,\mathcal{K}}|\mathcal{B}_{t,\mathcal{K}}, \mathcal{H}, \mathcal{I}_{\mathcal{T}_\tau})$ into a formula corresponding to (70). The posterior pdf of $\tilde{\mathcal{B}}_{t,\mathcal{K}}$ postulated by the optimal detector, defined in the same manner as in (14), is given by

$$p(\tilde{\mathcal{B}}_{t,\mathcal{K}}|\mathcal{Y}_t, \mathcal{S}_t, \mathcal{I}_{\mathcal{T}_\tau}) = \frac{\int p(\tilde{\mathcal{Y}}_t = \mathcal{Y}_t|\tilde{\mathcal{B}}_t, \mathcal{S}_t, \mathcal{I}_{\mathcal{T}_\tau})p(\tilde{\mathcal{B}}_t)d\tilde{\mathcal{B}}_{t,\setminus\mathcal{K}}}{\int p(\tilde{\mathcal{Y}}_t = \mathcal{Y}_t|\tilde{\mathcal{B}}_t, \mathcal{S}_t, \mathcal{I}_{\mathcal{T}_\tau})p(\tilde{\mathcal{B}}_t)d\tilde{\mathcal{B}}_t}, \quad (118)$$

with $\tilde{\mathcal{B}}_{t,\setminus\mathcal{K}} = \{\tilde{\mathcal{B}}_{t,k} : \text{for all } k \notin \mathcal{K}\}$. In (118), the pdf $p(\tilde{\mathcal{Y}}_t|\tilde{\mathcal{B}}_t, \mathcal{S}_t, \mathcal{I}_{\mathcal{T}_\tau})$ is given by (15) with $\mathcal{I}_{t-1} = \mathcal{I}_{\mathcal{T}_\tau}$. The equivalent channel between the users in \mathcal{K} and their decoders is represented as

$$p(\tilde{\mathcal{B}}_{t,\mathcal{K}}|\mathcal{B}_{t,\mathcal{K}}, \mathcal{H}, \mathcal{I}_{\mathcal{T}_\tau}) = \mathbb{E}_{\mathcal{S}_t} \left[\int p(\tilde{\mathcal{B}}_{t,\mathcal{K}}|\mathcal{Y}_t, \mathcal{S}_t, \mathcal{I}_{\mathcal{T}_\tau})p(\mathcal{Y}_t|\mathcal{H}, \mathcal{S}_t, \mathcal{B}_t)p(\mathcal{B}_{t,\setminus\mathcal{K}})d\mathcal{Y}_td\mathcal{B}_{t,\setminus\mathcal{K}} \right], \quad (119)$$

with $\mathcal{B}_{t,\setminus\mathcal{K}} = \{\mathcal{B}_{t,k} : \text{for all } k \notin \mathcal{K}\}$. In (119), the pdf $p(\mathcal{Y}_t|\mathcal{H}, \mathcal{S}_t, \mathcal{B}_t)$ represents the true MIMO DS-CDMA channel (2). Introducing a real number n , we obtain

$$\lim_{K,L \rightarrow \infty} p(\tilde{\mathcal{B}}_{t,\mathcal{K}}|\mathcal{B}_{t,\mathcal{K}}, \mathcal{H}, \mathcal{I}_{\mathcal{T}_\tau}) = \lim_{K,L \rightarrow \infty} \lim_{n \rightarrow +0} \Xi_n(\tilde{\mathcal{B}}_{t,\mathcal{K}}, \mathcal{B}_{t,\mathcal{K}}, \mathcal{H}, \mathcal{I}_{\mathcal{T}_\tau}), \quad (120)$$

with

$$\begin{aligned} \Xi_n(\tilde{\mathcal{B}}_{t,\mathcal{K}}, \mathcal{B}_{t,\mathcal{K}}, \mathcal{H}, \mathcal{I}_{\mathcal{T}_\tau}) &= \mathbb{E}_{\mathcal{S}_t} \left[\int \left\{ \int p(\tilde{\mathcal{Y}}_t = \mathcal{Y}_t|\tilde{\mathcal{H}}, \mathcal{S}_t, \tilde{\mathcal{B}}_t)p(\tilde{\mathcal{B}}_t)d\tilde{\mathcal{B}}_tp(\tilde{\mathcal{H}}|\mathcal{I}_{\mathcal{T}_\tau})d\tilde{\mathcal{H}} \right\}^{n-1} \right. \\ &\quad \left. \times p(\tilde{\mathcal{Y}}_t = \mathcal{Y}_t|\tilde{\mathcal{H}}, \mathcal{S}_t, \tilde{\mathcal{B}}_t)p(\tilde{\mathcal{H}}|\mathcal{I}_{\mathcal{T}_\tau})d\tilde{\mathcal{H}}p(\tilde{\mathcal{B}}_t)d\tilde{\mathcal{B}}_{t,\setminus\mathcal{K}}p(\mathcal{Y}_t|\mathcal{H}, \mathcal{S}_t, \mathcal{B}_t)p(\mathcal{B}_{t,\setminus\mathcal{K}})d\mathcal{Y}_td\mathcal{B}_{t,\setminus\mathcal{K}} \right], \end{aligned} \quad (121)$$

where the posterior pdf $p(\tilde{\mathcal{H}}|\mathcal{I}_{\mathcal{T}_\tau})$ is given by (13) with $\mathcal{I}_{t-1} = \mathcal{I}_{\mathcal{T}_\tau}$.

B. Average over Quenched Randomness

We evaluate (121) only for $n \in \mathbb{N}$ in the large-system limit. Let $\mathcal{B}_{t,k}^{\{a\}} = \{b_{t,k,m}^{\{a\}} \in \mathbb{C} : \text{for all } m\}$ and $\tilde{\mathcal{H}}_k^{\{a\}} = \{\tilde{h}_{k,m}^{\{a\}} \in \mathbb{C}^N : \text{for all } m\}$ denote replicas of $\tilde{\mathcal{B}}_{t,k}$ and $\tilde{\mathcal{H}}_k$ for $a = 2, 3, \dots$, respectively: $\{\mathcal{B}_{t,k}^{\{a\}}\}$ are independently drawn from $p(\mathcal{B}_{t,k})$ for all k and a , and $\{\tilde{\mathcal{H}}_k^{\{a\}}\}$ conditioned on $\mathcal{I}_{\mathcal{T}_\tau}$ are mutually independent random vectors following $p(\tilde{\mathcal{H}}_k | \mathcal{I}_{\mathcal{T}_\tau})$, defined by (11), for all k and a . For notational convenience, we introduce $\mathcal{B}_{t,k}^{\{0\}} = \mathcal{B}_{t,k}$, $\mathcal{B}_{t,k}^{\{1\}} = \tilde{\mathcal{B}}_{t,k}$, $\tilde{\mathcal{H}}_k^{\{0\}} = \mathcal{H}_k$, and $\tilde{\mathcal{H}}_k^{\{1\}} = \tilde{\mathcal{H}}_k$. Note that $\tilde{\mathcal{H}}_k^{\{a\}}$ and $\mathcal{H}_k^{\{a\}}$ for $a = 1, \dots, n$ should not be confused with each other. $\{\tilde{\mathcal{H}}_k^{\{a\}}\}$ conditioned on $\mathcal{I}_{\mathcal{T}_\tau}$ are mutually independent for all k , while $\{\mathcal{H}_k^{\{a\}}\}$ conditioned on $\mathcal{I}_{\mathcal{T}_\tau}$ have dependencies for all k . Taking the averages in (121) over \mathcal{Y}_t and \mathcal{S}_t in the same manner as in the derivation of (79), we have

$$\Xi_n(\tilde{\mathcal{B}}_{t,\mathcal{K}}, \mathcal{B}_{t,\mathcal{K}}, \mathcal{H}, \mathcal{I}_{\mathcal{T}_\tau}) = p(\tilde{\mathcal{B}}_{t,\mathcal{K}}) \mathbb{E} \left[e^{LG_1(\mathcal{Q}_t; n)} \Big| \tilde{\mathcal{B}}_{t,\mathcal{K}}, \mathcal{B}_{t,\mathcal{K}}, \mathcal{H}, \mathcal{I}_{\mathcal{T}_\tau} \right], \quad (122)$$

where $G_1(\mathcal{Q}_t, n)$ is given by (80). In (122), the positive definite Hermitian matrix $\mathcal{Q}_t \in \mathcal{M}_{(n+1)N}^+$ is given by

$$\mathcal{Q}_t = \frac{1}{K} \sum_{k=1}^K \sum_{m=1}^M \omega_{t,k,m}^{(c)} (\omega_{t,k,m}^{(c)})^H, \quad (123)$$

with $\omega_{t,k,m}^{(c)} = ((\omega_{t,k,m}^{(c),\{0\}})^T, \dots, (\omega_{t,k,m}^{(c),\{n\}})^T)^T$, in which $\omega_{t,k,m}^{(c),\{a\}} \in \mathbb{C}^N$ is given by

$$\omega_{t,k,m}^{(c),\{a\}} = \tilde{h}_{k,m}^{\{a\}} b_{t,k,m}^{\{a\}}. \quad (124)$$

C. Average over Replicated Randomness

We next evaluate the expectation in (122) with respect to \mathcal{Q}_t . In the same manner as in the derivation of (88), the pdf of \mathcal{Q}_t conditioned on $\tilde{\mathcal{B}}_{t,\mathcal{K}}$, $\mathcal{B}_{t,\mathcal{K}}$, \mathcal{H} , and $\mathcal{I}_{\mathcal{T}_\tau}$ is evaluated as

$$\mu_K^{(c)}(\mathcal{Q}_t; n) = \left(\frac{K}{2\pi i} \right)^{[(n+1)N]^2} \int \left\{ \prod_{k \in \mathcal{K}} M_k^{(c)}(\tilde{\mathcal{Q}}_t; n) \right\} e^{-K I_K^{(c)}(\mathcal{Q}_t, \tilde{\mathcal{Q}}_t; n)} d\tilde{\mathcal{Q}}_t, \quad (125)$$

where we have used the fact that $\{\tilde{\mathcal{H}}_k^{\{a\}} : a = 1, \dots, n\}$ conditioned on $\mathcal{I}_{\mathcal{T}_\tau}$ are mutually independent for all k . In (125), $\tilde{\mathcal{Q}}_t$ denotes an $(n+1)N \times (n+1)N$ non-singular Hermitian matrix, defined in the same manner as in (83). The integration in (125) with respect to each element of $\tilde{\mathcal{Q}}_t$ is taken along an imaginary axis. The moment generating function $M_k^{(c)}(\tilde{\mathcal{Q}}_t; n)$ for the users in \mathcal{K} is defined as

$$M_k^{(c)}(\tilde{\mathcal{Q}}_t; n) = \mathbb{E} \left[e^{\Lambda_k^{(c)}(\tilde{\mathcal{Q}}_t; n)} \Big| \mathcal{B}_{t,k}, \tilde{\mathcal{B}}_{t,k}, \mathcal{H}_k, \mathcal{I}_{\mathcal{T}_\tau} \right], \quad (126)$$

with

$$\Lambda_k^{(c)}(\tilde{\mathcal{Q}}_t; n) = \sum_{m=1}^M \text{Tr}[\omega_{t,k,m}^{(c)} (\omega_{t,k,m}^{(c)})^H \tilde{\mathcal{Q}}_t]. \quad (127)$$

Furthermore, the function $I_K^{(c)}(\mathcal{Q}_t, \tilde{\mathcal{Q}}_t; n)$ is given by

$$I_K^{(c)}(\mathcal{Q}_t, \tilde{\mathcal{Q}}_t; n) = \text{Tr}(\mathcal{Q}_t \tilde{\mathcal{Q}}_t) - \frac{1}{K} \sum_{k \notin \mathcal{K}} \ln \mathbb{E} \left[e^{\Lambda_k^{(c)}(\tilde{\mathcal{Q}}_t; n)} \Big| \mathcal{H}_k, \mathcal{I}_{\mathcal{T}_\tau} \right]. \quad (128)$$

Note that the second term of the right-hand side of (128) depends on \mathcal{H} and $\mathcal{I}_{\mathcal{T}_\tau}$, whereas that of (89) is a deterministic value. We use Lemma 1 to show that the second term on the right-hand side of (128) converges

in probability to a deterministic value in the large-system limit. We re-write $\mathbb{E}[\exp\{\Lambda_k^{(c)}(\tilde{\mathbf{Q}}_t; n)\} | \mathcal{H}_k, \mathcal{I}_{\mathcal{T}_\tau}]$ as $X_k(\mathcal{H}_k, \mathcal{I}_{\mathcal{T}_\tau})$, given by

$$X_k(\mathcal{H}_k, \mathcal{I}_{\mathcal{T}_\tau}) = \int f_k(\mathcal{H}_k, \{\tilde{\mathcal{H}}_k^{(a)}\}) \prod_{a=1}^n \left\{ p(\tilde{\mathcal{H}}_k^{(a)} | \mathcal{I}_{\mathcal{T}_\tau}) d\tilde{\mathcal{H}}_k^{(a)} \right\}, \quad (129)$$

with

$$f_k(\mathcal{H}_k, \{\tilde{\mathcal{H}}_k^{(a)}\}) = \mathbb{E} \left[e^{\Lambda_k^{(c)}(\tilde{\mathbf{Q}}_t; n)} \middle| \mathcal{H}_k, \{\tilde{\mathcal{H}}_k^{(a)}\} \right], \quad (130)$$

where $\{\tilde{\mathcal{H}}_k^{(a)}\} = \{\tilde{\mathcal{H}}_k^{(a)} : a = 1, \dots, n\}$ denotes all replicas of $\tilde{\mathcal{H}}_k^{(a)}$ for user k . Lemma 1 implies that $\{X_k(\mathcal{H}_k, \mathcal{I}_{\mathcal{T}_\tau}) : \text{for all } k\}$ converges in law to uncorrelated random variables $\underline{X}_k(\mathcal{H}_k, \underline{\mathcal{I}}_{\mathcal{T}_\tau, k})$ in the large-system limit, given by

$$\underline{X}_k(\mathcal{H}_k, \underline{\mathcal{I}}_{\mathcal{T}_\tau, k}) = \int f_k(\mathcal{H}_k, \{\tilde{\mathcal{H}}_k^{(a)}\}) \prod_{a=1}^n \prod_{m=1}^M \left\{ p(\mathbf{h}_{k,m} = \tilde{\mathbf{h}}_{k,m}^{(a)} | \underline{\mathcal{I}}_{\mathcal{T}_\tau, k, m}) d\tilde{\mathbf{h}}_{k,m}^{(a)} \right\}, \quad (131)$$

with $\underline{\mathcal{I}}_{\mathcal{T}_\tau, k} = \{\underline{\mathcal{I}}_{\mathcal{T}_\tau, k, m} : \text{for all } m\}$. From the weak law of large numbers, we find that (128) converges in probability to

$$I^{(c)}(\mathbf{Q}_t, \tilde{\mathbf{Q}}_t; n) = \text{Tr}(\mathbf{Q}_t \tilde{\mathbf{Q}}_t) - \lim_{K \rightarrow \infty} \frac{1}{K} \sum_{k \notin \mathcal{K}} \mathbb{E} \left[\ln \mathbb{E} \left\{ e^{\Lambda_k^{(c)}(\tilde{\mathbf{Q}}_t; n)} \middle| \mathcal{H}_k, \underline{\mathcal{I}}_{\mathcal{T}_\tau, k} \right\} \right], \quad (132)$$

in the large-system limit. The convergence in probability of (128) to (132) allows us to use the same method as in the derivation of (92). Consequently, (122) yields

$$\Xi_n(\tilde{\mathcal{B}}_{t, \mathcal{K}}, \mathcal{B}_{t, \mathcal{K}}, \mathcal{H}, \mathcal{I}_{\mathcal{T}_\tau}) = D_n^{(c)} p(\tilde{\mathcal{B}}_{t, \mathcal{K}}) \left\{ \prod_{k \in \mathcal{K}} M_k^{(c)}(\tilde{\mathbf{Q}}_t^{(s)}; n) \right\} e^{-K \Phi^{(c)}(\mathbf{Q}_t^{(s)}, \tilde{\mathbf{Q}}_t^{(s)}; n)} [1 + o(K)], \quad (133)$$

with

$$\Phi^{(c)}(\mathbf{Q}_t, \tilde{\mathbf{Q}}_t; n) = I^{(c)}(\mathbf{Q}_t, \tilde{\mathbf{Q}}_t; n) - \beta^{-1} G_1(\mathbf{Q}_t; n). \quad (134)$$

In (133), $D_n^{(c)}$ is given by $D_n^{(c)} = [\det \nabla_{\tilde{\mathbf{Q}}_t}^2 \Phi^{(c)}(\mathbf{Q}_t^{(s)}, \tilde{\mathbf{Q}}_t^{(s)}; n)]^{-1/2} |\det \nabla_{\tilde{\mathbf{Q}}_t}^2 I^{(c)}(\mathbf{Q}_t^{(s)}, \tilde{\mathbf{Q}}_t^{(s)}; n)|^{-1/2}$, with the Hesse matrices $\nabla_{\tilde{\mathbf{Q}}_t}^2 \Phi^{(c)}(\mathbf{Q}_t^{(s)}, \tilde{\mathbf{Q}}_t^{(s)}; n)$ and $\nabla_{\tilde{\mathbf{Q}}_t}^2 I^{(c)}(\mathbf{Q}_t^{(s)}, \tilde{\mathbf{Q}}_t^{(s)}; n)$ of (134) and (132) with respect to \mathbf{Q}_t and $\tilde{\mathbf{Q}}_t$ at the saddle-point $(\mathbf{Q}_t, \tilde{\mathbf{Q}}_t) = (\mathbf{Q}_t^{(s)}, \tilde{\mathbf{Q}}_t^{(s)})$, respectively, which is a solution to the coupled fixed-point equations

$$\mathbf{Q}_t = \lim_{K \rightarrow \infty} \frac{1}{K} \sum_{k \notin \mathcal{K}} \sum_{m=1}^M \mathbb{E} \left[\frac{\mathbb{E} \left\{ \omega_{t,k,m}^{(c)} (\omega_{t,k,m}^{(c)})^H e^{\Lambda_k^{(c)}(\tilde{\mathbf{Q}}_t; n)} \middle| \mathcal{H}_k, \underline{\mathcal{I}}_{\mathcal{T}_\tau, k} \right\}}{\mathbb{E} \left\{ e^{\Lambda_k^{(c)}(\tilde{\mathbf{Q}}_t; n)} \middle| \mathcal{H}_k, \underline{\mathcal{I}}_{\mathcal{T}_\tau, k} \right\}} \right], \quad (135)$$

$$\tilde{\mathbf{Q}}_t = -\beta^{-1} (\mathbf{I} + \mathbf{A}_1(n) \mathbf{Q}_t)^{-1} \mathbf{A}_1(n). \quad (136)$$

If the coupled fixed-point equations (135) and (136) have multiple solutions, the solution to minimize (134) is chosen.

Remark 5. A non-negative-entropy condition would be defined via the entropy of (125) if (123) is discrete or if the data symbols and the channel vectors were discrete random variables [18]. However, it is unrealistic to assume that the channel vectors are discrete. Thus, the conventional non-negative-entropy condition is not defined for the no-CSI case. A non-negative-entropy condition might be defined via the entropy for the pdf of \mathbf{Q}_t marginalized over the channel vectors. However, its calculation is not straightforward.

D. Replica Continuity

The evaluation of (133), (135), and (136) under the RS assumption is almost the same as in the derivations of (117), (110), and (111). Therefore, we omit the details and only present the results:

$$\lim_{K, L \rightarrow \infty} p(\tilde{\mathcal{B}}_{t, \mathcal{K}} | \mathcal{B}_{t, \mathcal{K}}, \mathcal{H}, \mathcal{I}_{\mathcal{T}_\tau}) = \prod_{k \in \mathcal{K}} \int q(\tilde{\mathcal{B}}_{t, k} | \underline{\mathcal{Y}}_{t, k}, \mathcal{I}_{\mathcal{T}_\tau}) \prod_{m=1}^M \left\{ g_N(\underline{\mathbf{y}}_{t, k, m} - \mathbf{h}_{k, m} b_{t, k, m}; \Sigma_0^{(t)}) d\underline{\mathbf{y}}_{t, k, m} \right\}, \quad (137)$$

for $\underline{\mathbf{y}}_{t, k, m} \in \mathbb{C}^N$. In (137), $g_N(\underline{\mathbf{y}}_{t, k, m} - \mathbf{h}_{k, m} b_{t, k, m}; \Sigma_0^{(t)})$ is defined as (1). Furthermore, $q(\tilde{\mathcal{B}}_{t, k} | \underline{\mathcal{Y}}_{t, k}, \mathcal{I}_{\mathcal{T}_\tau})$, with $\underline{\mathcal{Y}}_{t, k} = \{\underline{\mathbf{y}}_{t, k, m} : \text{for all } m\}$, is given by

$$q(\tilde{\mathcal{B}}_{t, k} | \underline{\mathcal{Y}}_{t, k}, \mathcal{I}_{\mathcal{T}_\tau}) = \frac{\int \prod_{m=1}^M g_N(\underline{\mathbf{y}}_{t, k, m} - \tilde{\mathbf{h}}_{k, m} \tilde{b}_{t, k, m}; \Sigma^{(t)}) p(\tilde{\mathcal{B}}_{t, k}) p(\tilde{\mathcal{H}}_k | \mathcal{I}_{\mathcal{T}_\tau}) d\tilde{\mathcal{H}}_k}{\int \prod_{m=1}^M g_N(\underline{\mathbf{y}}_{t, k, m} - \tilde{\mathbf{h}}_{k, m} \tilde{b}_{t, k, m}; \Sigma^{(t)}) p(\tilde{\mathcal{B}}_{t, k}) p(\tilde{\mathcal{H}}_k | \mathcal{I}_{\mathcal{T}_\tau}) d\tilde{\mathcal{B}}_{t, k} d\tilde{\mathcal{H}}_k}. \quad (138)$$

In these expressions, $(\Sigma_0^{(t)}, \Sigma^{(t)})$ is a solution to the coupled fixed-point equations

$$\Sigma_0^{(t)} = N_0 \mathbf{I}_N + \lim_{K \rightarrow \infty} \frac{\beta}{K} \sum_{k \notin \mathcal{K}} \sum_{m=1}^M \mathbb{E} \left[(\tilde{\mathbf{h}}_{k, m}^{(0)} b_{t, k, m}^{(0)} - \langle \tilde{\mathbf{h}}_{k, m}^{(1)} b_{t, k, m}^{(1)} \rangle) (\tilde{\mathbf{h}}_{k, m}^{(0)} b_{t, k, m}^{(0)} - \langle \tilde{\mathbf{h}}_{k, m}^{(1)} b_{t, k, m}^{(1)} \rangle)^H \right], \quad (139)$$

$$\Sigma^{(t)} = N_0 \mathbf{I}_N + \lim_{K \rightarrow \infty} \frac{\beta}{K} \sum_{k \notin \mathcal{K}} \sum_{m=1}^M \mathbb{E} \left[(\tilde{\mathbf{h}}_{k, m}^{(1)} b_{t, k, m}^{(1)} - \langle \tilde{\mathbf{h}}_{k, m}^{(1)} b_{t, k, m}^{(1)} \rangle) (\tilde{\mathbf{h}}_{k, m}^{(1)} b_{t, k, m}^{(1)} - \langle \tilde{\mathbf{h}}_{k, m}^{(1)} b_{t, k, m}^{(1)} \rangle)^H \right], \quad (140)$$

where $\langle \tilde{\mathbf{h}}_{k, m}^{(a)} b_{t, k, m}^{(a)} \rangle$ denotes the mean of $\tilde{\mathbf{h}}_{k, m}^{(a)} b_{t, k, m}^{(a)}$ with respect to $q(b_{t, k, m}^{(a)}, \tilde{\mathbf{h}}_{k, m}^{(a)} | \underline{\mathcal{Y}}_{t, k, m}, \underline{\mathcal{I}}_{\mathcal{T}_\tau, k, m}) d\tilde{b}_{t, k, m} d\tilde{\mathbf{h}}_{k, m}$, given by

$$q(b_{t, k, m}^{(a)}, \tilde{\mathbf{h}}_{k, m}^{(a)} | \underline{\mathcal{Y}}_{t, k, m}, \underline{\mathcal{I}}_{\mathcal{T}_\tau, k, m}) = \frac{g_N(\underline{\mathbf{y}}_{t, k, m} - \tilde{\mathbf{h}}_{k, m}^{(a)} b_{t, k, m}^{(a)}; \Sigma_a^{(t)}) p(b_{t, k, m}^{(a)}) p(\tilde{\mathbf{h}}_{k, m}^{(a)} | \underline{\mathcal{I}}_{\mathcal{T}_\tau, k, m})}{\int g_N(\underline{\mathbf{y}}_{t, k, m} - \tilde{\mathbf{h}}_{k, m}^{(a)} b_{t, k, m}^{(a)}; \Sigma_a^{(t)}) p(b_{t, k, m}^{(a)}) p(\tilde{\mathbf{h}}_{k, m}^{(a)} | \underline{\mathcal{I}}_{\mathcal{T}_\tau, k, m}) db_{t, k, m}^{(a)} d\tilde{\mathbf{h}}_{k, m}^{(a)}}, \quad (141)$$

with $\Sigma_1^{(t)} = \Sigma^{(t)}$. In the right-hand sides of (139) and (140), the expectations are taken with respect to the measure $g_N(\underline{\mathbf{y}}_{t, k, m} - \mathbf{h}_{k, m} b_{t, k, m}; \Sigma_0^{(t)}) d\underline{\mathbf{y}}_{t, k, m} p(b_{t, k, m}) db_{t, k, m} p(\mathbf{h}_{k, m} | \underline{\mathcal{I}}_{\mathcal{T}_\tau, k, m}) p(\underline{\mathcal{I}}_{\mathcal{T}_\tau, k, m}) d\mathbf{h}_{k, m} d\underline{\mathcal{I}}_{\mathcal{T}_\tau, k, m}$.

Let us assume $\Sigma_0^{(t)} = \Sigma^{(t)}$. Then, the coupled fixed-point equations (139) and (140) reduce to the single fixed-point equation

$$\Sigma_0^{(t)} = N_0 \mathbf{I}_N + \lim_{K \rightarrow \infty} \frac{\beta}{K} \sum_{k \notin \mathcal{K}} \sum_{m=1}^M \mathbb{E} \left[(\mathbf{h}_{k, m} b_{t, k, m} - \langle \mathbf{h}_{k, m} b_{t, k, m} \rangle) (\mathbf{h}_{k, m} b_{t, k, m} - \langle \mathbf{h}_{k, m} b_{t, k, m} \rangle)^H \right]. \quad (142)$$

In (142), $\langle \mathbf{h}_{k, m} b_{t, k, m} \rangle$ denotes the mean of $\mathbf{h}_{k, m} b_{t, k, m}$ with respect to the posterior pdf (30). Furthermore, the expectation is taken with respect to the same measure as that for (139). It is shown in Appendix E that (142) reduces to (37) under the assumption of $\Sigma_0^{(t)} = \sigma_c^2 \mathbf{I}_N$. Furthermore, it is straightforward to find that (137) is equivalent to (36) under Assumption 1.

E. Multiple Solutions

We consider the case in which the coupled fixed-point equations (139) and (140) have multiple solutions. In this case, we should choose the solution minimizing (134) under the RS assumption for $n \in [0, \epsilon)$, with a sufficiently

small $\epsilon > 0$. Since $\lim_{n \rightarrow +0} \Phi^{(c)}(\underline{\mathcal{Q}}_t^{(s)}, \tilde{\underline{\mathcal{Q}}}_t^{(s)}; n) = 0$, that solution is given as the solution minimizing the derivative of (134) with respect to n in the limit $n \rightarrow +0$:

$$F_{\text{rs}} \equiv \lim_{n \rightarrow +0} \frac{\partial}{\partial n} \Phi^{(c)}(\underline{\mathcal{Q}}_t^{(s)}, \tilde{\underline{\mathcal{Q}}}_t^{(s)}; n) = \lim_{n \rightarrow +0} \frac{\partial}{\partial n} \Phi^{(c)}(\underline{\mathcal{Q}}_t^{(s)}, \tilde{\underline{\mathcal{Q}}}_t^{(s)}; n), \quad (143)$$

with $\underline{\mathcal{Q}}_t^{(s)} = \lim_{n \rightarrow +0} \underline{\mathcal{Q}}_t^{(s)}$ and $\tilde{\underline{\mathcal{Q}}}_t^{(s)} = \lim_{n \rightarrow +0} \tilde{\underline{\mathcal{Q}}}_t^{(s)}$, in which we have used the stationarity condition (136) to obtain the last expression.

We calculate (80) and (132) in (134) under the RS assumption in the same manner as in the derivations of (113) and (115) and subsequently differentiate the obtained formula with respect to n in $n \rightarrow +0$, to have

$$\lim_{n \rightarrow +0} \frac{\partial G_1}{\partial n}(\underline{\mathcal{Q}}_t^{(s)}; n) = -\ln \det \Sigma^{(t)} - \text{Tr} \left[(\Sigma^{(t)})^{-1} \Sigma_0^{(t)} \right] - N \ln \pi, \quad (144)$$

$$\begin{aligned} & \lim_{n \rightarrow +0} \frac{\partial I}{\partial n}(\underline{\mathcal{Q}}_t^{(s)}, \tilde{\underline{\mathcal{Q}}}_t^{(s)}; n) \\ &= \lim_{K \rightarrow \infty} \frac{1}{K} \sum_{k \notin \mathcal{K}} \sum_{m=1}^M \mathbb{E}[\tilde{C}_{k,m}] \ln 2 - \frac{1}{\beta} \text{Tr} \left[\mathbf{I}_N - 2N_0(\Sigma^{(t)})^{-1} + N_0(\Sigma^{(t)})^{-1} \Sigma_0^{(t)} (\Sigma^{(t)})^{-1} \right], \end{aligned} \quad (145)$$

with

$$\tilde{C}_{k,m} = \int g_N(\underline{\mathbf{y}}_{t,k,m} - \mathbf{h}_{k,m} b_{t,k,m}; \Sigma_0^{(t)}) p(b_{t,k,m}) \log \frac{g_N(\underline{\mathbf{y}}_{t,k,m} - \mathbf{h}_{k,m} b_{t,k,m}; \Sigma^{(t)})}{\mathbb{E} \left[g_N(\underline{\mathbf{y}}_{t,k,m} - \mathbf{h}_{k,m} b_{t,k,m}; \Sigma^{(t)}) \middle| \underline{\mathcal{I}}_{\mathcal{T},k,m} \right]} d\underline{\mathbf{y}}_{t,k,m} db_{t,k,m}, \quad (146)$$

where the conditional expectation is taken with respect to $\mathbf{h}_{k,m}$ and $b_{t,k,m}$. Substituting (144) and (145) into (143), we obtain

$$\begin{aligned} \frac{\beta}{\ln 2} F_{\text{rs}} &= \lim_{K \rightarrow \infty} \frac{\beta}{K} \sum_{k \notin \mathcal{K}} \sum_{m=1}^M \mathbb{E}[\tilde{C}_{k,m}] + 2D(N_0 \mathbf{I}_N \| \Sigma^{(t)}) + D(\Sigma_0^{(t)} \| \Sigma^{(t)}) - D(N_0 \mathbf{I}_N \| \Sigma^{(t)} (\Sigma_0^{(t)})^{-1} \Sigma^{(t)}) \\ &+ N \log(\pi e N_0). \end{aligned} \quad (147)$$

It is straightforward to find that (147) reduces to (39) with the exception of the constant $N \log(\pi e N_0)$, by substituting $\Sigma_0^{(t)} = \Sigma^{(t)} = \sigma_c^2 \mathbf{I}_N$ into (147).

APPENDIX E

DERIVATION OF (37)

We assume $\Sigma_0^{(t)} = \sigma_c^2 \mathbf{I}_N$. Taking the traces for both sides of (142) divided by N , we obtain

$$\sigma_c^2 = N_0 + \lim_{K \rightarrow \infty} \frac{\beta}{NK} \sum_{k \notin \mathcal{K}} \sum_{m=1}^M \text{MMSE}_{t,k,m}, \quad (148)$$

with

$$\text{MMSE}_{t,k,m} = \mathbb{E} [\| \mathbf{h}_{k,m} b_{t,k,m} - \langle \mathbf{h}_{k,m} b_{t,k,m} \rangle \|^2]. \quad (149)$$

In (149), $\langle \mathbf{h}_{k,m} b_{t,k,m} \rangle$ denotes the mean of $\mathbf{h}_{k,m} b_{t,k,m}$ with respect to the posterior pdf (30).

We first calculate the conditional joint pdf $p(\underline{\mathbf{y}}_{t,k,m}, \mathbf{h}_{k,m} | b_{t,k,m}, \underline{\mathcal{I}}_{\mathcal{T}_\tau, k, m})$ to evaluate the posterior mean of $\mathbf{h}_{k,m} b_{t,k,m}$. The channel vector $\mathbf{h}_{k,m}$ conditioned on $\underline{\mathcal{I}}_{\mathcal{T}_\tau, k, m}$ follows $\mathcal{CN}(\hat{\underline{\mathbf{h}}}_{k,m}^{\mathcal{T}_\tau}, \xi^2 \mathbf{I}_N)$, with $\hat{\underline{\mathbf{h}}}_{k,m}^{\mathcal{T}_\tau}$ and $\xi^2 = \xi^2(\sigma_{\text{tr}}^2(\tau), \tau)$ given by (31) and (32), respectively. On the other hand, (27) yields

$$p(\underline{\mathbf{y}}_{t,k,m} | \mathbf{h}_{k,m}, b_{t,k,m}) = \frac{1}{(\pi\sigma_c^2)^N} \exp\left(-\frac{\|\underline{\mathbf{y}}_{t,k,m} - \mathbf{h}_{k,m} b_{t,k,m}\|^2}{\sigma_c^2}\right). \quad (150)$$

Calculating $p(\underline{\mathbf{y}}_{t,k,m}, \mathbf{h}_{k,m} | b_{t,k,m}, \underline{\mathcal{I}}_{\mathcal{T}_\tau, k, m}) = p(\underline{\mathbf{y}}_{t,k,m} | \mathbf{h}_{k,m}, b_{t,k,m}) p(\mathbf{h}_{k,m} | \underline{\mathcal{I}}_{\mathcal{T}_\tau, k, m})$, we obtain

$$p(\underline{\mathbf{y}}_{t,k,m}, \mathbf{h}_{k,m} | b_{t,k,m}, \underline{\mathcal{I}}_{\mathcal{T}_\tau, k, m}) = p(\mathbf{h}_{k,m} | \underline{\mathcal{I}}_{\mathcal{T}_\tau, k, m}) p(\underline{\mathbf{y}}_{t,k,m} | \mathbf{h}_{k,m}, b_{t,k,m}), \quad (151)$$

with

$$p(\mathbf{h}_{k,m} | \underline{\mathcal{I}}_{\mathcal{T}_\tau, k, m}) = \frac{(P/M)\xi^2 + \sigma_c^2}{\pi\xi^2\sigma_c^2} \exp\left\{-\frac{(P/M)\xi^2 + \sigma_c^2}{\xi^2\sigma_c^2} \left\| \mathbf{h}_{k,m} - \frac{\xi^2}{(P/M)\xi^2 + \sigma_c^2} (b_{t,k,m})^* \underline{\mathbf{y}}_{t,k,m} - \frac{\sigma_c^2}{(P/M)\xi^2 + \sigma_c^2} \hat{\underline{\mathbf{h}}}_{k,m}^{\mathcal{T}_\tau} \right\|^2\right\}, \quad (152)$$

where we have used the fact that $|b_{t,k,m}|^2$ equals P/M with probability one. By definition, the posterior mean of $\mathbf{h}_{k,m} b_{t,k,m}$ is given by

$$\langle \mathbf{h}_{k,m} b_{t,k,m} \rangle = \frac{(P/M)\xi^2}{(P/M)\xi^2 + \sigma_c^2} \underline{\mathbf{y}}_{t,k,m} + \frac{\sigma_c^2}{(P/M)\xi^2 + \sigma_c^2} \hat{\underline{\mathbf{h}}}_{k,m}^{\mathcal{T}_\tau} \langle b_{t,k,m} \rangle. \quad (153)$$

We next evaluate (149). Substituting (27) and (153) into (149) yields

$$\text{MMSE}_{t,k,m} = \mathbb{E} \left[\left\| \mathbf{c}_{t,k,m} + \frac{\sigma_c^2}{(P/M)\xi^2 + \sigma_c^2} \hat{\underline{\mathbf{h}}}_{k,m}^{\mathcal{T}_\tau} (b_{t,k,m} - \langle b_{t,k,m} \rangle) \right\|^2 \right], \quad (154)$$

where $\mathbf{c}_{t,k,m}$ is defined as

$$\mathbf{c}_{t,k,m} = \frac{\sigma_c^2}{(P/M)\xi^2 + \sigma_c^2} (\mathbf{h}_{k,m} - \hat{\underline{\mathbf{h}}}_{k,m}^{\mathcal{T}_\tau}) b_{t,k,m} - \frac{(P/M)\xi^2}{(P/M)\xi^2 + \sigma_c^2} \underline{\mathbf{y}}_{t,k,m}. \quad (155)$$

The fact that $\mathbf{c}_{t,k,m}$ and $\underline{\mathbf{y}}_{t,k,m}$ conditioned on $b_{t,k,m}$ and $\underline{\mathcal{I}}_{\mathcal{T}_\tau, k, m}$ are jointly CSCG is useful for showing that the two terms on the right-hand side of (154) are mutually independent under the same conditions. The means of $\mathbf{c}_{t,k,m}$ and $\underline{\mathbf{y}}_{t,k,m}$ conditioned on $b_{t,k,m}$ and $\underline{\mathcal{I}}_{\mathcal{T}_\tau, k, m}$ are zero and $\hat{\underline{\mathbf{h}}}_{k,m}^{\mathcal{T}_\tau} b_{t,k,m}$, respectively. Also, the covariance matrix of $(\mathbf{c}_{t,k,m}^T, \underline{\mathbf{y}}_{t,k,m}^T)^T$ conditioned on $b_{t,k,m}$ and $\underline{\mathcal{I}}_{\mathcal{T}_\tau, k, m}$ is evaluated as the diagonal matrix $\text{diag}\{(P/M)\xi^2\sigma_c^2 / \{(P/M)\xi^2 + \sigma_c^2\} \mathbf{I}_N, \{(P/M)\xi^2 + \sigma_c^2\} \mathbf{I}_N\}$. Therefore, $\mathbf{c}_{t,k,m}$ and $\underline{\mathbf{y}}_{t,k,m}$ conditioned on $b_{t,k,m}$ and $\underline{\mathcal{I}}_{\mathcal{T}_\tau, k, m}$ are mutually independent. This fact indicates that the two terms on the right-hand side of (154) conditioned on $b_{t,k,m}$ and $\underline{\mathcal{I}}_{\mathcal{T}_\tau, k, m}$ are independent of each other, since the second term on the right-hand side of (154) conditioned on $b_{t,k,m}$ and $\underline{\mathcal{I}}_{\mathcal{T}_\tau, k, m}$ is a function of $\underline{\mathbf{y}}_{t,k,m}$. Hence, from (154), we have

$$\text{MMSE}_{t,k,m} = \frac{N(P/M)\xi^2\sigma_c^2}{(P/M)\xi^2 + \sigma_c^2} + \left(\frac{\sigma_c^2}{(P/M)\xi^2 + \sigma_c^2} \right)^2 \mathbb{E} \left[\|\hat{\underline{\mathbf{h}}}_{k,m}^{\mathcal{T}_\tau}\|^2 |b_{t,k,m} - \langle b_{t,k,m} \rangle|^2 \right]. \quad (156)$$

We substitute (156) into the fixed-point equation (148) to obtain (37).

APPENDIX F

PROOF OF PROPOSITION 2

We take the expectation of (36) for $\mathcal{K} = \{k\}$ with respect to $p(\mathcal{H}_k|\mathcal{I}_{\mathcal{T}_\tau})$ to obtain

$$\lim_{K,L \rightarrow \infty} p(\tilde{\mathcal{B}}_{t,k}|\mathcal{B}_{t,k}, \mathcal{I}_{\mathcal{T}_\tau}, \mathcal{S}_t) = p(\tilde{\mathcal{B}}_{t,k} = \tilde{\mathcal{B}}_{t,k}|\mathcal{B}_{t,k}, \mathcal{I}_{\mathcal{T}_\tau}) \quad \text{in law.} \quad (157)$$

Applying this expression to (21), we have

$$\lim_{K,L \rightarrow \infty} C_{\text{sep}} = \beta \left(1 - \frac{\tau}{T_c}\right) \lim_{K,L \rightarrow \infty} I(\mathcal{B}_{\tau+1,1}, \underline{\mathcal{Y}}_{\tau+1,1}|\mathcal{I}_{\mathcal{T}_\tau}), \quad (158)$$

where we have used the fact that $\tilde{\mathcal{B}}_{t,k}$ contains all information about the received vectors $\underline{\mathcal{Y}}_{t,k}$ in the single-user SIMO channel (27) for the estimation of $\mathcal{B}_{t,k}$.

In order to show that the right-hand side of (158) is equal to (41), we regard the conditional pdf $p(\underline{\mathcal{Y}}_{t,k}|\mathcal{B}_{t,k}, \mathcal{I}_{\mathcal{T}_\tau})$ as a random variable and write it as $X_k(\mathcal{I}_{\mathcal{T}_\tau}; \Theta) \geq 0$, with $\Theta = \{\mathcal{B}_{t,k}, \{\underline{\mathbf{n}}_{t,k,m} : \text{for all } m\}\}$, given by

$$X_k(\mathcal{I}_{\mathcal{T}_\tau}; \Theta) = \int f_k(\mathcal{H}_k; \Theta) p(\mathcal{H}_k|\mathcal{I}_{\mathcal{T}_\tau}) d\mathcal{H}_k, \quad (159)$$

with

$$f_k(\mathcal{H}_k; \Theta) = \prod_{m=1}^M p(\underline{\mathbf{y}}_{t,k,m} = \mathbf{h}_{k,m} b_{t,k,m} + \underline{\mathbf{n}}_{t,k,m} | \mathbf{h}_{k,m}, b_{t,k,m}), \quad (160)$$

where $p(\underline{\mathbf{y}}_{t,k,m} | \mathbf{h}_{k,m}, b_{t,k,m})$ represents the single-user SIMO channel (27). There exists the moment generating function of (159) since (159) is bounded. Then, Lemma 1 implies that $X_k \sim \prod_{m=1}^M \underline{X}_{k,m}(\underline{\mathcal{I}}_{\mathcal{T}_\tau, k, m}; \Theta)$ given Θ , defined as

$$\underline{X}_{k,m}(\underline{\mathcal{I}}_{\mathcal{T}_\tau, k, m}; \Theta) = \int p(\underline{\mathbf{y}}_{t,k,m} = \mathbf{h}_{k,m} b_{t,k,m} + \underline{\mathbf{n}}_{t,k,m} | \mathbf{h}_{k,m}, b_{t,k,m}) p(\mathbf{h}_{k,m} | \underline{\mathcal{I}}_{\mathcal{T}_\tau, k, m}) d\mathbf{h}_{k,m}. \quad (161)$$

In evaluating (161), $\sigma_t^2 = \sigma_{\text{tr}}^2(\tau)$ for $t \in \mathcal{T}_\tau$ is given by the solution to the fixed-point equation (38). Applying this result to (158), we find that the right-hand side of (158) is equal to (41).

APPENDIX G

LIST OF SEVERAL SETS

Table II lists several sets used in this paper. The other sets, such as \mathcal{Y} , $\mathcal{I}_{\mathcal{T}_\tau}$, and so on, are defined according to the rule described in Section I-A. The indices of chips, symbol periods, users, transmit antennas, and replicas are denoted by l , t , k , m , and a , respectively. The indices l , t , k , and m move from 1 to the spreading factor L , the coherence time T_c , the number of users K , and the number of transmit antennas M , respectively. The index a runs from 0 to \tilde{n} (n) for Appendix C (Appendix D), which denotes the number of replicas. In this paper, indices themselves have meanings, as noted in Section I-A. For example, \mathcal{X}_t should not be confused with \mathcal{X}_k . The former denotes the pilot symbols in symbol period t , while the latter represents all pilot symbols for user k .

TABLE II
LIST OF SEVERAL SETS.

Sets	Definitions	Eqs
\mathcal{K}	finite subset of $\{1, \dots, K\}$	–
\mathcal{T}_t	$\{1, \dots, t\}$	–
\mathcal{C}_t	$\{t, \dots, T_c\}$	–
$\{\mathcal{A}_k\}$	disjoint subsets of $\{2, \dots, n\}$	(42)
\mathcal{Y}_t	$\{\mathbf{y}_{l,t} \in \mathbb{C}^N : \text{for all } l\}$	(2)
$\tilde{\mathcal{Y}}_t$	$\{\tilde{\mathbf{y}}_{l,t} \in \mathbb{C}^N : \text{for all } l\}$	(12)
\mathcal{S}_t	$\{s_{l,t,k,m} \in \mathbb{C} : \text{for all } t, k, m\}$	(2)
\mathcal{H}_k	$\{\mathbf{h}_{k,m} \in \mathbb{C}^N : \text{for all } m\}$	(2)
$\mathcal{H}_k^{\{a\}}$	replica of \mathcal{H}_k	–
$\mathcal{H}_k^{\{0\}}$	\mathcal{H}_k	–
$\tilde{\mathcal{H}}_k$	$\{\tilde{\mathbf{h}}_{k,m} \in \mathbb{C}^N : \text{for all } m\}$	(13)
$\tilde{\mathcal{H}}_k^{\{a\}}$	replica of $\tilde{\mathcal{H}}_k$	–
$\tilde{\mathcal{H}}_k^{\{0\}}$	$\tilde{\mathcal{H}}_k$	–
$\mathcal{X}_{t,k}$	$\{x_{t,k,m} \in \mathbb{C} : \text{for all } m\}$	(3)
$\mathcal{B}_{t,k}$	$\{b_{t,k,m} \in \mathbb{C} : \text{for all } m\}$	(3)
$\tilde{\mathcal{B}}_{t,k}$	$\{\tilde{b}_{t,k,m} \in \mathbb{C} : \text{for all } m\}$	(12)
$\mathcal{B}_{t,k}^{\{a\}}$	replica of $\tilde{\mathcal{B}}_{t,k}$	–
$\mathcal{B}_{t,k}^{\{0\}}$	$\mathcal{B}_{t,k}$	–
\mathcal{U}_t	$\{u_{t,k,m} \in \mathbb{C} : \text{for all } k, m\}$	(2)
\mathcal{I}_t	$\{\mathcal{Y}_t, \mathcal{S}_t, \mathcal{U}_t\}$	–
$\tilde{\mathcal{I}}_t$	$\{\tilde{\mathcal{Y}}_t, \mathcal{S}_t\}$	–
$\underline{\mathcal{Y}}_{t,k}$	$\{\underline{\mathbf{y}}_{t,k,m} \in \mathbb{C}^N : \text{for all } m\}$	(27)
$\underline{\mathcal{I}}_{t,k,m}$	$\{u_{t,k,m}, \underline{\mathbf{y}}_{t,k,m}\}$	(27)

REFERENCES

- [1] F. Adachi, M. Sawahashi, and H. Suda, "Wideband DS-CDMA for next-generation mobile communications systems," *IEEE Commun. Mag.*, vol. 36, no. 9, pp. 56–69, Sep. 1998.
- [2] E. Dahlman, B. Gudmundson, M. Nilsson, and J. Sköld, "UMTS/IMT-2000 based on wideband CDMA," *IEEE Commun. Mag.*, vol. 36, no. 9, pp. 70–80, Sep. 1998.
- [3] T. Ojanperä and R. Prasad, "An overview of air interface multiple access for IMT-2000/UMTS," *IEEE Commun. Mag.*, vol. 36, no. 9, pp. 82–95, Sep. 1998.
- [4] A. Mantravadi, V. V. Veeravalli, and H. Viswanathan, "Spectral efficiency of MIMO multiaccess systems with single-user decoding," *IEEE J. Sel. Areas Commun.*, vol. 21, no. 3, pp. 382–394, Apr. 2003.
- [5] Z. Ni and D. Li, "Spectral efficiency of distributed MIMO code division multiple access systems over multipath fading channels," *Wirel. Commun. Mob. Comput.*, vol. 5, pp. 35–43, 2005.
- [6] M. Juntti, M. Vehkaperä, J. Leinonen, Z. Li, D. Tujkovic, S. Tsumura, and S. Hara, "MIMO MC-CDMA communications for future cellular systems," *IEEE Commun. Mag.*, vol. 43, no. 2, pp. 118–124, Feb. 2005.
- [7] H. Li and H. V. Poor, "Spectral efficiency of equal-rate DS-CDMA systems with multiple transmit antennas," *IEEE Trans. Wireless Commun.*, vol. 5, no. 12, pp. 3680–3688, Dec. 2006.

- [8] A. Nordin and G. Taricco, "Linear receivers for the multiple-input multiple-output multiple-access channel," *IEEE Trans. Commun.*, vol. 54, no. 8, pp. 1446–1456, Aug. 2006.
- [9] S. Buzzi, "Multipass channel estimation and joint multiuser detection and equalization for MIMO long-code DS/CDMA systems," *EURASIP J. Wirel. Commun. Netw.*, vol. 2006, pp. 1–13, 2006, article ID 24132.
- [10] W. Choi and J. G. Andrews, "Spatial multiplexing in cellular MIMO-CDMA systems with linear receivers: Outage probability and capacity," *IEEE Trans. Wireless Commun.*, vol. 6, no. 7, pp. 2612–2621, Jul. 2007.
- [11] K. Takeuchi, T. Tanaka, and T. Yano, "Asymptotic analysis of general multiuser detectors in MIMO DS-CDMA channels," *IEEE J. Sel. Areas Commun.*, vol. 26, no. 3, pp. 486–496, Apr. 2008.
- [12] S. V. Hanly and D. N. C. Tse, "Resource pooling and effective bandwidths in CDMA networks with multiuser receivers and spatial diversity," *IEEE Trans. Inf. Theory*, vol. 47, no. 4, pp. 1328–1351, May 2001.
- [13] L. Cottatellucci and R. R. Müller, "CDMA systems with correlated spatial diversity: A generalized resource pooling result," *IEEE Trans. Inf. Theory*, vol. 53, no. 3, pp. 1116–1136, Mar. 2007.
- [14] S. Verdú, *Multiuser Detection*. New York: Cambridge University Press, 1998.
- [15] D. N. C. Tse and S. V. Hanly, "Linear multiuser receivers: effective interference, effective bandwidth and user capacity," *IEEE Trans. Inf. Theory*, vol. 45, no. 2, pp. 641–657, Mar. 1999.
- [16] S. Verdú and S. Shamai (Shitz), "Spectral efficiency of CDMA with random spreading," *IEEE Trans. Inf. Theory*, vol. 45, no. 2, pp. 622–640, Mar. 1999.
- [17] S. Shamai (Shitz) and S. Verdú, "The impact of frequency-flat fading on the spectral efficiency of CDMA," *IEEE Trans. Inf. Theory*, vol. 47, no. 4, pp. 1302–1327, May 2001.
- [18] T. Tanaka, "A statistical-mechanics approach to large-system analysis of CDMA multiuser detectors," *IEEE Trans. Inf. Theory*, vol. 48, no. 11, pp. 2888–2910, Nov. 2002.
- [19] R. R. Müller and W. H. Gerstacker, "On the capacity loss due to separation of detection and decoding," *IEEE Trans. Inf. Theory*, vol. 50, no. 8, pp. 1769–1778, Aug. 2004.
- [20] D. Guo and S. Verdú, "Randomly spread CDMA: Asymptotics via statistical physics," *IEEE Trans. Inf. Theory*, vol. 51, no. 6, pp. 1983–2010, Jun. 2005.
- [21] P. D. Alexander, A. J. Grant, and M. C. Reed, "Iterative detection in code-division multiple-access with error control coding," *Euro. Trans. Telecommun.*, vol. 9, no. 5, pp. 419–425, Sep.–Oct. 1998.
- [22] M. C. Reed, C. B. Schlegel, P. D. Alexander, and J. A. Asenstorfer, "Iterative multiuser detection for CDMA with FEC: near-single-user performance," *IEEE Trans. Commun.*, vol. 46, no. 12, pp. 1693–1699, Dec. 1998.
- [23] M. Moher, "An iterative multiuser decoder for near-capacity communications," *IEEE Trans. Commun.*, vol. 46, no. 7, pp. 870–880, Jul. 1998.
- [24] X. Wang and H. V. Poor, "Iterative (turbo) soft interference cancellation and decoding for coded CDMA," *IEEE Trans. Commun.*, vol. 47, no. 7, pp. 1046–1061, Jul. 1999.
- [25] J. Boutros and G. Caire, "Iterative multiuser joint decoding: Unified framework and asymptotic analysis," *IEEE Trans. Inf. Theory*, vol. 48, no. 7, pp. 1772–1793, Jul. 2002.
- [26] G. Caire, R. R. Müller, and T. Tanaka, "Iterative multiuser joint decoding: Optimal power allocation and low-complexity implementation," *IEEE Trans. Inf. Theory*, vol. 50, no. 9, pp. 1950–1973, Sep. 2004.
- [27] K. Takeuchi and T. Tanaka, "Hierarchical decoupling principle of a MIMO-CDMA channel in asymptotic limits," in *Proc. 2007 IEEE Int. Symp. Inf. Theory*, Nice, France, Jun. 2007, pp. 1271–1275.
- [28] P. D. Alexander and A. J. Grant, "Iterative channel and information sequence estimation in CDMA," in *Proc. IEEE 6th Int. Symp. Spread-Spectrum Tech. & Appl.*, vol. 2, New Jersey, USA, Sep. 2000, pp. 593–597.
- [29] H. E. Gamal and E. Geraniotis, "Iterative multiuser detection for coded CDMA signals in AWGN and fading channels," *IEEE J. Sel. Areas Commun.*, vol. 18, no. 1, pp. 30–41, Jan. 2000.
- [30] A. Lampe, "Iterative multiuser detection with integrated channel estimation for coded DS-CDMA," *IEEE Trans. Commun.*, vol. 50, no. 8, pp. 1217–1223, Aug. 2002.
- [31] T. L. Marzetta and B. M. Hochwald, "Capacity of a mobile multiple-antenna communication link in Rayleigh flat fading," *IEEE Trans. Inf. Theory*, vol. 45, no. 1, pp. 139–157, Jan. 1999.

- [32] M. Médard, “The effect upon channel capacity in wireless communications of perfect and imperfect knowledge of the channel,” *IEEE Trans. Inf. Theory*, vol. 46, no. 3, pp. 933–946, May 2000.
- [33] B. Hassibi and B. M. Hochwald, “How much training is needed in multiple-antenna wireless link?” *IEEE Trans. Inf. Theory*, vol. 49, no. 4, pp. 951–963, Apr. 2003.
- [34] J. Evans and D. N. C. Tse, “Large system performance of linear multiuser receivers in multipath fading channels,” *IEEE Trans. Inf. Theory*, vol. 46, no. 6, pp. 2059–2078, Sep. 2000.
- [35] H. Li, S. M. Betz, and H. V. Poor, “Performance analysis of iterative channel estimation and multiuser detection in multipath DS-CDMA channels,” *IEEE Trans. Signal Process.*, vol. 55, no. 5, pp. 1981–1993, May 2007.
- [36] M. Vehkaperä, K. Takeuchi, R. R. Müller, and T. Tanaka, “Iterative channel and data estimation: Framework and analysis via replica method,” in *Proc. 2009 IEEE Int. Symp. Inf. Theory*, Seoul, Korea, Jun. 2009, pp. 2689–2693.
- [37] H. Nishimori, *Statistical Physics of Spin Glasses and Information Processing*. New York: Oxford University Press, 2001.
- [38] K. H. Fischer and J. A. Hertz, *Spin Glasses*. Cambridge, UK: Cambridge University Press, 1991.
- [39] Mézard, G. Parisi, and M. A. Virasoro, *Spin Glass Theory and Beyond*. Singapore: World Scientific, 1987.
- [40] K. Takeda, S. Uda, and Y. Kabashima, “Analysis of CDMA systems that are characterized by eigenvalue spectrum,” *Europhys. Lett.*, vol. 76, no. 6, pp. 1193–1199, 2006.
- [41] A. L. Moustakas, S. H. Simon, and A. M. Sengupta, “MIMO capacity through correlated channels in the presence of correlated interferers and noise: A (not so) large N analysis,” *IEEE Trans. Inf. Theory*, vol. 49, no. 10, pp. 2545–2561, Oct. 2003.
- [42] C. K. Wen and K. K. Wong, “Asymptotic analysis of spatially correlated MIMO multiple-access channels with arbitrary signaling inputs for joint and separate decoding,” *IEEE Trans. Inf. Theory*, vol. 53, no. 1, pp. 252–268, Jan. 2007.
- [43] R. R. Müller, D. Guo, and A. L. Moustakas, “Vector precoding for wireless MIMO systems and its replica analysis,” *IEEE J. Sel. Areas Commun.*, vol. 26, no. 3, pp. 530–540, Apr. 2008.
- [44] B. M. Zaidel, R. R. Müller, A. L. Moustakas, and R. de Miguel, “Vector precoding for Gaussian MIMO broadcast channels: Impact of replica symmetry breaking,” submitted to *IEEE Trans. Inf. Theory*, 2010, [Online]. Available: <http://arxiv.org/abs/1001.3790>.
- [45] F. Guerra, “Broken replica symmetry bounds in the mean field spin glass model,” *Commun. Math. Phys.*, vol. 233, pp. 1–12, 2003.
- [46] M. Talagrand, “The Parisi formula,” *Annals of Mathematics*, vol. 163, pp. 221–263, 2006.
- [47] S. B. Korada and A. Montanari, “Applications of the Lindeberg principle in communications and statistical learning,” *IEEE Trans. Inf. Theory*, vol. 57, no. 4, pp. 2440–2450, Apr. 2011.
- [48] F. D. Neeser and J. L. Massey, “Proper complex random processes with applications to information theory,” *IEEE Trans. Inf. Theory*, vol. 39, no. 4, pp. 1293–1302, Jul. 1993.
- [49] K. Takeuchi and T. Tanaka, “Statistical-mechanics-based analysis of multiuser MIMO channels with linear dispersion codes,” *J. Phys.: Conf. Ser.*, vol. 95, pp. 012 008–1–11, Jan. 2008.
- [50] K. Takeuchi, M. Vehkaperä, T. Tanaka, and R. R. Müller, “Asymptotic performance bounds of joint channel estimation and multiuser detection in frequency-selective fading DS-CDMA channels,” in *Proc. 2008 Int. Symp. Inf. Theory and its Appl.*, Auckland, New Zealand, Dec. 2008, pp. 359–364.
- [51] T. M. Cover and J. A. Thomas, *Elements of Information Theory*, 2nd ed. New Jersey: Wiley, 2006.
- [52] T. Li and O. M. Collins, “A successive decoding strategy for channels with memory,” *IEEE Trans. Inf. Theory*, vol. 53, no. 2, pp. 628–646, Feb. 2007.
- [53] K. Padmanabhan, S. Venkatraman, and O. M. Collins, “Tight upper and lower bounds on the constrained capacity of non-coherent multi-antenna channels,” in *Proc. 2008 IEEE Int. Symp. Inf. Theory*, Toronto, Canada, Jul. 2008, pp. 2588–2592.
- [54] S. B. Korada and N. Macris, “Tight bounds on the capacity of binary input random CDMA systems,” *IEEE Trans. Inf. Theory*, vol. 56, no. 11, pp. 5590–5613, Nov. 2010.
- [55] Y. Kabashima, “A CDMA multiuser detection algorithm on the basis of belief propagation,” *J. Phys. A: Math. Gen.*, vol. 36, no. 43, pp. 11 111–11 121, Oct. 2003.
- [56] J. R. L. de Almeida and D. J. Thouless, “Stability of the Sherrington-Kirkpatrick solution of a spin glass model,” *J. Phys. A: Math. Gen.*, vol. 11, no. 5, pp. 983–990, 1978.
- [57] H. Nishimori, “Comment on “statistical mechanics of CDMA multiuser demodulation” by Tanaka,” *Europhys. Lett.*, vol. 57, no. 2, pp. 302–303, Jan. 2002.

- [58] D. N. C. Tse and P. Viswanath, *Fundamentals of Wireless Communication*. Cambridge, UK: Cambridge University Press, 2005.
- [59] M. Yoshida, T. Uezu, T. Tanaka, and M. Okada, "Statistical mechanical study of code-division multiple-access multiuser detectors," *J. Phys. Soc. Jpn.*, vol. 76, pp. 054 003–1–10, 2007.
- [60] E. Biglieri, G. Taricco, and A. Tulino, "How far aways is infinity? using asymptotic analyses in multiple-antenna systems," in *Proc. IEEE 7th Int. Symp. Spread-Spectrum Tech. & Appl.*, vol. 1, Prague, Czech Republic, Sep. 2002, pp. 1–6.
- [61] K. Nakamura and T. Tanaka, "Microscopic analysis for decoupling principle of linear vector channel," in *Proc. 2008 IEEE Int. Symp. Inf. Theory*, Toronto, Canada, Jul. 2008, pp. 519–523.